Report to

THE NATIONAL SCIENCE FOUNDATION
Washington, D.C.
Grant No. ENV77-15333

EARTHQUAKE RESISTANT STRUCTURAL WALLS - TESTS OF WALLS WITH AND WITHOUT OPENINGS

by

K. N. Shiu
J. I. Daniel
J. D. Aristizabal-Ochoa
A. E. Fiorato
W. G. Corley

Submitted by

CONSTRUCTION TECHNOLOGY LABORATORIES
A Division of the Portland Cement Association
5420 Old Orchard Road
Skokie, Illinois 60077

July, 1981

50272-101

REPORT DOCUMENTATION PAGE	1. REPORT NO. NSF/CEE-81033	2.	3. Recipient's Accession No. PB82 131947
4. Title and Subtitle Earthquake Resistant Structural Walls - Tests of Walls With and Without Openings			5. Report Date July 1981 6. U328054
7. Author(s) W.G. Corley, PI, K.N. Shiu, J.I. Daniel, J.D. Aristizabal-Ochoa,*			8. Performing Organization Rept. No.
9. Performing Organization Name and Address Portland Cement Association Construction Technology Laboratories 5420 Old Orchard Road Skokie, Il 60077			10. Project/Task/Work Unit No. 11. Contract(C) or Grant(G) No. (C) (G) ENV7715333
12. Sponsoring Organization Name and Address Directorate for Engineering (ENG) National Science Foundation 1800 G Street, N.W. Washington, DC 20550			13. Type of Report & Period Covered 14.

15. Supplementary Notes

Submitted by: Communications Program (OPRM)
National Science Foundation
Washington, DC 20550

*A.E. Fiorato

16. Abstract (Limit: 200 words)

The effects of structural wall window openings on strength, deformation capacity, and energy dissipation capacity were determined and evaluated. Two one-third scale, six-story wall specimens were subjected to inelastic load reversals representing severe earthquake forces exerted by double acting hydraulic rams, located on both sides of the wall specimens, and applied to the top of each wall. The specimens were designed of earthquake resistant reinforced concrete wall elements in coupled wall systems based on the 1976 Uniform Building Code. The loading was calculated using a modified DRAIN two-dimensional computer program with two actual earthquake records used as input ground motion data. One specimen was a solid wall and the other included six openings simulating windows. When data was normalized by yield capacities, the response of the two walls to the inelastic loading was similar. The presence of window openings had little effect on the deformation characteristics of the sample walls in response to the cyclic loads. The solid wall failed through sliding shear along a horizontal crack that developed at the first-story level, while the pierced wall failed through shear-compression at the boundary elements.

17. Document Analysis a. Descriptors

Earthquake resistant structures
Concrete construction
Structural design
Loads (forces)
Walls
Dynamic structural analysis
Reinforced concrete
Dynamic tests

b. Identifiers/Open-Ended Terms

DRAIN (programming language)

c. COSATI Field/Group

I

18. Availability Statement	19. Security Class (This Report)	21. No. of Pages
NTIS	20. Security Class (This Page)	22. Price

(See ANSI-Z39.18) See Instructions on Reverse

OPTIONAL FORM 272 (4-77)
(Formerly NTIS-35)
Department of Commerce

TABLE OF CONTENTS

TABLE OF CONTENTS (Continued)

EARTHQUAKE RESISTANT STRUCTURAL WALLS - TESTS OF WALLS WITH AND WITHOUT OPENINGS

by

K. N. Shiu, J. I. Daniel, J. D. Aristizabal-Ochoa, A. E. Fiorato, and W. G. Corley*

HIGHLIGHTS

Effects of openings on behavior of structural walls under inelastic load reversals are discussed in this report. Two 1/3-scale structural wall specimens, with and without openings, were tested. The solid wall, Specimen CI-1, was designed according to UBC and ACI recommendations. The wall with openings, Specimen PW-1, was compared with Specimen CI-1. Reinforcement details around openings were adopted from current design practices. Specimen PW-1 had an opening-to-wall area ratio of 8.3% and lintels with a shear span-to-depth ratio of 0.35. Reversing loads representing effects of severe earthquakes were applied to both specimens.

Behavior of specimens was observed and compared. Effects of openings on strength, deformation capacity, and energy dissipation capacity were determined and evaluated.

*Respectively, Structural Engineer, Associate Structural Engineer, Former Structural Engineer, Structural Development Department; Manager, Construction Methods Section; Divisional Director, Engineering Development Division, Construction Technology Laboratories, a Division of Portland Cement Association, Skokie, Illinois 60077.

FINDINGS AND CONCLUSIONS

The following findings and conclusions are based on results from tests of Specimens CI-1 and PW-1.

1. Load capacity and deformation characteristics of solid wall Specimen CI-1 and pierced wall Specimen PW-1 were similar. Maximum rotational ductility measured over the lower 6 ft (1.8 m) was 5.6 for both specimens. Maximum nominal shear stresses sustained by Specimens CI-1 and PW-1 were 4.6 $\sqrt{f'_c}$ psi (0.38 $\sqrt{f'_c}$ MPa) and 4.8 $\sqrt{f'_c}$ psi (0.40 $\sqrt{f'_c}$ MPa), respectively. Top deflection ductilities for Specimens CI-1 and PW-1 were 4.3 and 3.5, respectively. Both specimens exhibited similar energy dissipation capacities.
2. Lintels in Specimen PW-1 had a shear span-to-depth ratio of 0.35. The short lintels were effective in connecting wall piers together. No special diagonal reinforcement was used in the lintels. There was no yielding of reinforcement in the lintels even after the vertical wall reinforcement yielded.
3. The design practice of placing discontinuous reinforcement to each side of openings functioned well.
4. Stress concentrations around openings were not observed to effect behavior of the pierced wall specimen.
5. Different failure modes were observed in each specimen. The solid wall, Specimen CI-1, lost its load carrying capacity through "sliding shear" along a horizontal

crack that developed at the first story level. The pierced wall, Specimen PW-1, lost capacity through shear-compression at the boundary elements.

6. Capacity of both specimens was limited by shear.
7. Premature failure of lintels between openings can be avoided by designing lintels to remain elastic until flexural capacity of the structural wall is reached.

INTRODUCTION

Behavior of structural walls under earthquake loadings has been extensively investigated in recent years.[1,2,3] A comprehensive analytical and experimental research project to evaluate strength and deformation capacities of isolated walls was initiated at Portland Cement Association in the late sixties.[1] It has been shown that structural walls are effective structural members for resisting earthquake motions. Results, findings, and recommendations for designing walls have been published in reports and papers in various technical journals.[1,4,5,6]

Structural walls are usually connected to other walls or frames by means of coupling beams to form structural systems. Openings for windows and doors in structural walls are also common. As illustrated in Fig. 1, there are generally three types of structural wall systems; coupled wall systems, wall frame systems, and pierced wall systems. Recent research efforts on structural walls have been primarily devoted to behavior of isolated walls, coupled wall systems, and wall

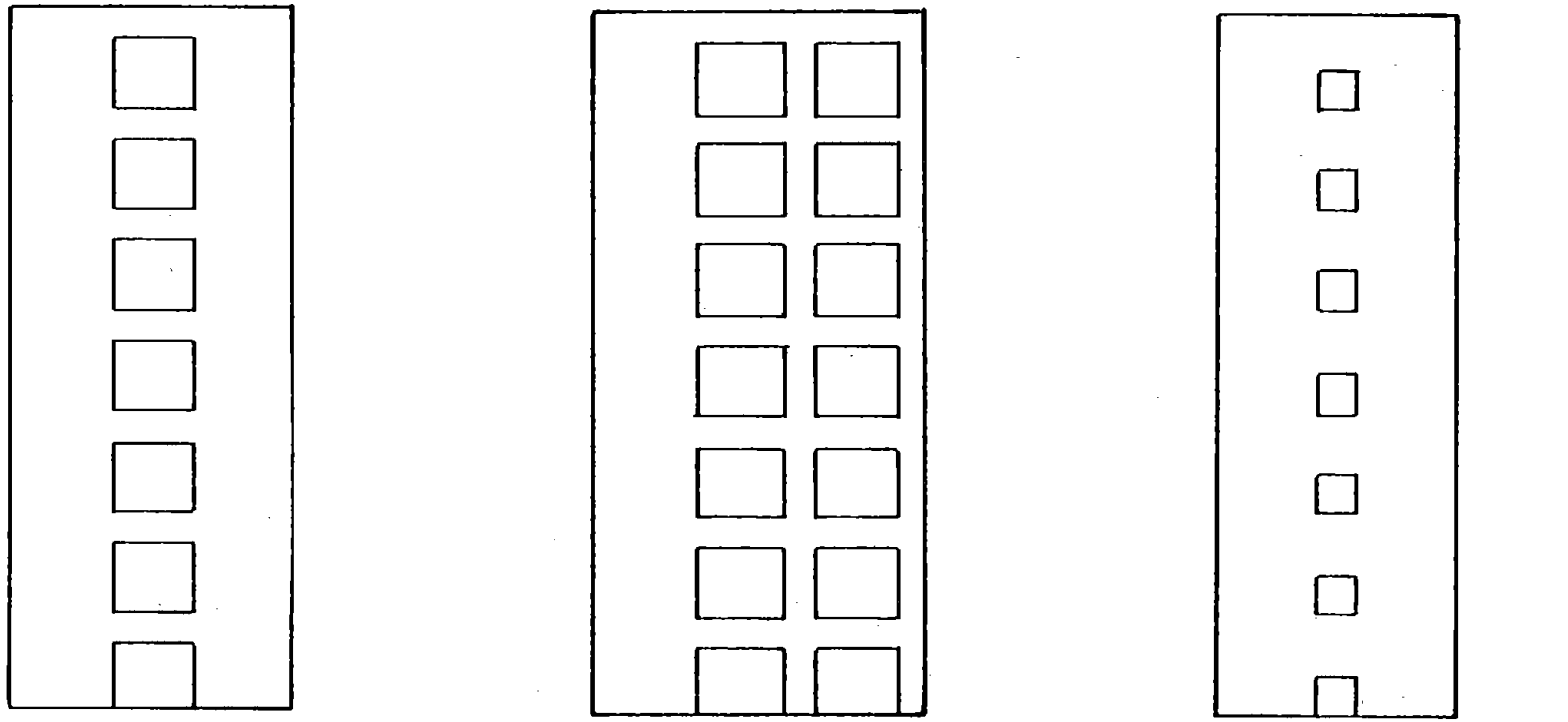

Fig. 1 Structural Wall Systems

frame systems.[1-7] Data on behavior of pierced wall systems under earthquake loadings is lacking.

Behavior of coupled wall systems with weak and strong beams was investigated at the Portland Cement Association.[5,6] Openings in the coupled wall systems represented proportions common for fire door openings. To complete the research on behavior of different earthquake resistant structural wall systems, a structural wall pierced with openings was also investigated. Openings simulated window areas or utility ducts. Effect of openings on the behavior of structural walls was determined.

Background

Effects of openings on concrete walls have been investigated by several researchers. Benjamin found that stress concentrations around corners of openings were significant.[8] High levels of stress around corners was found to reduce wall capacity if not properly considered in design.

Although experimental data on stress concentrations around openings and on effects of openings in beams and walls are available; reported test results deal mainly with inelastic behavior under monotonic loadings.[8,10,11,12] Information concerning inelastic behavior of structural walls with openings under load reversals is not available.

Test data are available on inelastic behavior of coupled wall systems with very short coupling beams. Paulay tested wall systems with coupling beams having a shear span-to-depth ratio of 0.67.[7] The area ratio of opening-to-wall was 7%.

Mirsa tested coupled wall systems with coupling beams having a shear span-to-depth ratio of 0.64.[13] The area ratio of opening-to-wall was 16%.

As the shear span-to-depth ratio decreases, behavior of coupled wall systems approaches that of pierced wall systems. However, there is a fundamental difference in behavior between the two systems. Coupled wall systems are designed to dissipate energy through coupling beams. Behavior of the coupled wall system depends on the amount of coupling provided by the beams, and the relative strength and deformation capacities of beam and wall elements. Pierced wall systems behave as isolated wall elements. Full coupling action is expected from lintels in pierced wall systems. The lintels or deep beams are not expected to undergo significant inelastic behavior before yielding of the wall system occurs.

Therefore, to further our understanding of the effects of openings on structural walls under reversing loads, wall specimens with and without openings were constructed and tested at Construction Technology Laboratories, a division of the Portland Cement Association.

Objectives and Scope

Objectives of this investigation were:

1. To determine effects of openings on strength and deformation capacity of structural walls under simulated earthquake loadings.

2. To verify design criteria and reinforcement details for earthquate resistant structural walls with openings.

Two wall specimens were tested. They represented structural walls at approximately 1/3-scale. A solid isolated wall, Specimen CI-1, was tested first. A companion isolated wall pierced with openings, Specimen PW-1, was then tested. Except for the presence of openings, Specimen PW-1 was nominally identical to Specimen CI-1. Openings in PW-1 were located in the center of the wall at each story level. The size of the openings represented typical window areas. No special reinforcement details were used around the openings.

Specimens were tested under similar load histories. Reversing loads were applied laterally to the top of each specimen as a fixed vertical cantilever. Load and deformation characteristics were recorded. Based on observed behavior and measured data, comparisons between the two specimens were made. Discussion of the effects of openings on behavior of structural walls is presented in this report.

EXPERIMENTAL PROGRAM

A brief description of the test specimens, test setup, and test procedure is presented in this section. Detailed description of the experimental program is presented in Appendix A.

Test Specimens

Overall dimensions of the wall specimens are shown in Fig. 2. Specimens were 1/3-scale representations of six-story

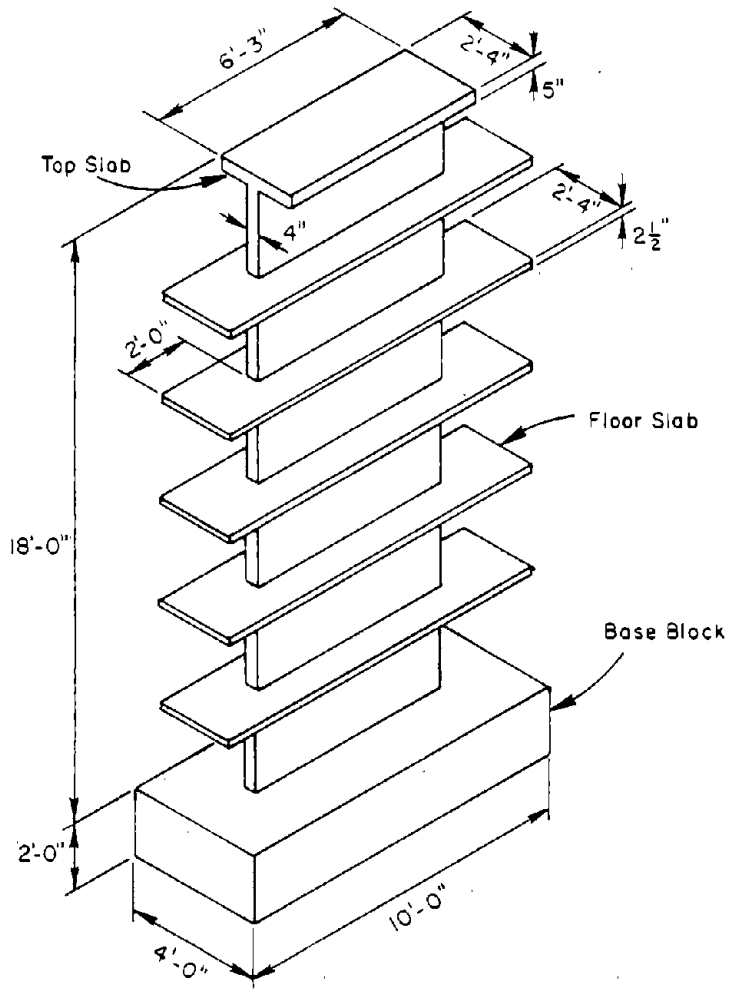

Fig. 2 Dimensions of Wall Specimens

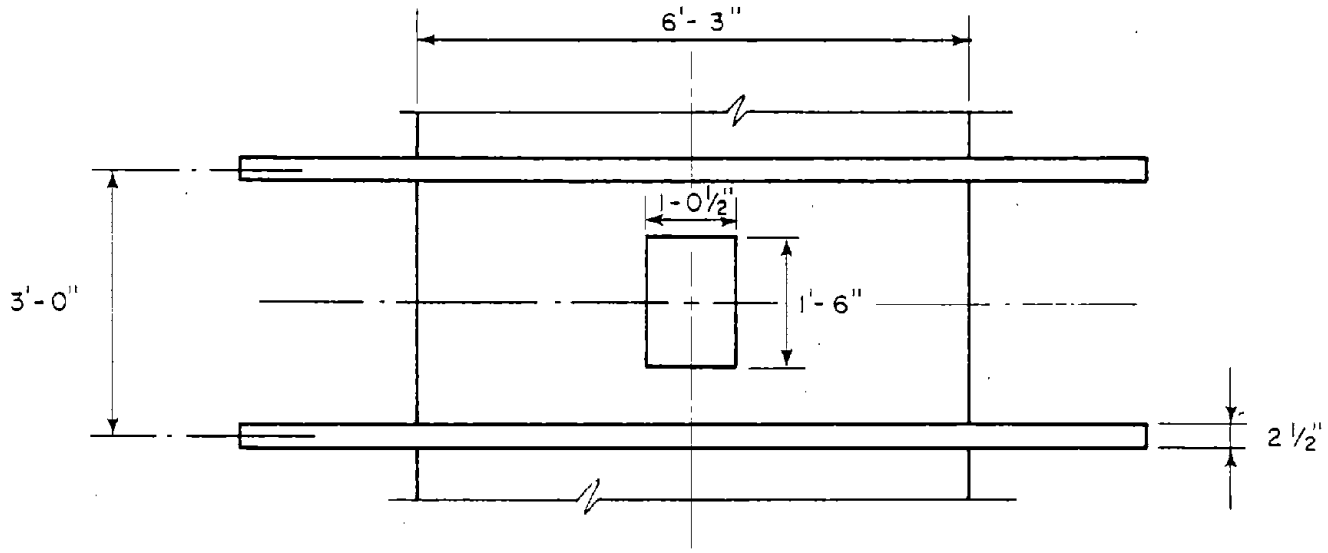

Fig. 3 Location and Dimensions of Openings

walls with short stubs representing floor slabs at each story level. Specimens had a total height of 18 ft (5.5 m), a horizontal length of 6 ft 3 in. (1.9 m), and a uniform wall thickness of 4 in. (106 mm). The height of each story level was 3 ft (0.9 m). Floor slabs were simulated by 2.5-in. (64 mm) thick stubs running full length along both sides of the walls. Specimens were attached to the test floor through a rigid foundation block. Foundation-soil interaction was not considered in this investigation.

With the exception of openings, Specimen PW-1 was nominally identical to Specimen CI-1. Openings in the pierced wall were located in the center of the wall at each story level. They were 12.5-in. by 18.0-in. (317 mm x 457 mm) rectangular openings simulating typical window areas. Locations and dimensions of openings are shown in Fig. 3.

Construction procedures were similar to common field practice. Specimens were cast vertically, one story at a time, with construction joints at each floor level.

Design and Reinforcement Details

Specimens were designed as wall elements for a coupled wall system. The design was made for a coupled wall prototype structure conforming to the provisions of the 1971 ACI Building Code,[14] and the 1976 Uniform Building Code.[15] The resulting design was later checked by dynamic analyses using actual recorded earthquake ground motions.

In design calculations, 3000 psi (20.7 mPa) concrete and Grade-60 steel were used. Reinforcement arrangement in Specimen PW-1 was identical to Specimen CI-1 with the exception of details around openings. Reinforcement interrupted by openings was moved in equal amount to the sides of openings. Flexural and shear capacity of lintels were designed to ensure full coupling between wall piers. Essentially, Specimen PW-1 was designed to behave as an isolated wall. Shear reinforcement in piers was selected to resist shear stresses corresponding to the flexural strength of the system.

Reinforcement details for Specimen CI-1 are shown in Fig. 4. Primary flexural reinforcement was provided by 12-No. 4 bars located to each side of the wall. Reinforcement percentage of these bars with respect to surrounding concrete area was approximately 6%. Confinement around primary reinforcement was provided by closed hoops of D-3 deformed wires. These hoops were spaced at 1-1/3 in. (34 mm) within the the first two stories and at 4 in. (102 mm) within the upper stories. Horizontal shear reinforcement was provided by two layers of 6 mm bars spaced at 6 in. (102 mm) on centers.

Reinforcement details around openings for Specimen PW-1 are shown in Fig. 5. Flexural reinforcement in lintels was provided by four 6 mm bars as shown in Fig. 6. Lintels were designed to remain elastic until capacity of wall piers was reached. Shear capacity of the lintels was provided by closed hoops of 6 mm bars spaced 2-3/8 in. (60.3 mm). These hoops provided confinement as well as shear capacity.

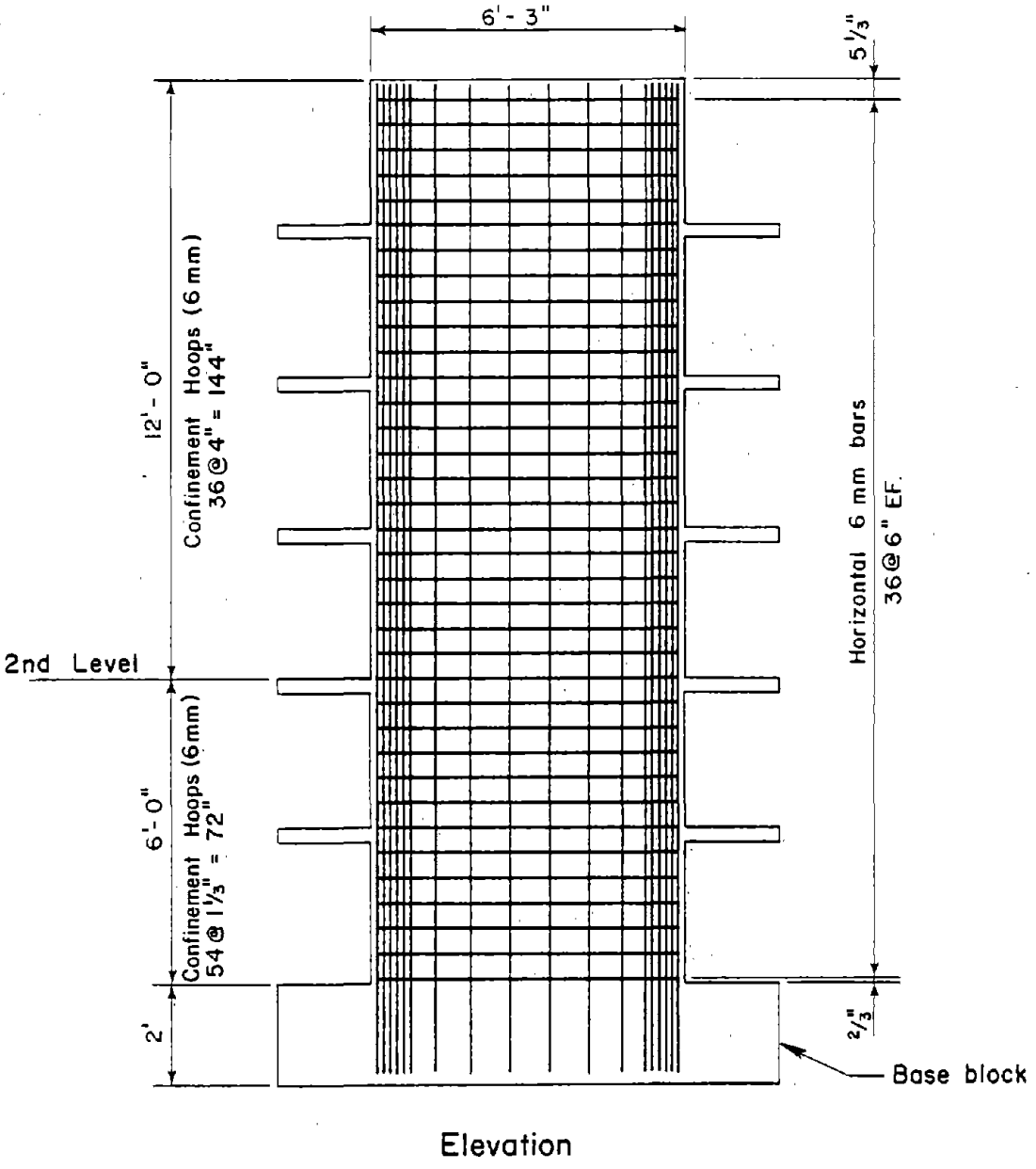

Fig. 4 Reinforcement Details of Specimens

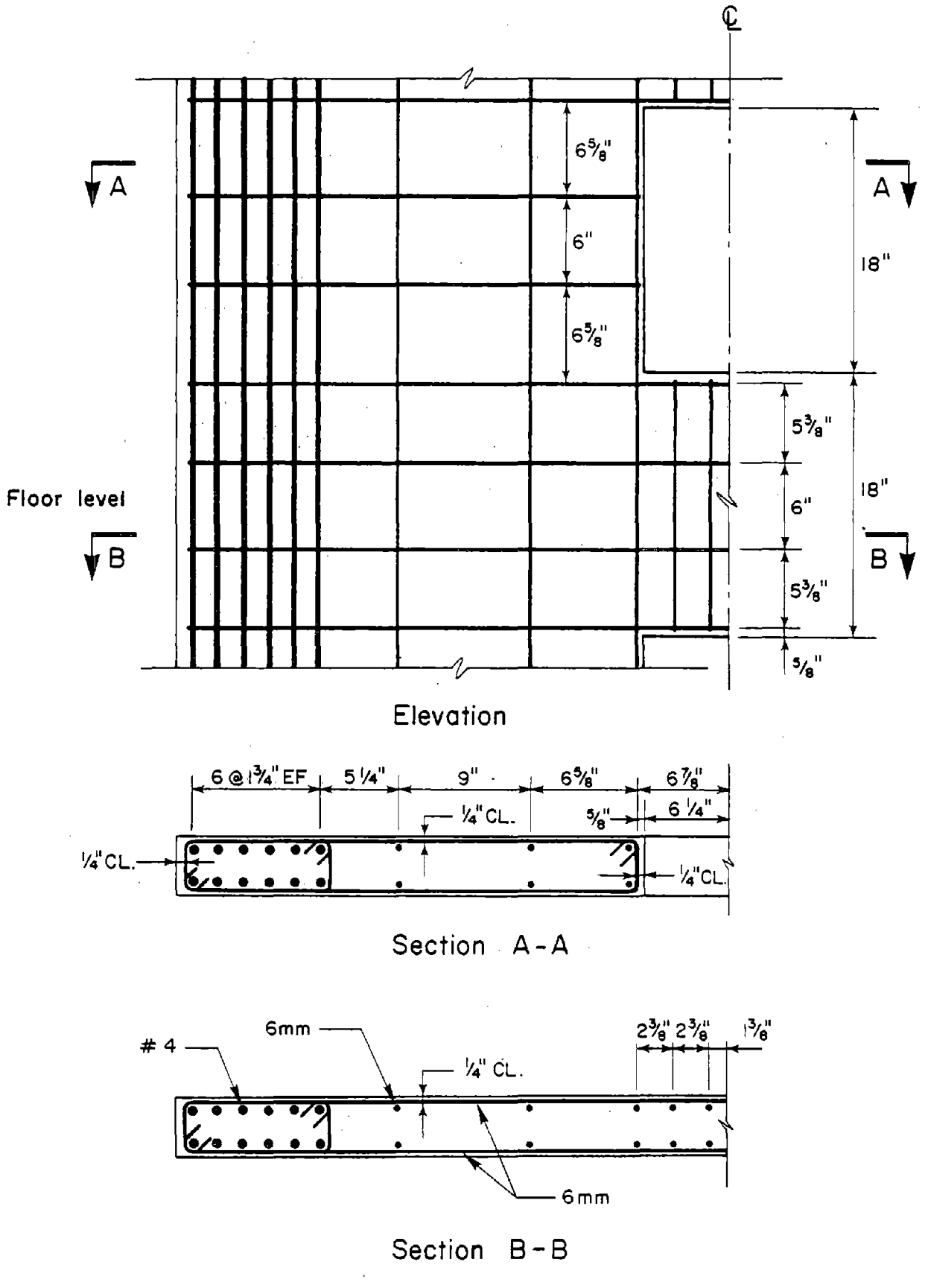

Fig. 5 Reinforcement Details Around Openings in Specimen PW-1

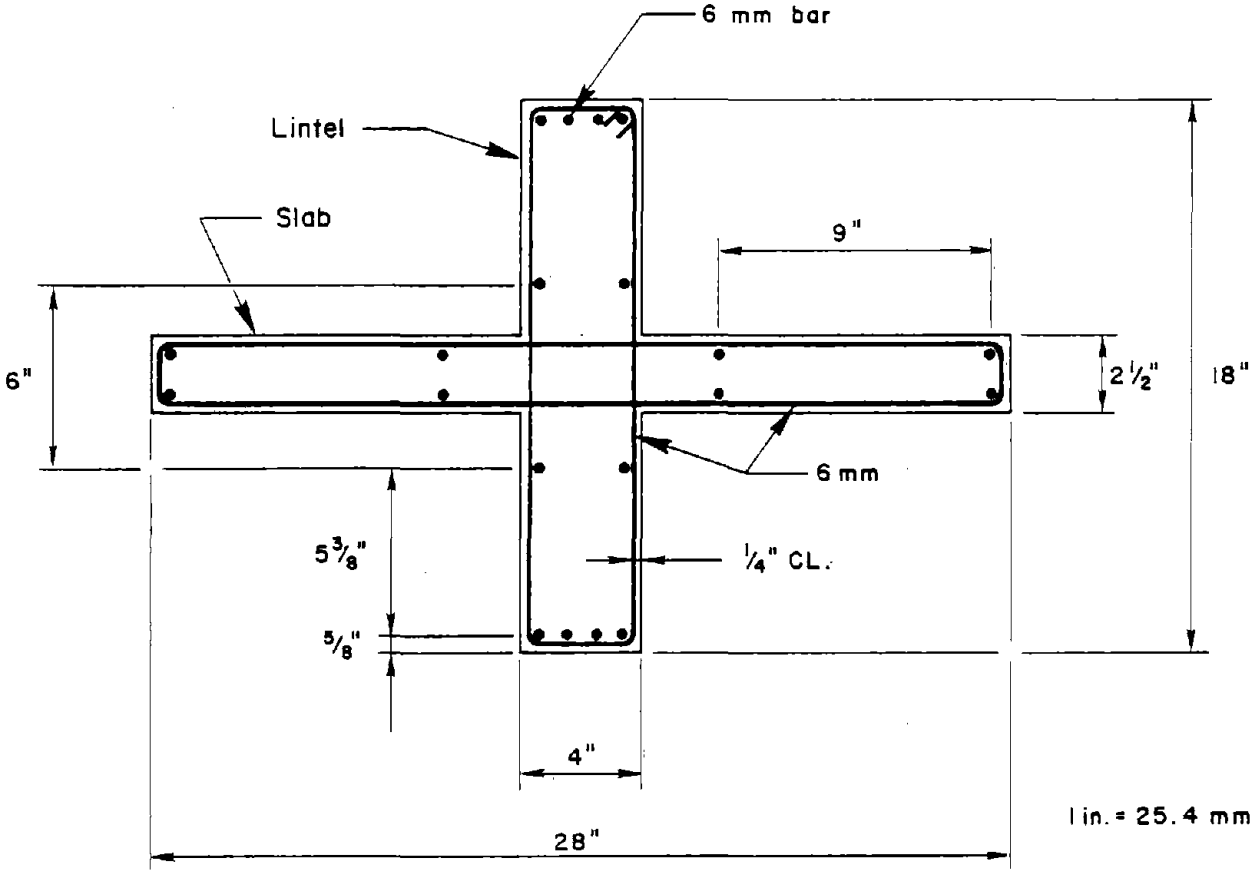

Cross Section of Lintel

Fig. 6 Reinforcement Details of Lintels for Specimen PW-1

Measured material properties for both specimens are given in Tables 1 and 2. Design of reinforcement details for both specimens is presented in Appendix A.

Test Setup

A photograph of the test setup for Specimens CI-1 and PW-1 is shown in Fig. 7. Specimens were located between two pairs of reaction walls. Specimens were post-tensioned to the laboratory floor.

To increase lateral stability, external frames were used to guide in-plane movements of the wall specimens. The frames were located on both sides of each wall specimen as shown in Fig. 7.

The following is a brief description of the loading system and instrumentation used for the two tests. Detailed description of the test setup is given in Appendix A.

Loading System

Specimens were loaded as vertical cantilevers using pulling forces applied through the top slab. Forces were exerted by double acting hydraulic rams located on both sides of the specimen. Pulling loads were applied to minimize out-of-plane movements.

Two loading boxes were attached to each side of the top slab. These boxes provided a pinned connection to loading rods. This ensured that loads were maintained horizontal throughout testing.

TABLE 1 - MEASURED CONCRETE PROPERTIES

Specimen	f'_c (psi)	f_t (psi)	E_c (ksi)
CI-1	3375	480	3385
PW-1	3030	430	2815

f'_c = compressive strength of concrete
f_t = splitting tensile strength of concrete
E_c = Modulus of elasticity of concrete
Metric Equivalents:
1 ksi = 1000 psi = 6.895 MPa

TABLE 2 - MEASURED STEEL PROPERTIES

Specimen	Reinforcing Steel	f_y (ksi)	f_{su} (ksi)	E_s (ksi x 10^3)
CI-1	No. 4 bar 6 mm bar D-3 wire	69.1 68.6 70.8	110.5 94.3 81.9	26.1 29.5 27.7
PW-1	No. 4 bar 6 mm bar D-3 wire	60.4 67.0 78.0	110.0 90.5 87.7	24.0 35.0 28.5

f_y = yield strength of reinforcing steel
f_{su} = ultimate strength of reinforcing steel
E_s = modulus of elasticity of reinforcing steel
Metric Equivalents:
1 ksi = 6.895 MPa

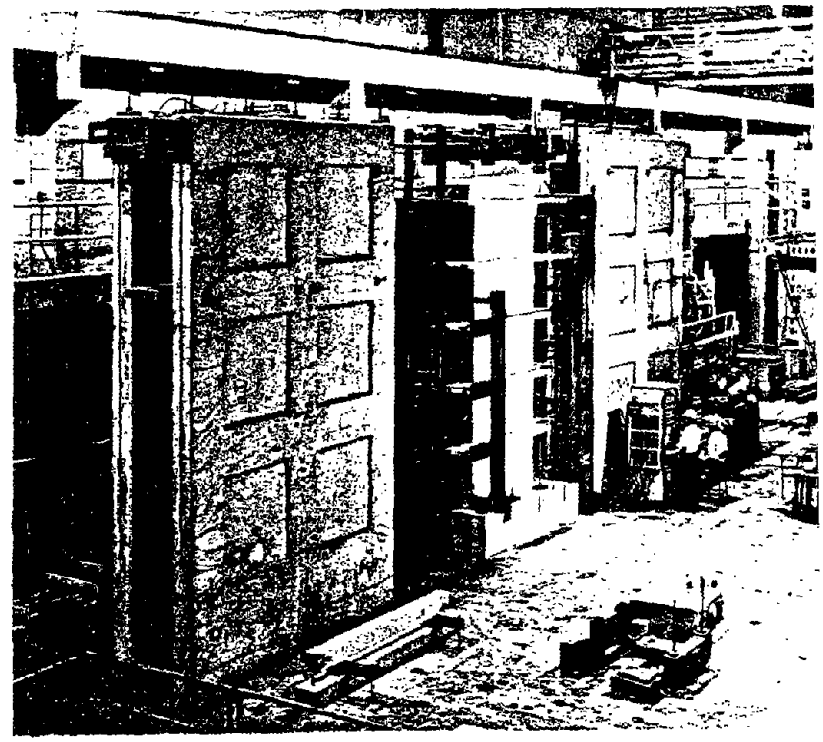

Fig. 7 Test Setup

Instrumentation

Specimens were instrumented both externally and internally. External gages measured applied loads, deflections, rotations, and shear distortions. Approximately 150 electrical resistance strain gages were placed at selected locations to measure reinforcement strains.

Test Procedure

Specimens CI-1 and PW-1 were subjected to similar load histories as shown in Fig. 8. Load histories were derived from a dynamic response analysis of a 6-story prototype structure using a modified DRAIN 2-D computer program.[16] Two actual earthquake records were used as input ground motion. They were the East-West Component of the 1940 El Centro Earthquake record, and the 16° South component of the 1971 Pacoima Dam Earthquake record. Detailed description and development of the load histories is presented in Appendix A.

Load histories were divided into three phases. The first two phases represented two severe earthquakes. Each phase consisted of ten complete reversing load cycles. Five cycles in each phase were beyond the elastic load level. For the initial cycle, rotational ductility over the lower 6 ft (1.83 m) was chosen as the control parameter. Subsequent load cycles were controlled by deflection.

After the first two phases of loading were applied, additional reversals were applied incrementally in series of three cycles. Testing was continued until significant loss of load

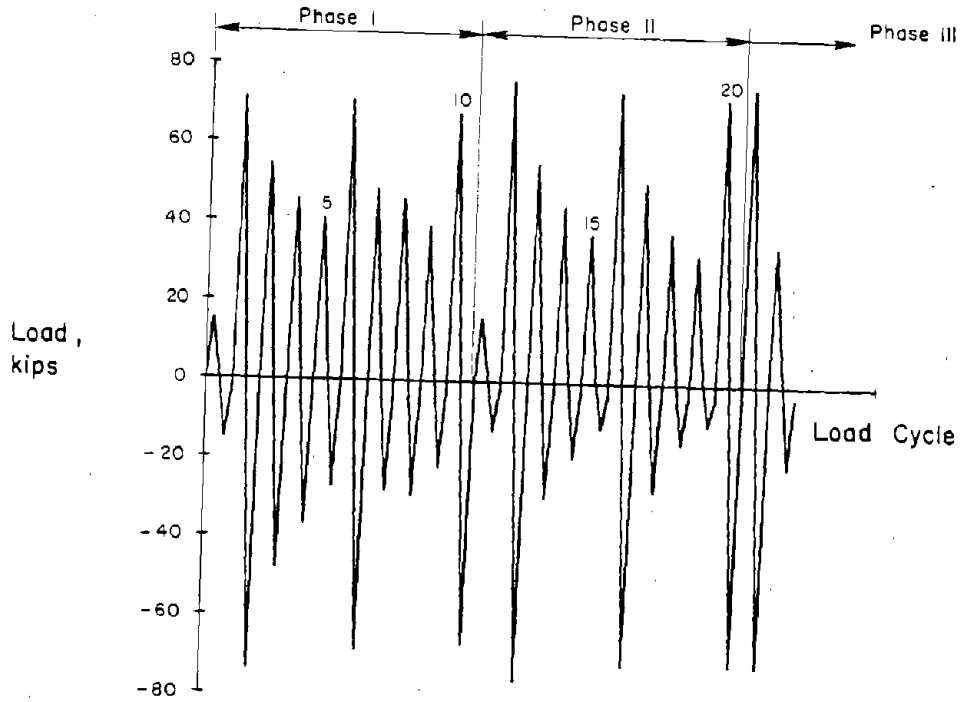

a) Specimen CI-1

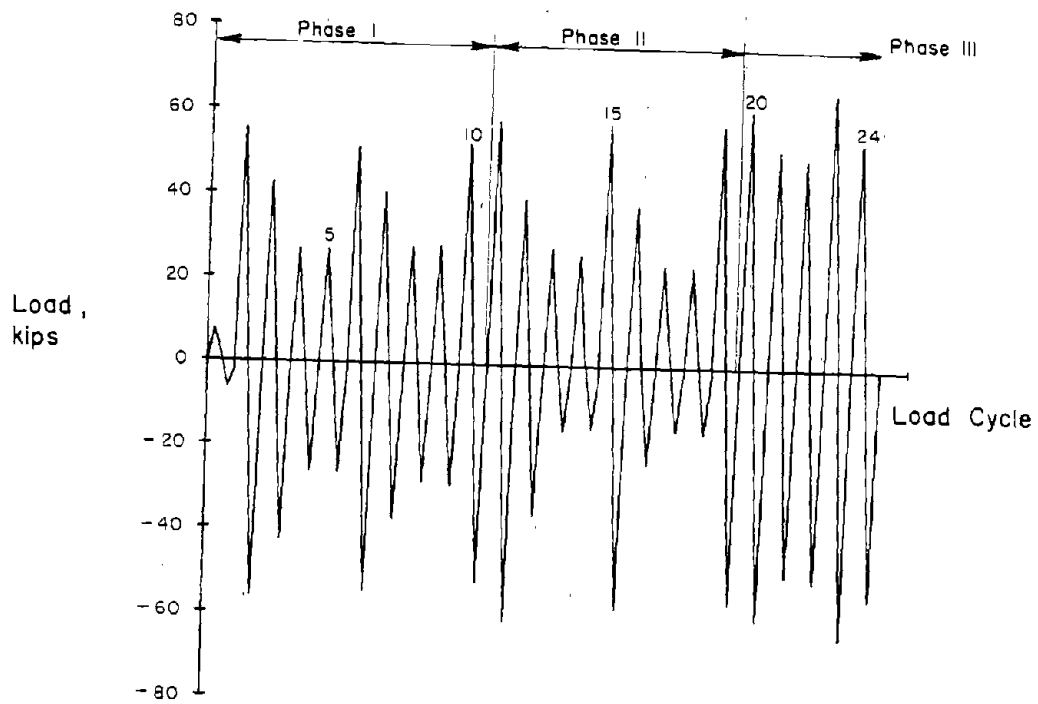

b) Specimen PW-1

Fig. 8 Load Histories

capacity was observed or unrealistically large deformations were encountered.

SUMMARY OF TEST RESULTS

Response of structural walls with and without openings to cyclic load reversals is described in this section.

Observed Behavior

Crack patterns, cyclic load versus top deflection relationships, and modes of behavior are discussed in this section. Principal experimental results are listed in Table 3.

Specimen CI-1

Specimen CI-1 was subjected to a total of 22 load cycles. Cyclic load versus top deflection relationship for Specimen CI-1 is shown in Fig. 9.

During Phase I loading, first cracking was observed at an applied load of 15.1 kips (67.2 kN). Diagonal cracks extended across the web of the wall. Primary cracking was limited to the first two stories. Several horizontal cracks were also noted at the first story level. As load reversals continued, horizontal cracks linked together to extend across the entire width of the wall. In particular, a major horizontal crack developed at 1.5 ft (0.46 m) above the base of the wall. As loads were reversed, sliding along this crack was observed. Crack pattern at the end of Phase I loading is shown in Fig. 10.

Yielding of the wall occurred at an applied load of 62.4 kips (278 kN) and a top deflection of 1.45 in. (37 mm). With

TABLE 3 - PRINCIPAL TEST RESULTS

Specimen	Yield Load (kips)	Yield Deflection (in.)	Maximum Load (kips)	Maximum Rotational Ductility Over Lower 6 ft
CI-1	62.4	1.45	76.1	5.6
PW-1	57.0	1.50	65.7	5.6

Metric Equivalent:

1 in. = 25.4 mm
1 kip = 4.45 kN

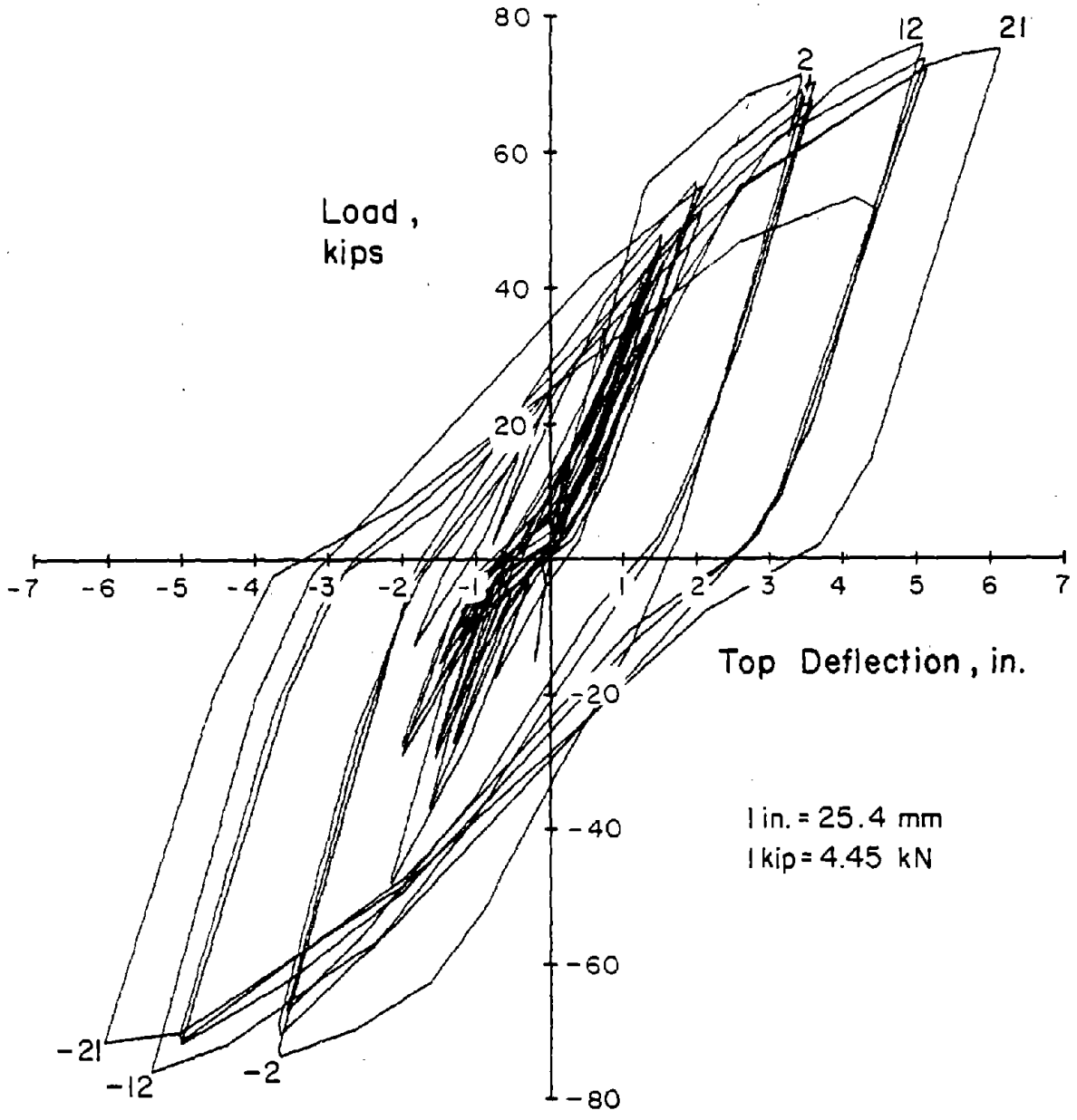

Fig. 9 Load versus Top Deflection Relationship for Specimen CI-1

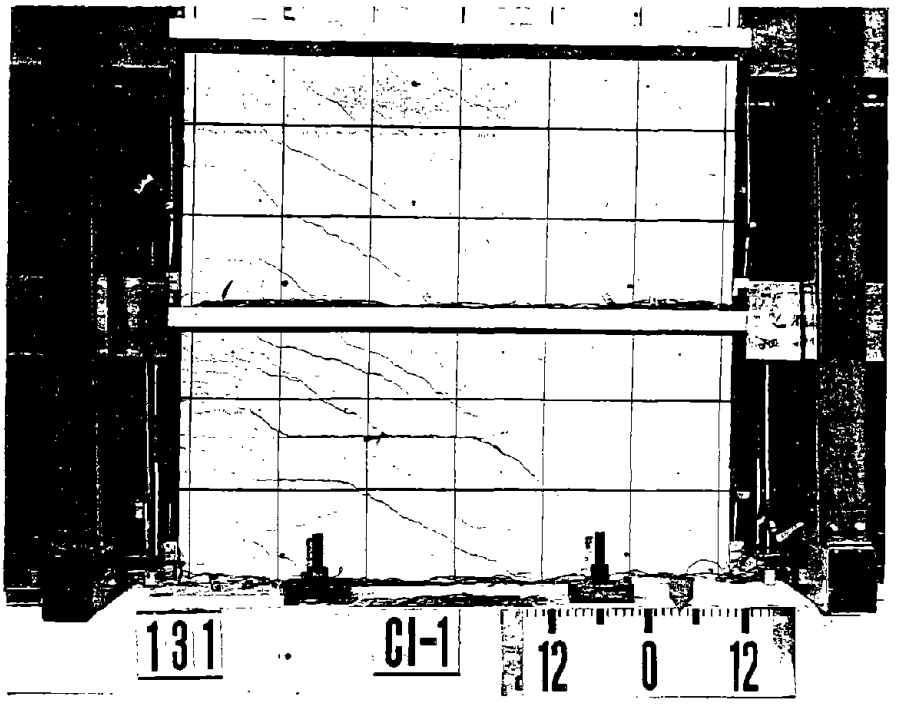

Fig. 10 Crack Pattern of Specimen CI-1 at End of Phase I

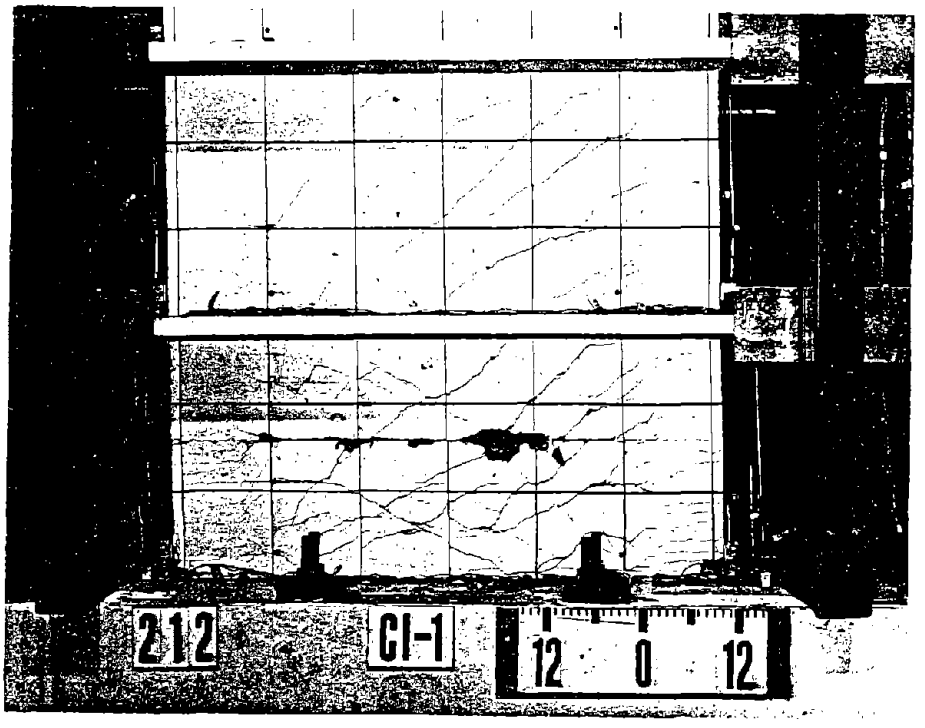

Fig. 11 Crack Pattern of Specimen CI-1 at End of Phase II

increasing numbers of load reversals, degradation of the shear resisting mechanism was observed across the major horizontal crack in the first story. Grinding and crushing of concrete along the horizontal crack was noted at the end of Phase II loading as can be seen in Fig. 11. Sliding along this crack accounted for 13% of the top deflection during Load Cycle 20. However, no major signs of distress or loss of load capacity were observed by the end of Phase II loading. The specimen was able to carry a maximum applied load of 76.1 kips (339 kN) at a top deflection of 5 in. (127 mm). This load corresponds to a nominal shear stress of $4.63\sqrt{f'_c}$ psi ($0.38\sqrt{f'_c}$ MPa).

During Phase III loading, a top deflection of 6 in. (152 mm) was imposed on the specimen. At this stage, resistance to sliding across the horizontal crack at mid-height of the first story was primarily provided by dowel action of the boundary elements. During Load Cycle 22, slip across the horizontal crack in the first story accounted for 21% of the top deflection. During the second half of Load Cycle 22, severe distress in the boundary elements at the height of the horizontal crack developed. Load carrying capacity of the specimen dropped to 34.7 kips (154 kN) and the test was terminated. This mode of failure is called "sliding shear." The specimen after testing is shown in Fig. 12.

Specimen PW-1

Specimen PW-1 was subjected to a total of 23 load cycles. Cyclic load versus top deflection relationship for Specimen PW-1 is shown in Fig. 13.

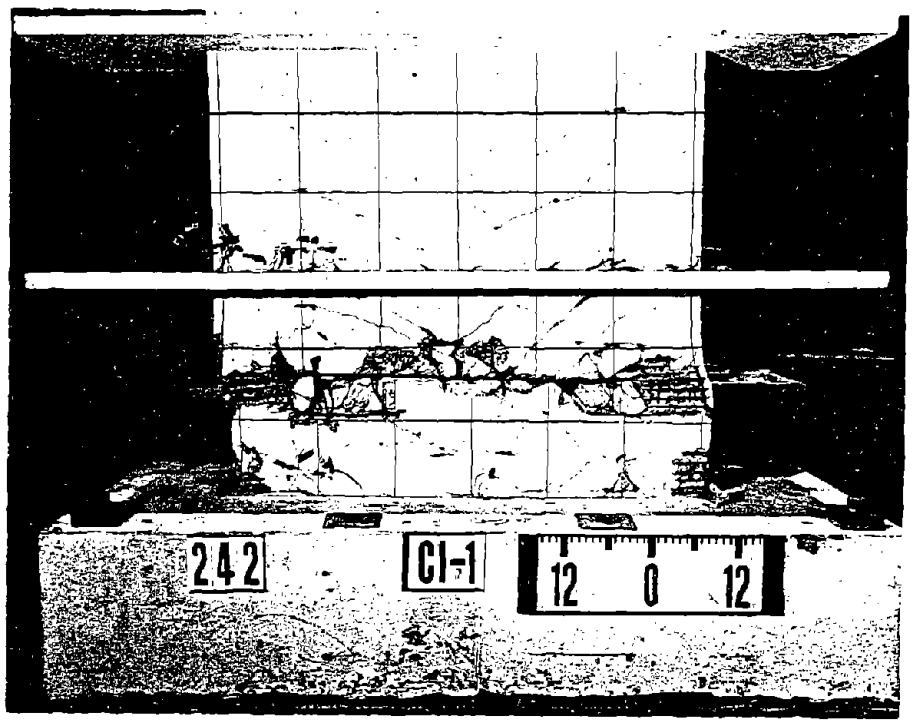

Fig. 12 Specimen CI-1 at End of Test

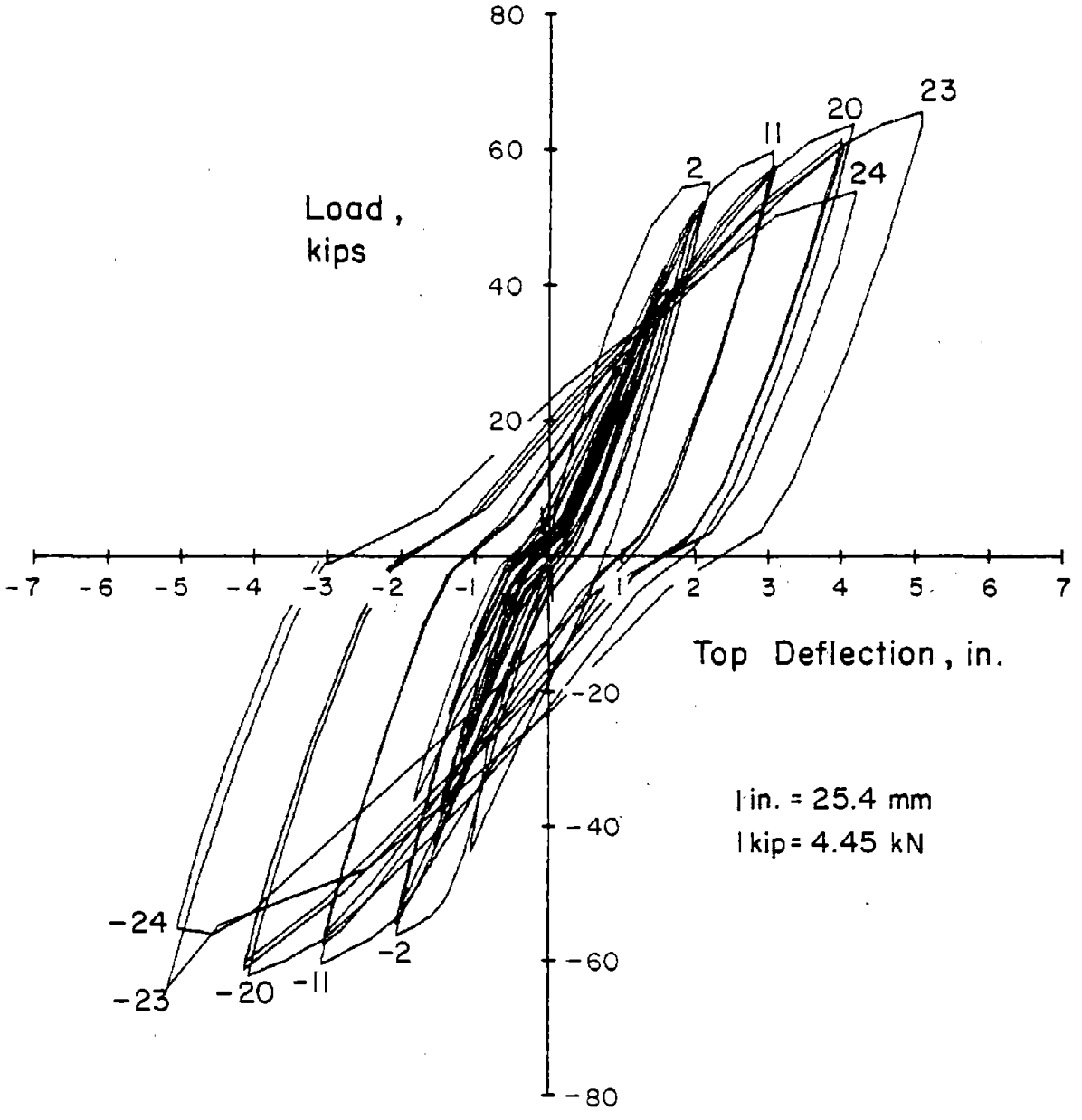

Fig. 13 Load versus Top Deflection Relationship for Specimen PW-1

First cracking of the specimen was observed at a load of 7.2 kips (32 kN). First, horizontal cracks were observed in the tension pier at the top of the first story opening. With the first reversal, diagonal cracks formed on the other side of the opening. With additional load reversals, diagonal cracks widened. Small diagonal cracks were also observed in the lintels. The cracking pattern indicated that the specimen behaved as an isolated wall. Cracks were concentrated in the lower 6 ft (1.83 m) of the wall. Yielding of the specimen occured at an applied load of 57.0 kips (254 kN) and a top deflection of 1.5 in. (38 mm). The specimen after the Phase I loading is shown in Fig. 14.

During Phase II, Specimen PW-1 reached a lateral load of 58.0 kips (258 kN) at a corresponding top deflection of 3 in. (76 mm). This load corresponded to nominal shear stress of $4.2\sqrt{f'_c}$ psi ($0.35\sqrt{f'_c}$ MPa) based on gross cross-sectional area of the piers. No significant degradation of strength was observed during Phase II loading. The cracking pattern at the end of Phase II is shown in Fig. 15.

During Phase III loading, diagonal cracks propagated into the boundary elements. Slipping and grinding of concrete along these cracks were observed. A maximum load of 65 kips (289 kN) was recorded in this phase. This load corresponds to a nominal shear stress of $4.75\sqrt{f'_c}$ psi ($0.40\sqrt{f'_c}$ MPa) in the piers. In the first half of Load Cycle 24, Specimen PW-1 lost its load carrying capacity by a shear-compression failure in the boundary

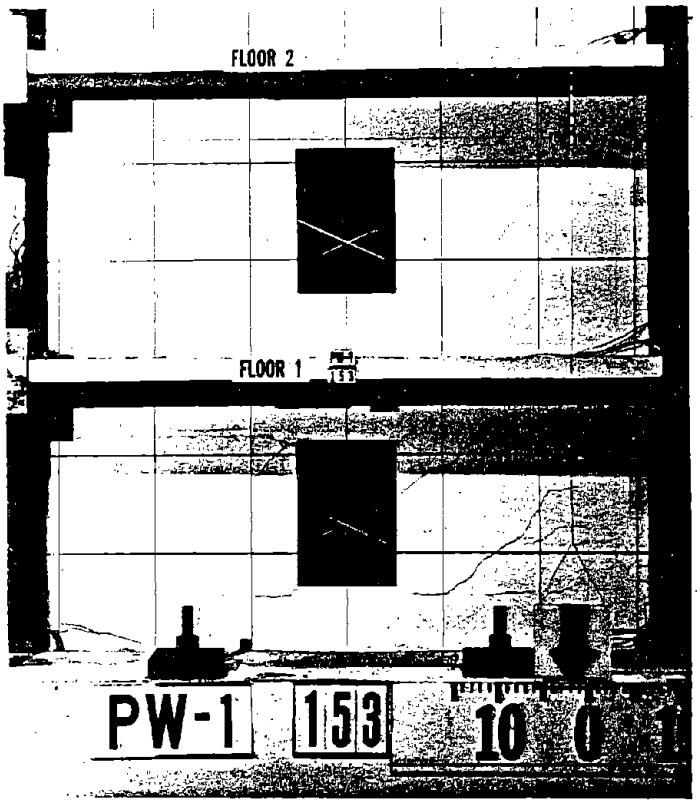

Fig. 14 Crack Pattern of Specimen PW-1 at End of Phase I

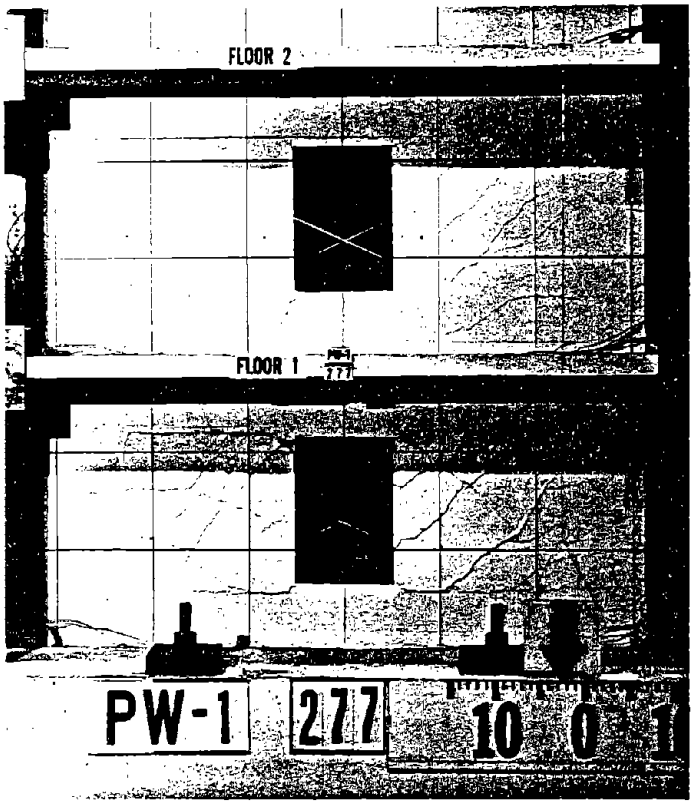

Fig. 15 Crack Pattern of Specimen PW-1 at End of Phase II

element. A photograph of the specimen at the end of the test is shown in Fig. 16.

Presence of openings interrupted formation of diagonal compression struts early in the test. This reduced the effective shear resistance offered by the wall web. The primary shear resisting mechanism at the end of the test was provided by the boundary elements.

Deformation Characteristics

A maximum top deflection of 6.2 in. (157 mm) was measured in Specimen CI-1. This deflection corresponds to 2.9% of the specimen height. The maximum top deflection in Specimen PW-1 was 5.2 in. (132 mm), which corresponds to 2.4% of the specimen height. Principal test results are listed in Table 3.

Lateral load versus rotation of the first story is shown in Fig. 17 for Specimens CI-1 and PW-1. Both specimens had similar load versus rotation relationships. Maximum rotation observed in Specimen CI-1 was noticably larger than that observed in Specimen PW-1. Initial rotational stiffness of Specimen CI-1 was slightly greater than Specimen PW-1.

Lateral load versus first story shear distortion is shown in Fig. 18. Both specimens underwent a maximum shear distortion of 0.04 rad. Initial shear stiffness of Specimen CI-1 was greater than Specimen PW-1. Pinching of load versus shear distortion curves was observed in both tests. This indicates the presence of sliding shear along horizontal cracks during load reversals.

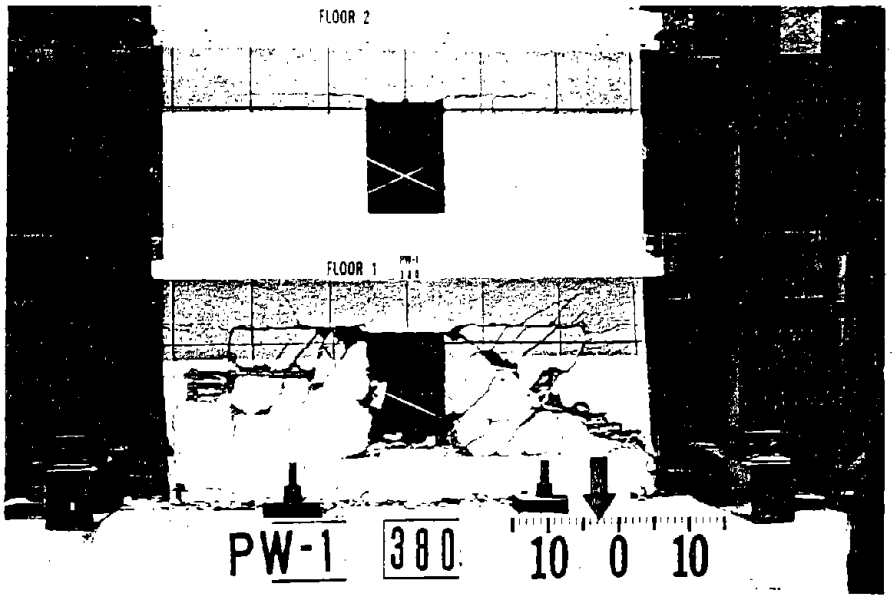

Fig. 16 Specimen PW-1 at End of Test

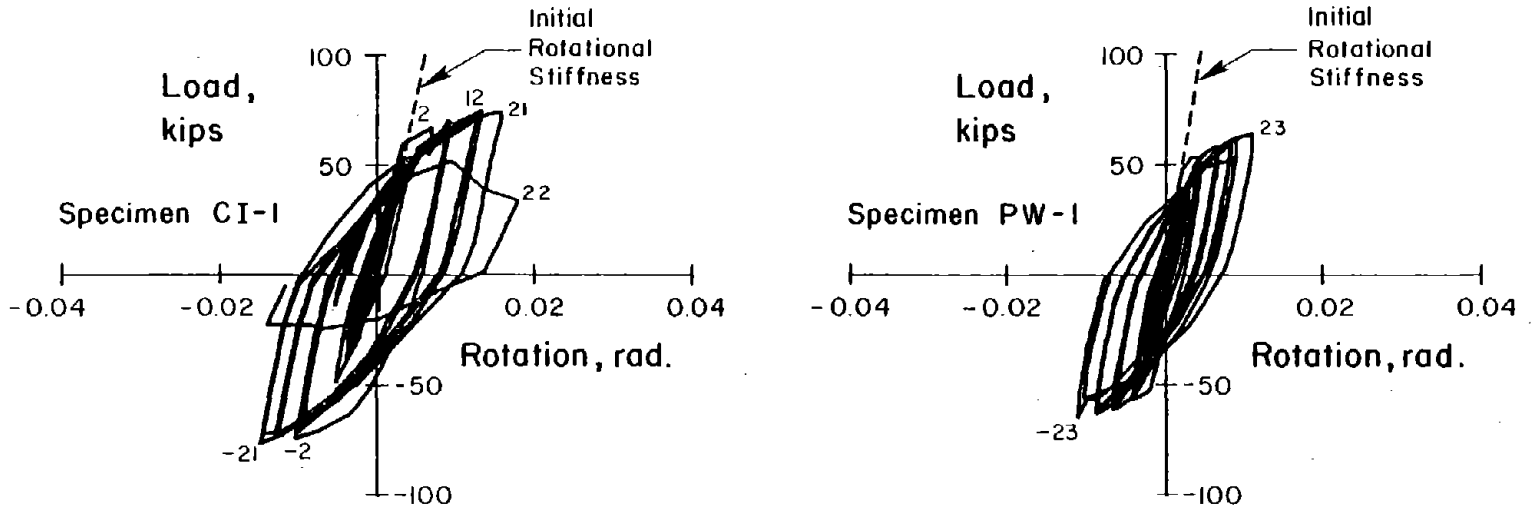

Fig. 17 Load versus First Story Rotation Relationships

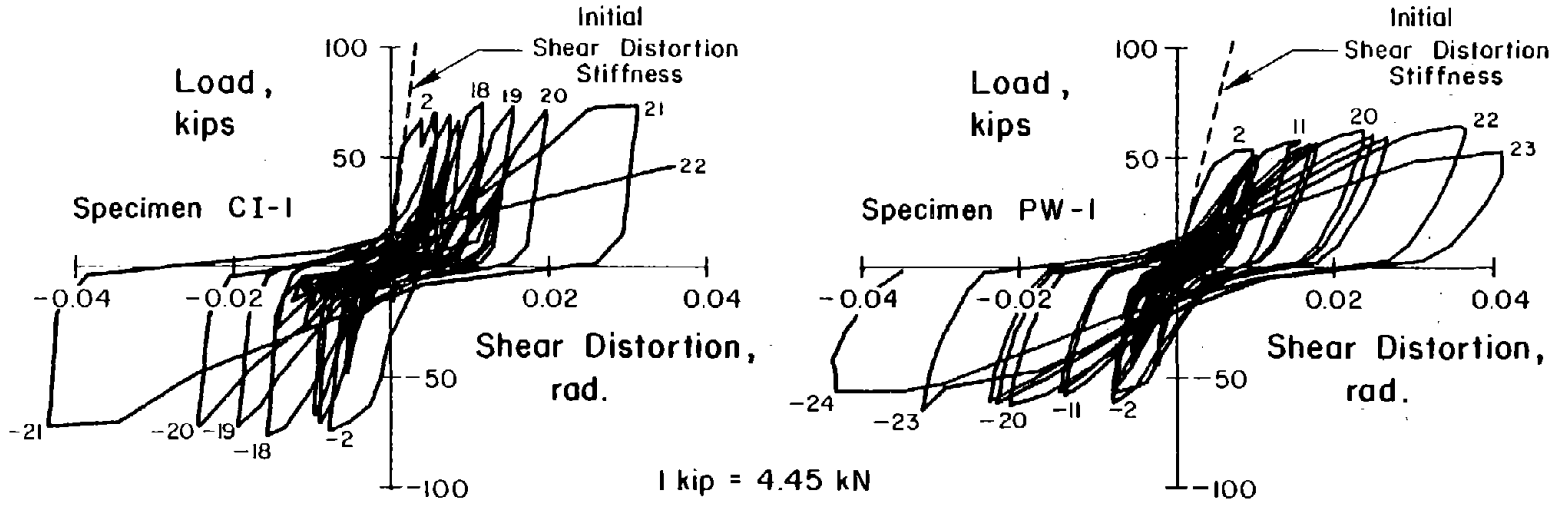

Fig. 18 Load versus First Story Shear Distortion Relationships

COMPARISON OF TEST RESULTS

To evaluate effects of openings on behavior of structural walls, comparisons between the two wall specimens were made. Load capacities, deformation characteristics, and energy dissipation characteristics were compared.

Strength and Deformation Comparisons

Positive load versus top deflection envelopes are presented in Fig. 19. Specimen CI-1 carried 14% more load than Specimen PW-1. However, there were differences in material properties between the two specimens. In particular, yield strength of the primary reinforcing steel (No. 4 bars) was different in the two specimens.

Envelopes of load ratio versus top deflection ductility ratio are presented in Fig. 20. Similar envelopes for first story deflection and rotation ductility are shown in Fig. 21. Load ratio is defined as applied load divided by the yield load of the specimen. Similarly, deflection ductility ratio and rotation ductility ratio are defined as specimen deflection or rotation divided by the corresponding deformation at yield.

When the data are normalized by yield capacities, both specimens exhibited similar behavior as shown in Figs. 20 and 21. These data indicate that presence of openings had little effect on load versus deformation characteristics of the specimens.

To further evaluate deformation characteristics, contributions of rotation and shear distortion to total deflection were estimated.

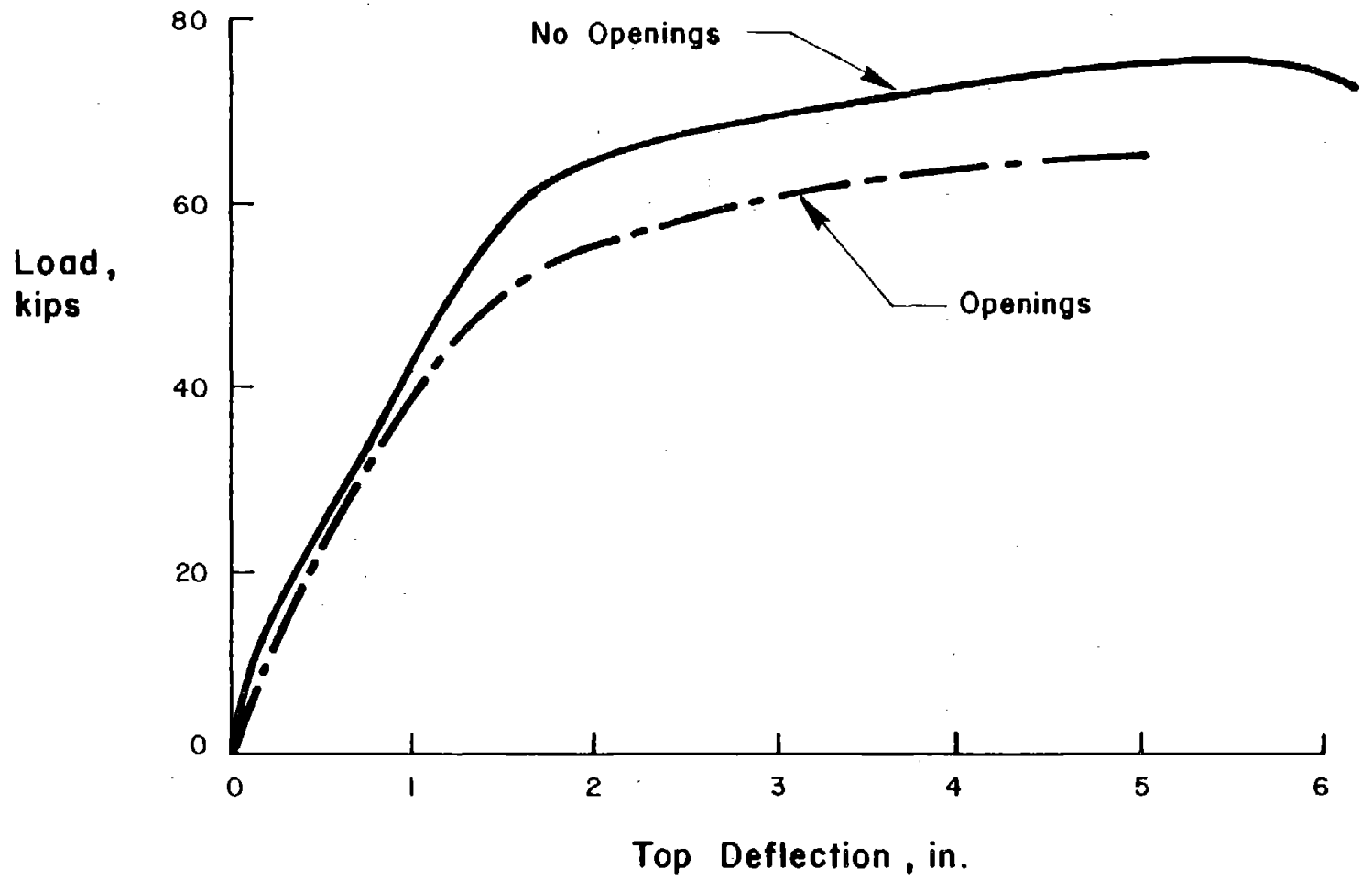

Fig. 19 Positive Load versus Top Deflection Envelopes

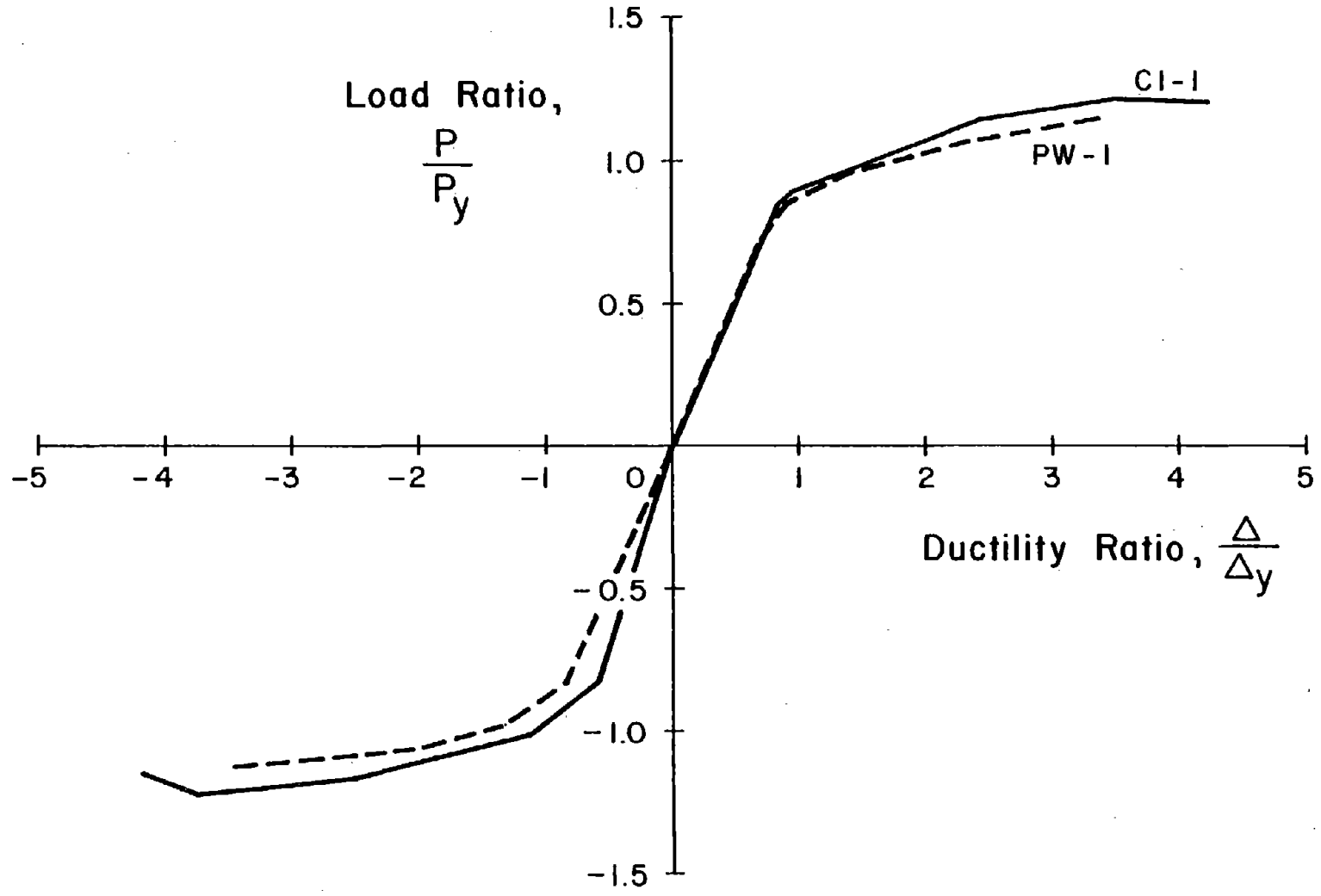

Fig. 20 Load Ratio versus Top Delfection Ductility Ratio Envelopes

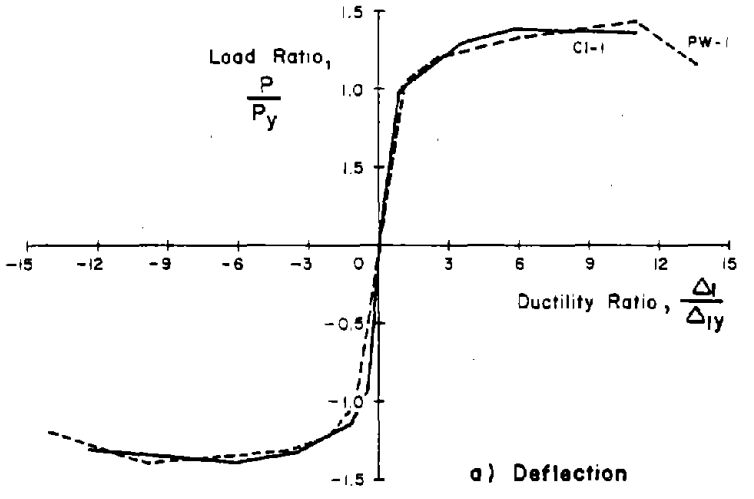

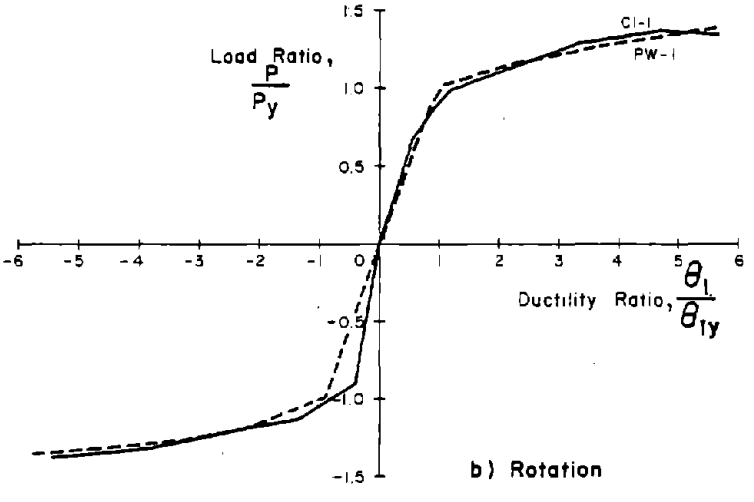

Fig. 21 Load versus First Story Deformation Envelopes

Deflection components at the end of Phase III loading are presented for Specimen CI-1 in Fig. 22a. Total deflection of the specimen at the 3-ft (0.91 m), 6-ft (1.83 m) and top levels were separated into components attributed to flexural rotation and shear distortion. The deflection components were calculated from measured rotation and shear distortion data obtained during the test. The sum of the rotation and shear components show excellent agreement with measured deflection data. Dashed lines are extrapolations of measured data.

Deflection components for Specimen PW-1 at the end of Phase III are presented in Fig. 22b. Unfortunately, instrumentation for measuring first story shear distortion malfunctioned during testing. Without measured shear distortions, shear deflection components were taken as the difference between the total deflection and the calculated rotation component. Assuming that actual deflection components for Specimen PW-1 agreed with the total deflection as they did for Specimen CI-1, this estimation of the shear deflection component is reasonable.

Deflection profiles of both wall specimens, as shown in Fig. 22 by solid lines, were found to be very similar. Deflection within the lower 6 ft (1.83 m) of the walls was primarily attributed to shear deformations. Above the 6-ft (1.83 m) level, shear distortion remained relatively constant and rotational deformations increased. Large shear distortions observed at the 3-ft (0.92 m) level indicated that shear was significant in the behavior of both specimens. The presence of the openings had little effect on the relative magnitudes of deflection components.

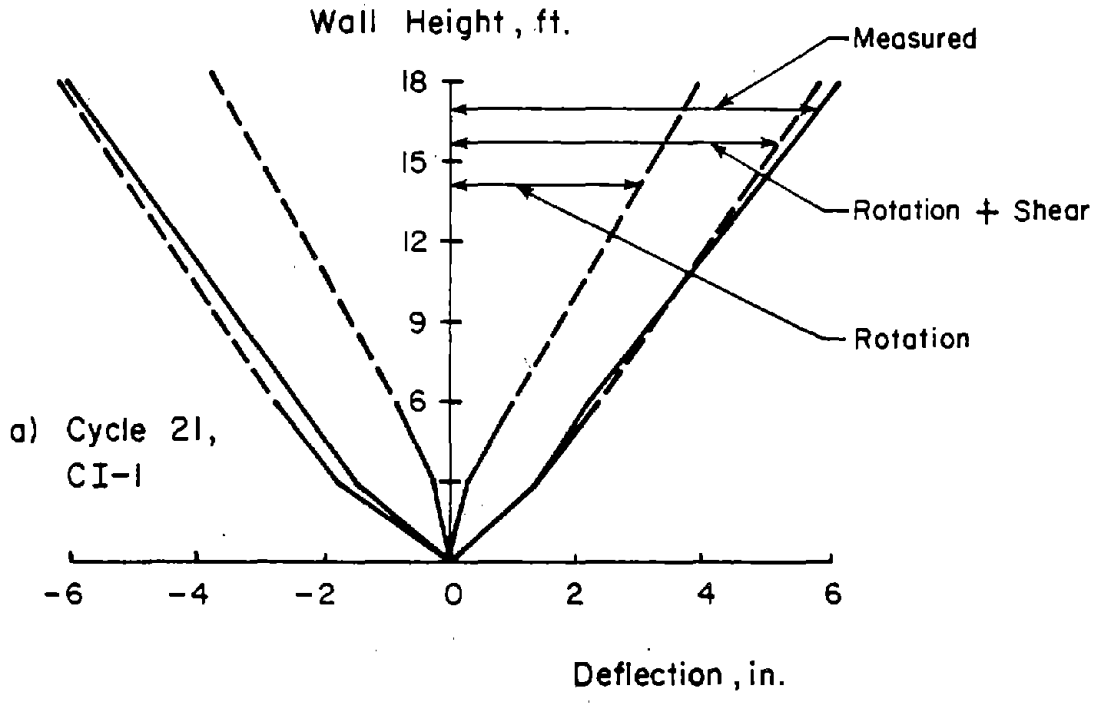

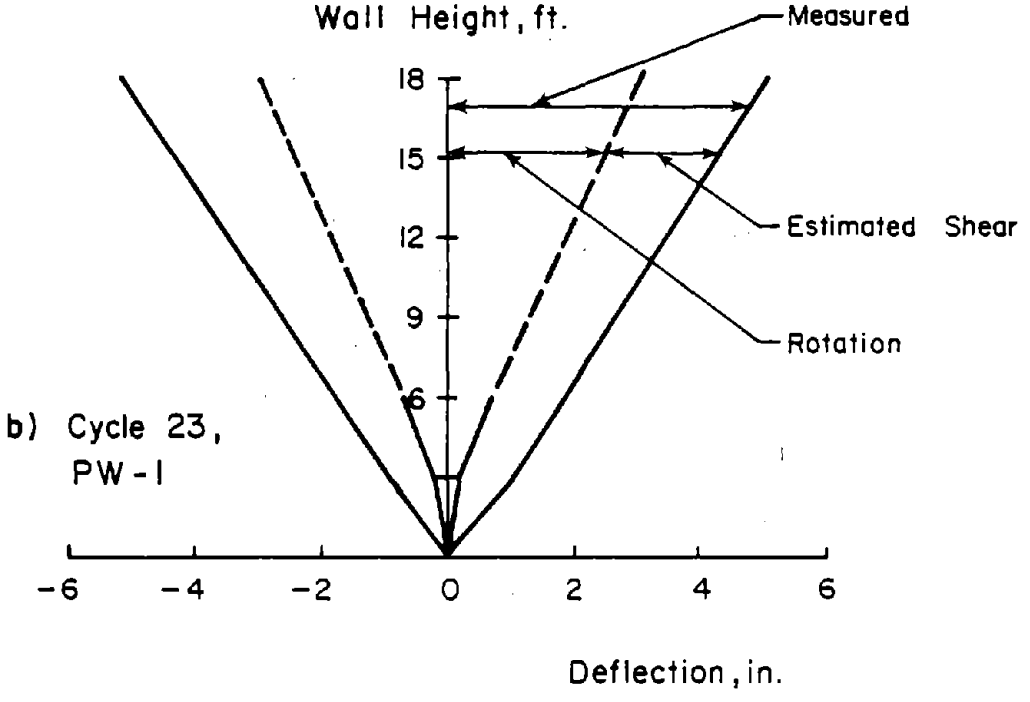

Fig. 22 Deflection Components

Energy dissipated by the specimen during a load cycle is defined as the area enclosed within the load-deflection hysteresis loop. As a means of comparing energy dissipation capacity, the ratio of dissipated energy to linear energy capacity was used. This energy ratio is defined in Fig. 23. Relationships of energy ratio versus top deflection ductility ratio are also presented in Fig. 23. The figure shows that both walls exhibited similar energy dissipation characteristics. That is, relative areas within hysteresis loops at a given ductility ratio were similar for both specimens.

Effect of Openings on Wall Behavior

Both specimens were subjected to moderately low maximum nominal shear stresses of approximately 4.7 $\sqrt{f'_c}$ psi (0.39 $\sqrt{f'_c}$ MPa). With initial inelastic load reversals, specimen behavior was characterized by the formation of horizontal cracks in the lower 3 ft (0.91 m) of the wall. At this stage, presence of openings did not alter response of Specimen PW-1.

With increasing nominal shear stresses the effect of openings on cracking became more evident. Diagonal cracks formed in Specimen C1-1 as increasing inelastic load cycles were applied. Much of the load was observed to be resisted by diagonal compression struts. Sliding was also observed along horizontal cracks in the wall web. With repeated grinding and sliding, shear resistance across horizontal cracks deteriorated rapidly. By the end of the test, the primary shear resisting

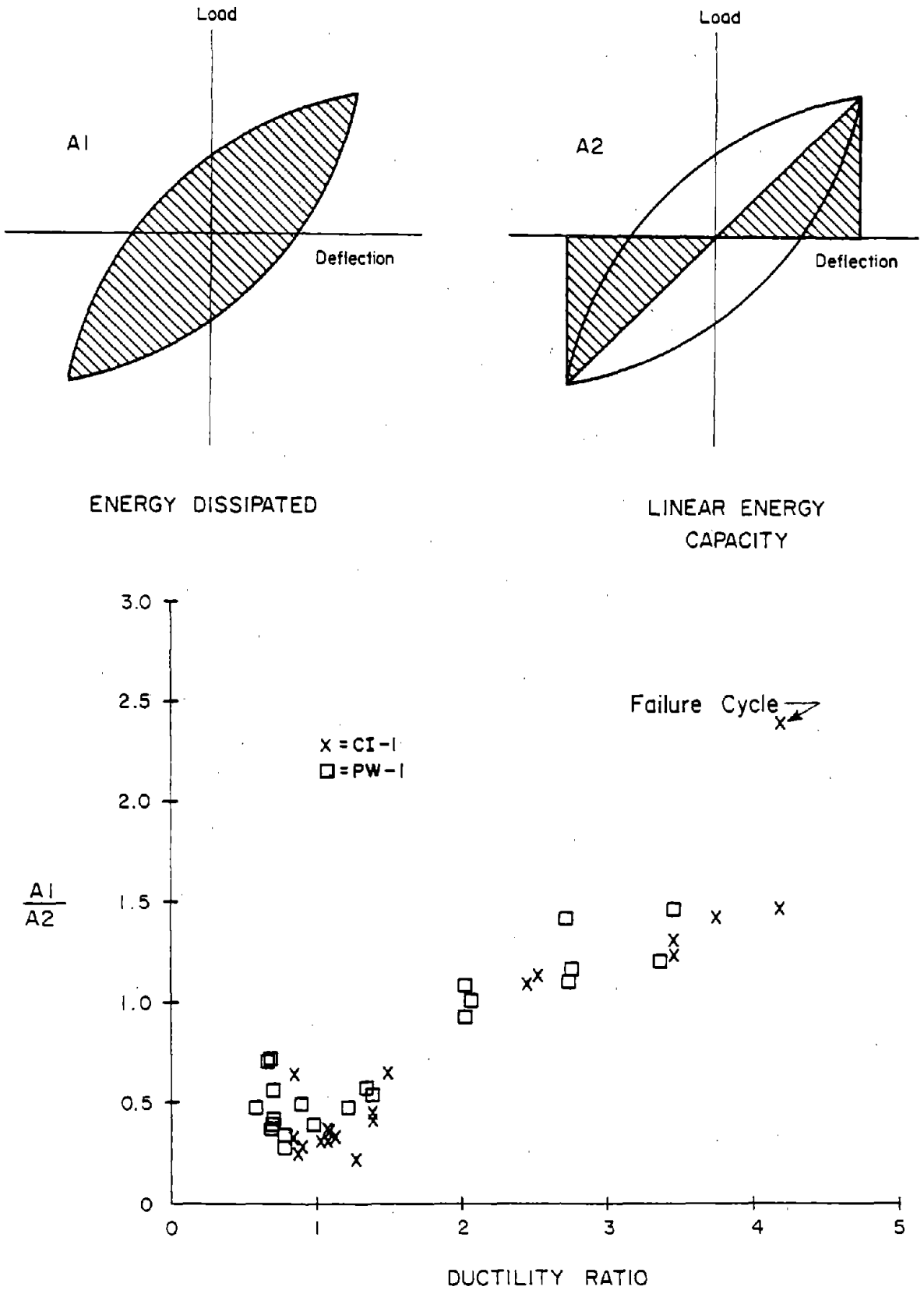

Fig. 23 Ratio of Dissipated Energy to Linear Energy Capacity versus Top Deflection Ductility Ratio

mechanism was provided by dowel action of the boundary elements.

Openings in Specimen PW-1 separated the wall web area into two independent piers coupled by lintels. Formation of diagonal compression struts across wall web was interrupted by openings. Therefore, shear resistance offered by the wall web was reduced. This explains why the initial shear stiffness was larger in Specimen CI-1 than in Specimen PW-1.

In spite of observed behavioral differences, the two specimens exhibited similar load, deformation, and energy dissipation characteristics.

Design Considerations

Based on test results presented in this report, the following should be considered in the design of structural walls pierced with openings.

1. Pierced walls should be designed to function as isolated walls without openings.
2. Flexural and shear capacity of lintels should be designed to ensure full coupling between wall piers. Lintels should not yield before yielding of wall piers.
3. Reinforcement interrupted by openings should be distributed in equal amounts to the sides of openings.

It has been suggested that drift control, or control of overall lateral displacements, should be emphasized in seismic design.[17,18] For proper selection of an earthquake resisting system, consideration of limits on interstory drifts as

well as deformation capacity of the structure are necessary. Interstory drift limits provide a means of controlling overall stability and damage. Interstory drift limits implied by UBC[15] and ATC 3-06[19] provisions are 1 to 2%. These limits correspond to values acceptable to many designers for stability and damage control.[17,18]

Specimens CI-1 and PW-1 had maximum recorded top deflections of 5.2 and 6.2 in., respectively. This is equivalent to interstory drifts of nearly than 3%. Using 2% drift as a design criterion, Specimens CI-1 and PW-1 exhibited a reserve of deformation capacity.

CONCLUSIONS

Major conclusions are summarized in FINDINGS AND CONCLUSIONS at the beginning of this report.

ACKNOWLEDGEMENTS

This investigation was part of a combined experimental and analytical research program on earthquake resistant structural walls jointly sponsored by National Science Foundation under Grant Nos. ENV74-14766 and ENV77-15333, and by Construction Technology Laboratories, a division of the Portland Cement Association. Research was conducted in the Structural Development Department, Dr. H.G. Russell, Director.

Fabrication and testing of specimens was completed in the Structural Laboratory under the supervision of R. K. Richter, Laboratory Foreman. Lead technicians on construction and instrumentation were P. P. Hordorwich, Senior Technician, and W. J. Hummerich, Jr., Assistant Foreman. Their efforts for making the experimental program a success are appreciated.

Helpful advice and suggestions were thankfully accepted throughout the program from M. Fintel, Director, Advanced Engineering Services. His contributions to the project are appreciated.

Any opinions, findings and conclusions being expressed in this report are based solely on the reported experimental results and are those of the authors. They do not necessarily reflect the views of the National Science Foundation.

REFERENCES

1. Corley, W.G., Fintel, M., Fiorato, A.E., and Derecho, A.T., "Earthquake Engineering Research at the Portland Cement Association - A Progress Report," Proceedings of Seven World Conference on Earthquake Engineering, Ankara, Turkey, September 8-13, 1980.

2. Paulay, T. and Uzumeri, M., "A Critical Review of the Seismic Design Provisions for Ductile Shear Walls of the Canadian Code and Commentary," Canadian Journal of Civil Engineering, Vol. 2, No. 4, 1975, pp. 592-610.

3. Mahin, S.A. and Bertero, V.V., "Nonlinear Seismic Response of a Coupled Wall System," Journal of the Structural Division, ASCE, Vol. 102, No. ST9, September 1976, pp. 1759-1780.

4. Oesterle, R.G., Aristizabal-Ochoa, J.D., Fiorato, A.E., Russell, H.G., and Corley, W.G., "Earthquake Resistant Structural Walls - Tests of Isolated Walls Phase II" Report to National Science Foundation, Portland Cement Association, Skokie, Oct. 1979, 263 pp. (Available through National Technical Information Service, U.S. Department of Commerce, 5285 Port Royal Rd., Springfield, VA., 22161, No. PB271465/AS).

5. Shiu, K.N., Aristizabal-Ochoa, J.D., Barney, G.B., Fiorato, A.E., and Corley, W.G. "Earthquake Resistant Structural Walls - Coupled Wall Tests." Report to National Science Foundation, Portland Cement Association, Skokie, IL., July 1981.

6. Aristizabal-Ochoa, J.D., Shiu, K.N., and Corley, W.G. "Effects of Beam Strength and Stiffness on Coupled Wall Behavior." Proceedings, U.S. National Conference on Earthquake Engineering - 1979, Stanford, California, August 1979.

7. Paulay, T. and Santhakumar, A.R., "Ductile Behavior of Coupled Shear Walls," Journal of the Structural Division, ASCE, Vol. 102, No. ST1, Proc. Paper 11852, January 1976, pp. 93-108.

8. Benjamin, J.R., and Williams, H.A., "Behavior of One-Story Reinforced Concrete Shear Walls Containaing Openings," Journal ACI, Proc. Vol. 55, No. 5, Nov. 1958, pp. 605-618.

9. Yamada, M., Kawamura, H., and Katagihara, K., "Reinforced Concrete Shear Walls with Openings; Test and Analysis," Shear in Reinforced Concrete Publ. SP-42, ACI, Detroit, 1974, pp. 559-578.

10. Matsui, Gengo, and Ogawa, Takahisa, "Study on Methods of Arranging Openings in Box Frame Type Construction and Shearing Stress Distribution," Transactions of the Architectural Institute of Japan No. 286, December 1979, pp. 37-43.

11. Barney, G.B., Corley, W.G., Hanson, J.M., and Parmelee, R.A., "Behavior and Design of Prestressed Concrete Beams with Large Web Openings," Journal of the Prestressed Concrete Institute, Nov./Dec. 1977, pp. 32-61. (Also PCA Research and Development Bulletin RD054.01D.)

12. Seya, Y. and Matsui, Gengo, "Study of Stress and Displacement of Shear Wall with Opening," Transactions of the Architectural Institute of Japan No. 286, December 1979, pp. 45-53.

13. Mirza, M.S. "A Study of Behavior of Coupled Shear Wall Systems," Department of Civil Engineering and Applied Mechanics, McGill University, 33 pp.

14. ACI Committee 318, Building Code Requirements for Reinforced Concrete ACI Standard 318-71, American Concrete Institute, Detroit, 1971, 78 pp.

15. International Conference of Building Officials, Uniform Building Code, 1976 Edition, Whittier, California, 1976, pp. 2626.

16. Saatcioglu, M., Derecho, A.T., and Corley, W.G., "Coupled Walls in Earthquake-Resistant Buildings," Report to National Science Foundation, Portland Cement Association, Skokie, Illinois, June, 1980, 135 pp.

17. Sozen, M.A., "Review of Earthquake Response of R/C Buildings with a View to Drift Control," Proceedings of the Seventh World Conference on Earthquake Engineering, Instanbul, Turkey, Sept. 1980.

18. Oesterle, R.G., Fiorato, A.E., and Corley, W.G., "Effects of Reinforcement Details on Seismic Performance of Walls," to be published in Proceedings of Conference on Earthquake and Earthquake Engineering: The Eastern U.S., Knoxville, Tennessee, Sept., 1981.

19. Applied Technology Council "Tentative Provisions for the Development of Seismic Regulations for Buildings," ATC 3-06, National Bureau of Standards Special Publication 510, Washington, D.C., June 1978, 505 pp.

APPENDIX A - EXPERIMENTAL PROGRAM

Two tests were carried out to determine effects of openings on isolated structural walls. Specimen CI-1 was a solid wall with no openings. Speciman PW-1 was pierced with rectangular openings to represent windows at each floor level.

This appendix presents a detailed description of the test specimens, test setup, and load histories.

Test Specimens

Overall dimensions of test specimens are shown in Fig. A-1. Test specimens were a 1/3-scale representations of walls in a six-story building. Specimens were 18-ft (5.5 m) high with a horizontal length of 6 ft 3 in. (1.9 m) and a uniform wall thickness of 4 in. (106 mm). The height of each story was 3 ft (0.9 m). Floor slabs at each story level were simulated by 2.5-in. (64 mm) thick by 1 ft (0.3 m) wide stubs running full length on both sides of the walls. Slabs overhung the ends of each specimen by 2 ft (0.6 m). The top slab was 5-in. (127-mm) thick to permit transfer of loads to the specimen. The base of each specimen was attached to the test floor through a rigid foundation block. The reinforced concrete base block was 2x4x10 ft (0.6x1.2x3.1 m). The base block was stressed to the laboratory floor.

The pierced wall Specimen (PW-1) was nominally identical to the solid wall Specimen (CI-1) except for the openings. Openings in the pierced wall specimen were located at the center of the wall at every story level. They were 12.5-in. by 1-ft 6-in.

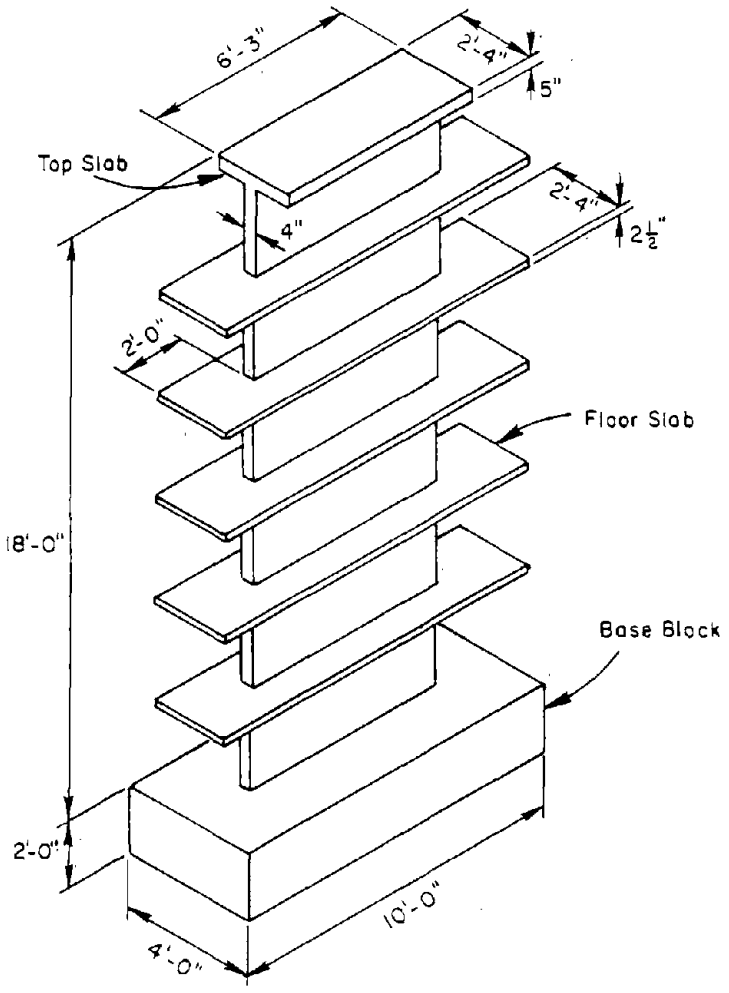

Fig. A-1 Dimensions of Wall Specimens

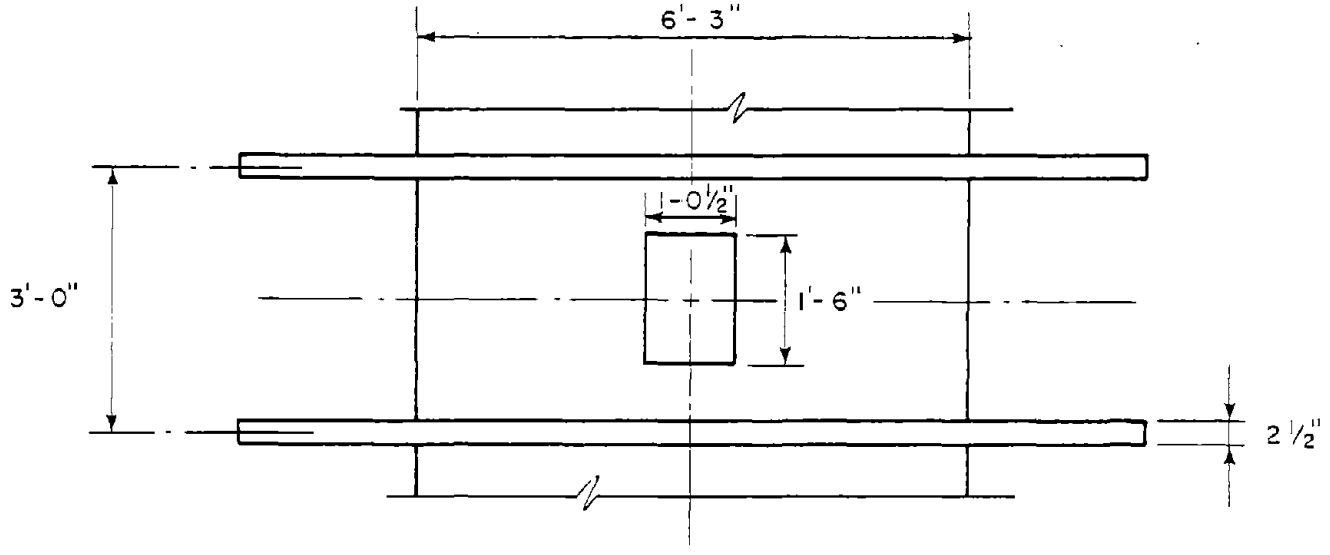

Fig. A-2 Location and Dimensions of Openings

(317 mm x 457 mm) rectangular openings simulating typical window areas. Locations and dimensions of openings in the pierced wall specimen are shown in Fig. A-2.

Design

Specimens were designed as wall elements in coupled wall systems. Wall design was made for the arbitrary prototype structure shown in Fig. A-3. Design followed provisions of the 1971 ACI Building Code.[14] The structural wall was designed to resist earthquake forces as defined by the 1976 Uniform Building Code.[15] Design was further checked by dynamic analyses using actual recorded earthquake ground motions. The prototype structure was then scaled down proportionately to obtain the wall specimens.

In the analysis, concrete was assumed to have a compressive strength of 3000 psi (20.7 MPa) and unit weight of 150 pcf (2403 kg/m^3). Live load of 40 psf (1915 Pa) was used in design calculations. Lateral design forces were determined for a box system located in Earthquake Zone 4 as defined by the 1976 Uniform Building Code.[15] Based on this analysis, reinforcement was selected according to the 1971 ACI Building Code.[14]

Flexural design for Specimen PW-1 was identical to Specimen CI-1. Lintels were designed to provide full coupling between wall piers so that the specimen would behave as an isolated wall.

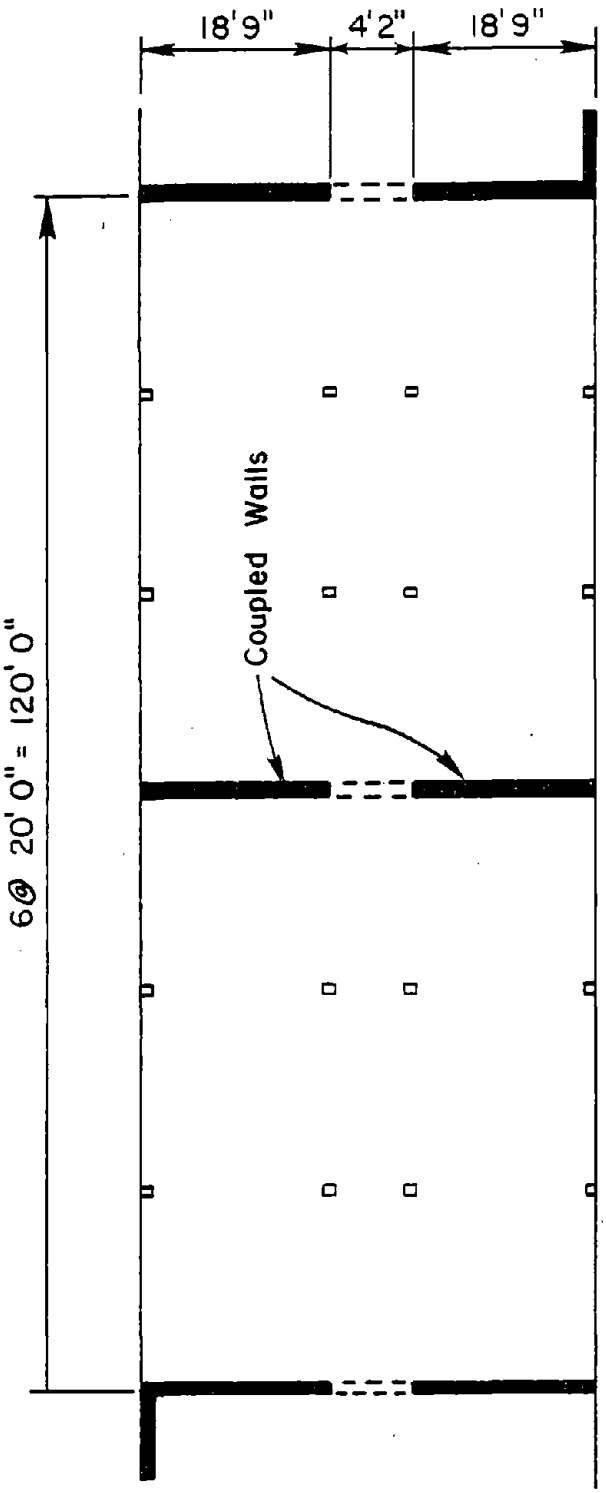

Fig. A-3 Prototype Floor Plan

Material Properties

A concrete mix design with 3/8-in. (9.5 mm) maximum size aggregate was selected for both wall specimens. The design compressive strength was 3000 psi (20.7 MPa) at 28 days. Physical properties of concrete are summarized in Table A1 for both specimens. Tests were performed according to ASTM specifications. A representative stress-strain curve for concrete in both specimens is shown in Fig. A-4.

Physical properties of steel reinforcement used in both specimens are listed in Table A2. Representative stress-strain relationships for reinforcing bars are presented in Fig. A-5.

Reinforcement Details

Reinforcement details for the wall specimens are shown in Fig. A-6. Primary flexural reinforcement was concentrated along the sides of each specimen to form boundary elements. Boundary elements consisted of 12-No. 4 bars of Grade-60 steel. Reinforcement percentage of these bars with respect to surrounding concrete area was approximately 6%. This percentage is the maximum allowed by the 1971 ACI Building Code for columns in earthquake resistant structures.

Confinement around the primary flexural reinforcement was provided by closed hoops of D-3 deformed wires. These hoops were spaced at 1-1/3 in. (34 mm) within the first two stories. Hoops were spaced at 4 in. (102 mm) above the second story level. Horizontal shear reinforcement was provided by two layers of 6 mm bars spaced at 6 in. (102 mm).

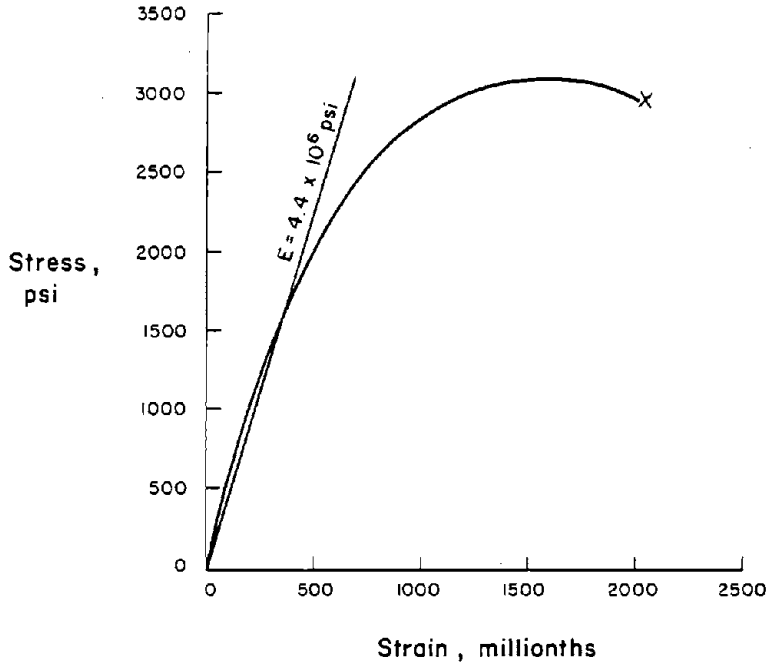

Fig. A-4 Representative Concrete Stress-Strain Curve

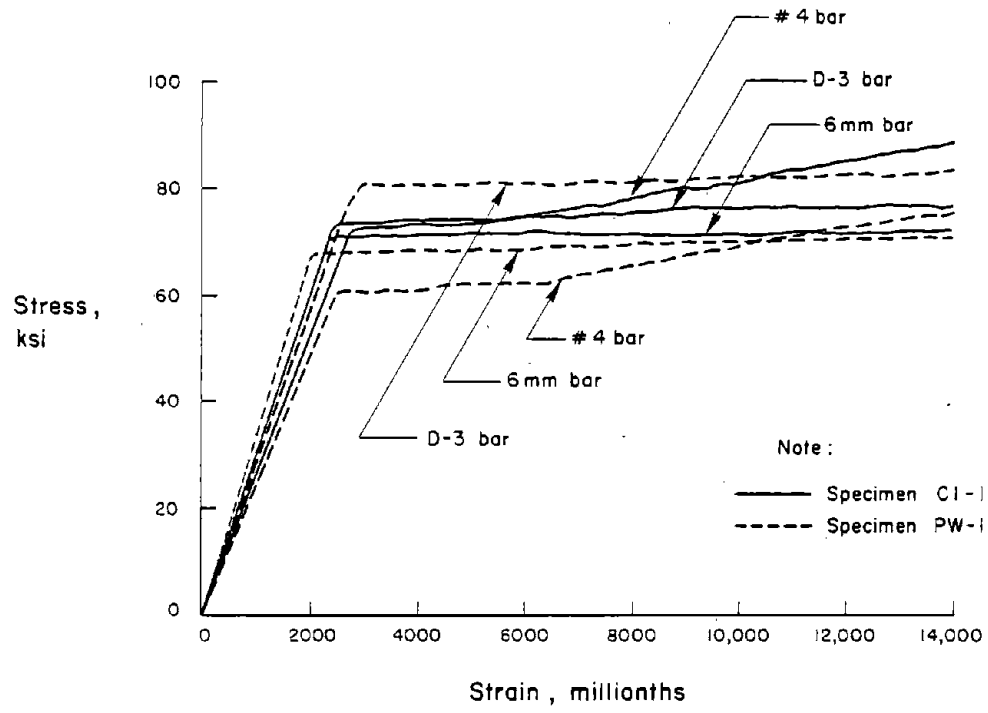

Fig. A-5 Representative Reinforcement Stress-Strain Curves

TABLE A1 - MEASURED CONCRETE PROPERTIES

Specimen	f'_c (psi)	f_t (psi)	E_c (ksi)
CI-1	3375	480	3385
PW-1	3030	430	2815

f'_c = compressive strength of concrete
f_t = splitting tensile strength of concrete
E_c = Modulus of elasticity of concrete
Metric Equivalents:
1 ksi = 1000 psi = 6.895 MPa

TABLE A2 - MEASURED STEEL PROPERTIES

Specimen	Reinforcing Steel	f_y (ksi)	f_{su} (ksi)	E_s (ksi x 10^3)
CI-1	No. 4 bar 6 mm bar D-3 wire	69.1 68.6 70.8	110.5 94.3 81.9	26.1 29.5 27.7
PW-1	No. 4 bar 6 mm bar D-3 wire	60.4 67.0 78.0	110.0 90.5 87.7	24.0 35.0 28.5

f_y = yield strength of reinforcing steel
f_{su} = ultimate strength of reinforcing steel
E_s = modulus of elasticity of reinforcing steel
Metric Equivalents:
1 ksi = 6.895 MPa

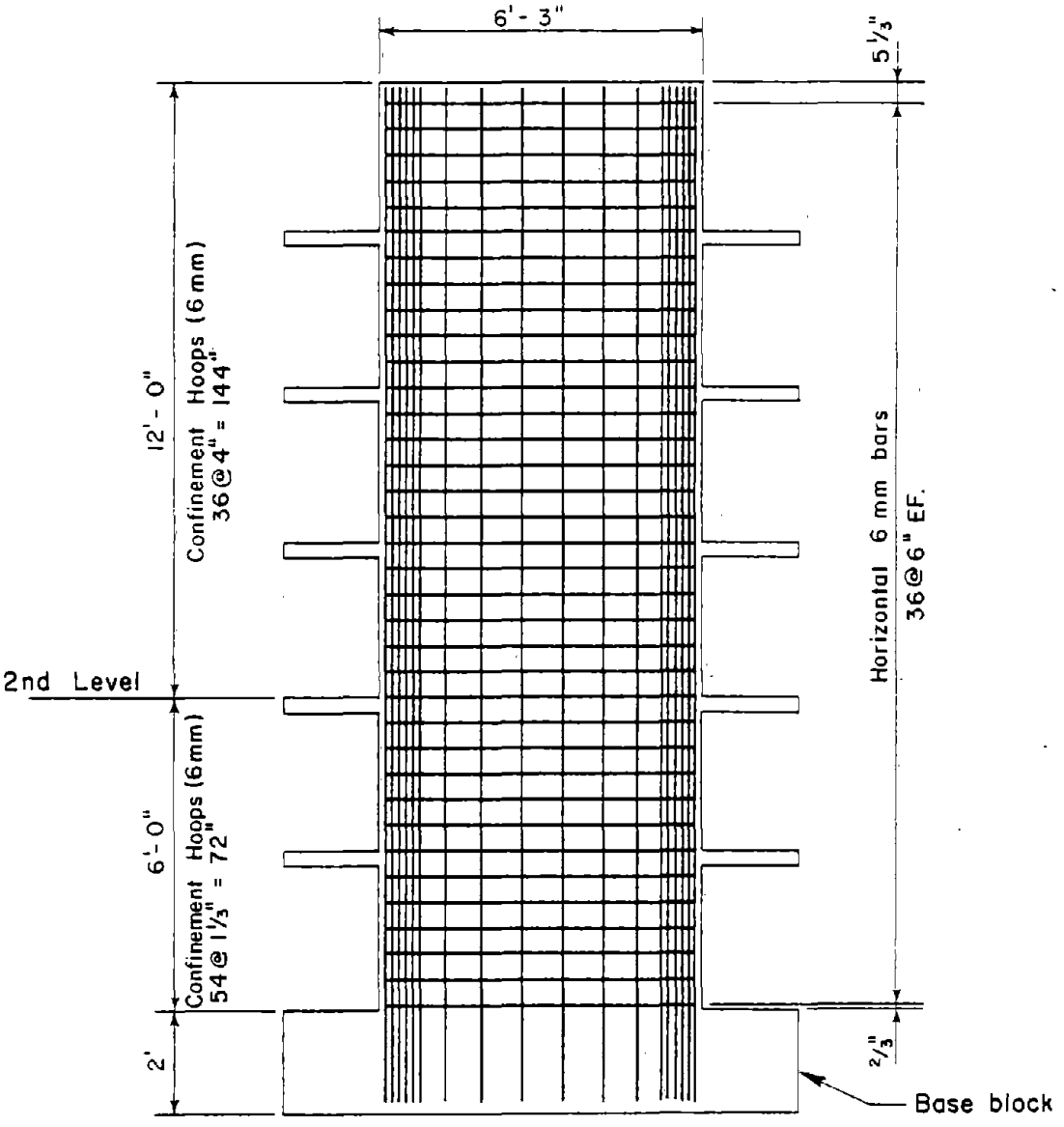

Elevation

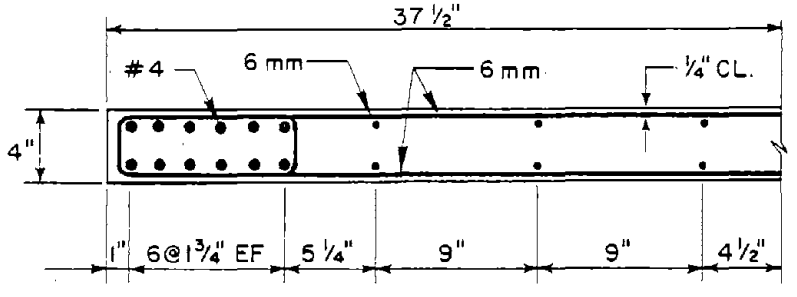

Section

Fig. A-6 Reinforcement Details for Specimens

Reinforcement layout for Specimen PW-1 was similar to Specimen CI-1 except for details around openings. Reinforcement details around openings are shown in Fig. A-7. Vertical and horizontal reinforcement interrupted by openings was placed in equal amount to the sides of the openings. Therefore, two continuous 6 mm bars were put on each side of the openings as shown in Fig. A-7. Photographs of reinforcement layouts for Specimens CI-1 and PW-1 are shown in Fig. A-8.

Flexural reinforcement in the lintels was provided by four 6 mm bars, as shown in Fig. A-9. Lintels were designed to remain elastic until capacity of wall piers was reached. Shear capacity of the lintels was provided by stirrups of 6 mm bars. Stirrups were designed to provide shear capacity as well as concrete confinement.

To avoid premature shear failure of lintels, nominal shear stress was limited to 10 $\sqrt{f'_c}$ (0.83 $\sqrt{f'_c}$ MPa). Nominal shear stress in the lintels was calculated to be 7.9 $\sqrt{f'_c}$ (0.66 $\sqrt{f'_c}$ MPa) at yield of vertical wall steel. Piers were checked to ensure that sufficient shear and flexural capacity was available so that the specimen would behave as an isolated wall.

Reinforcement details of floor slabs are shown in Fig. A-10. Slab reinforcement parallel to the plane of the wall was provided by four D-3 deformed wires. Reinforcement perpendicular to the wall was designed using the "equivalent frame method". Reinforcement consisted of two layers of 6 mm bars spaced at 4 in. (132 mm). Additional reinforcement was provided in the

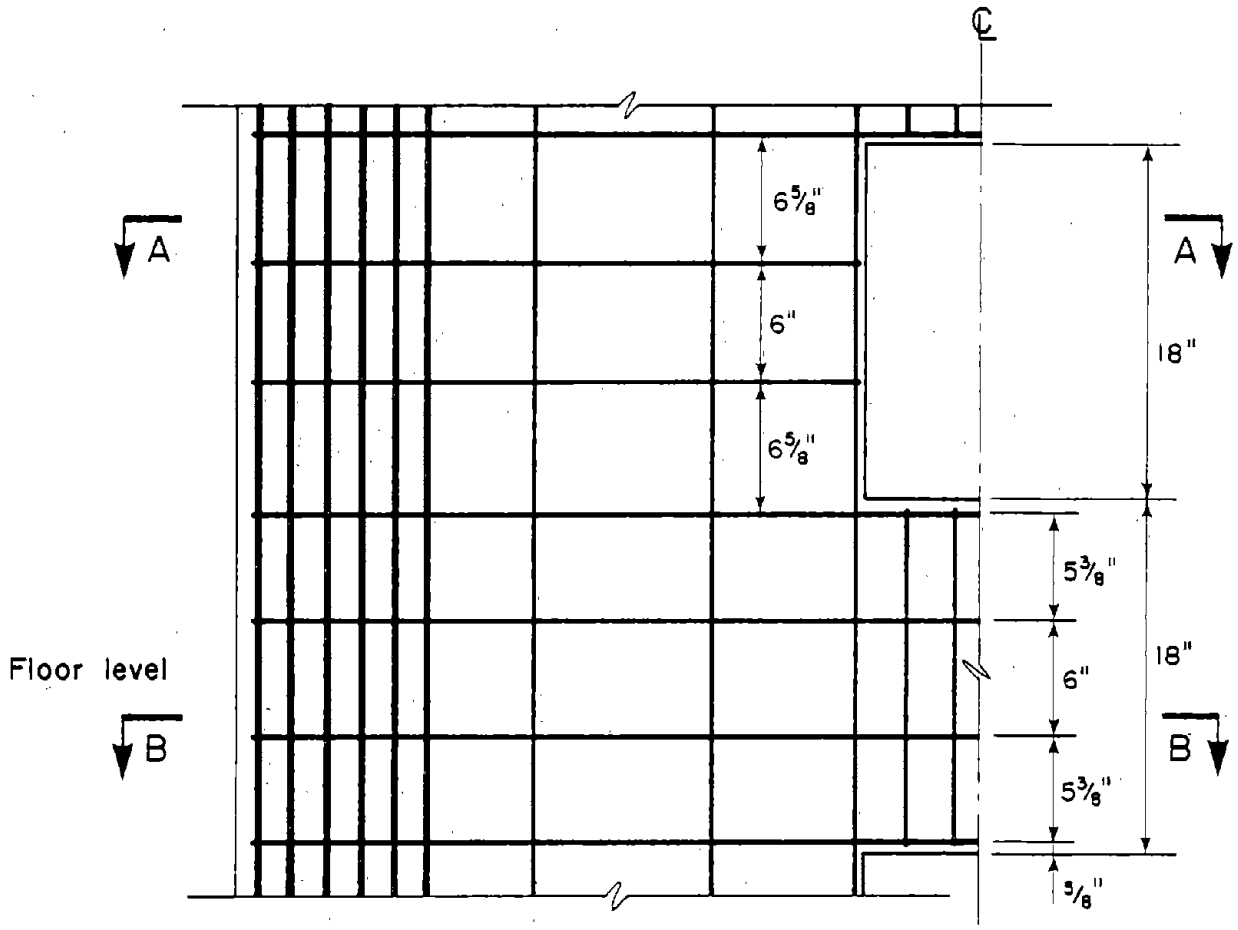

Elevation

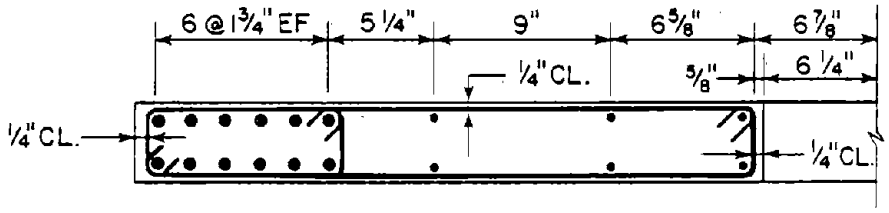

Section A-A

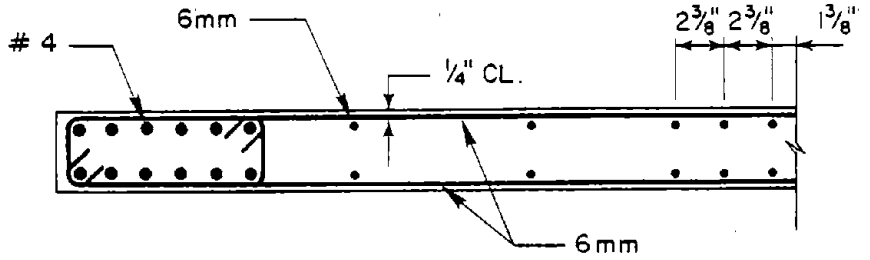

Section B-B

Fig. A-7 Reinforcement Details Around Openings for Specimen PW-1

(a) Specimen CI-1

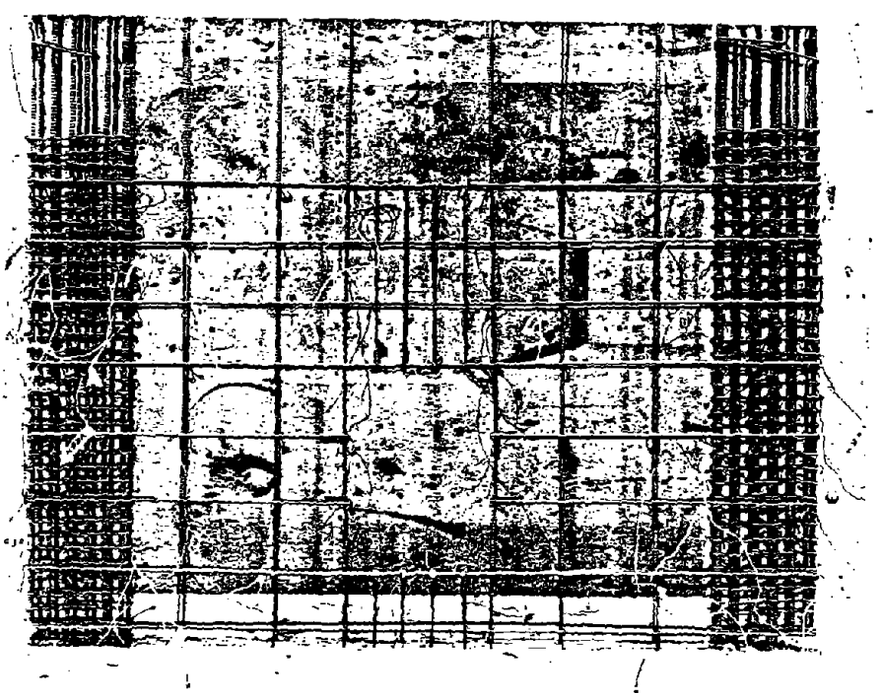

(b) Specimen PW-1

Fig. A-8 Reinforcement Layout in Walls

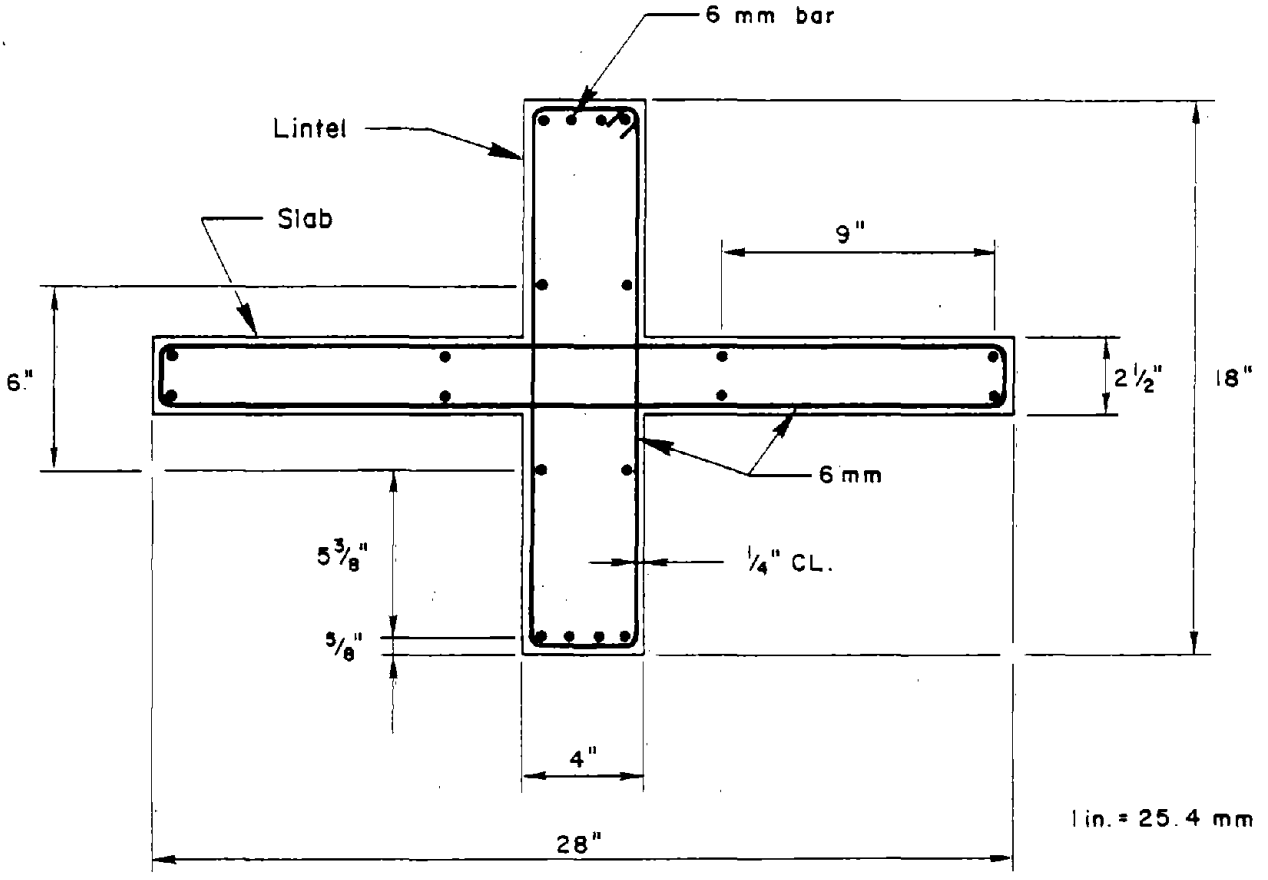

Cross Section of Lintel

Fig. A-9 Reinforcement Details of Lintels for Specimen PW-1

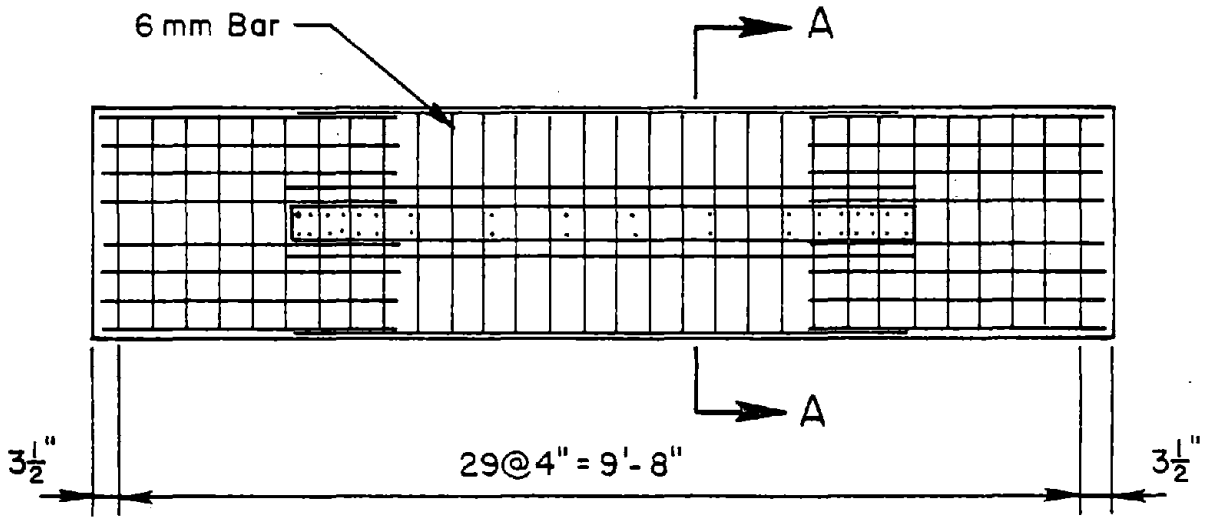

Plan View

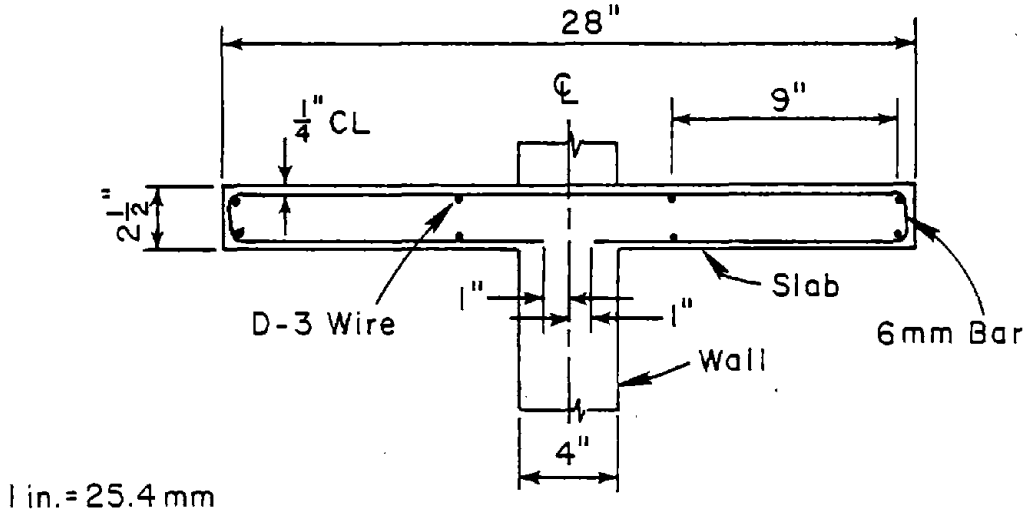

1 in. = 25.4 mm

Section A-A

Fig. A-10 Slab Reinforcement Details

overhanging portion of the slab at both ends of the wall. The extra reinforcement was to strengthen the slab section to resist forces induced by the vertical restraining frames. These frames were used to prevent from out-of-plane movement of specimens. A photograph of the slab reinforcement layout is shown in Fig. A-11.

Construction

Specimens CI-1 and PW-1 were constructed vertically against a stationary formwork. Construction of specimens began with casting of the base block as shown in Fig. A-12. Inserts and vertical conduits for instrumentation and post-tensioning were cast into the base block. In addition, all flexural steel was anchored in the base block and extended continuously into the upper stories.

The specimen was cast one story at a time with construction joints at the top of every floor slab. Prior to placing forms for each story, horizontal wall steel was tied in position.

Initially, formwork for the first story was fastened to inserts in the base block. For stories above the first level, formwork was secured to the preceding floor slab as shown in Fig. A-13. Vertical alignment was maintained by laterally tying the wall to the stationary formwork. Vertical and horizontal alignment were checked before each cast using a theodolite. A photograph of Specimen PW-1 during construction is shown in Fig. A-14.

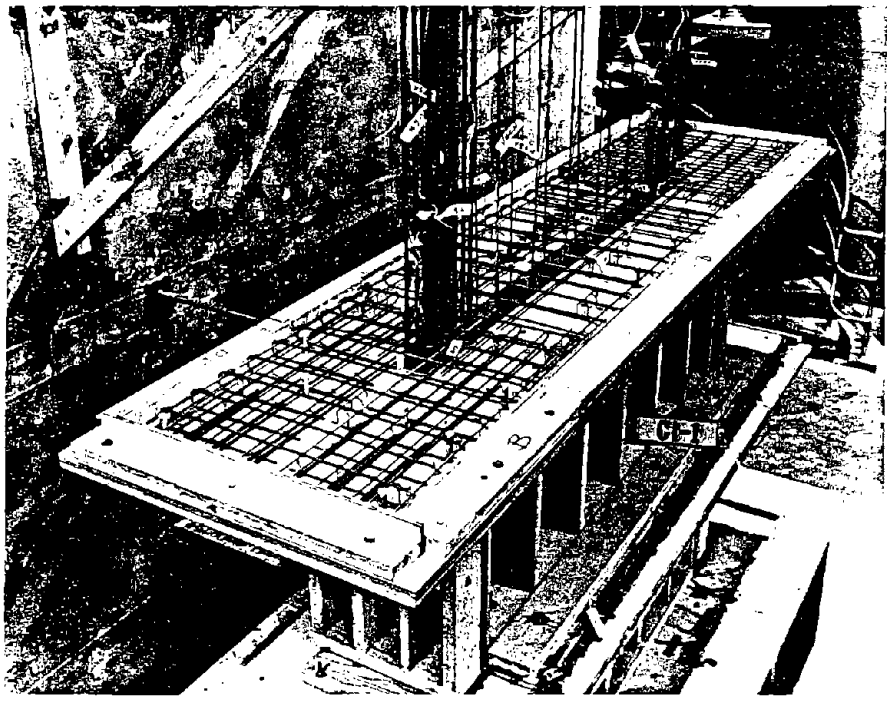

Fig. A-11 Reinforcement Layout of Slabs

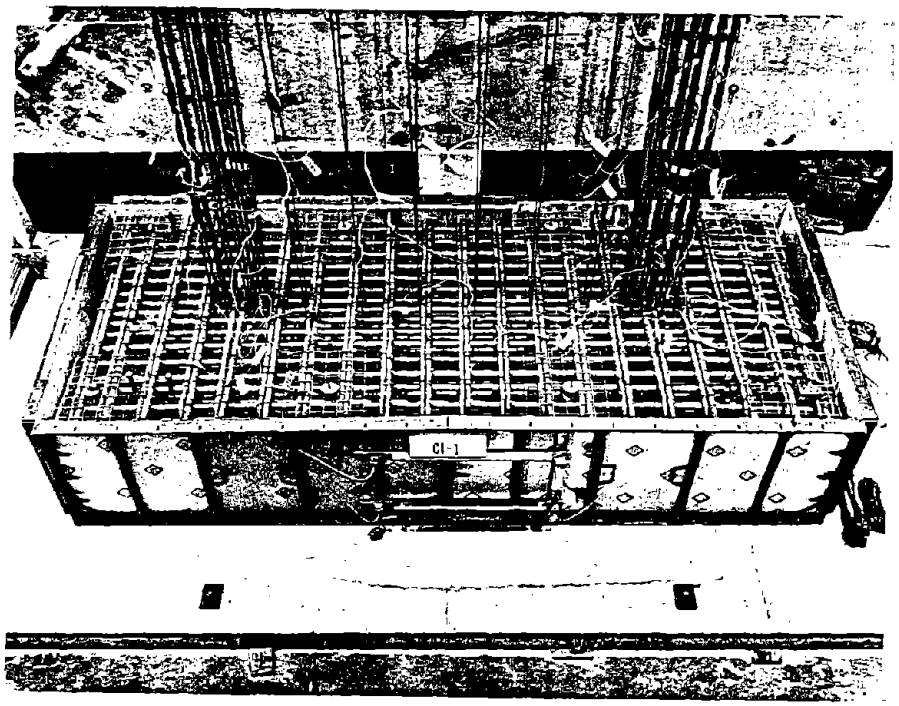

Fig. A-12 Base Block under Construction for Specimen CI-1

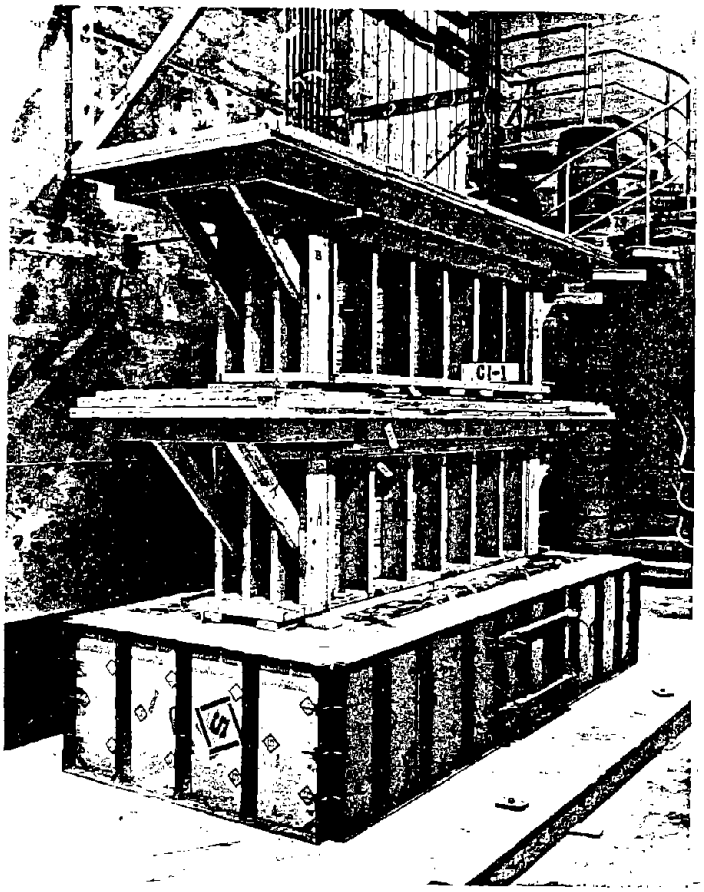

Fig. A-13 Forms Used for Casting Specimen CI-1

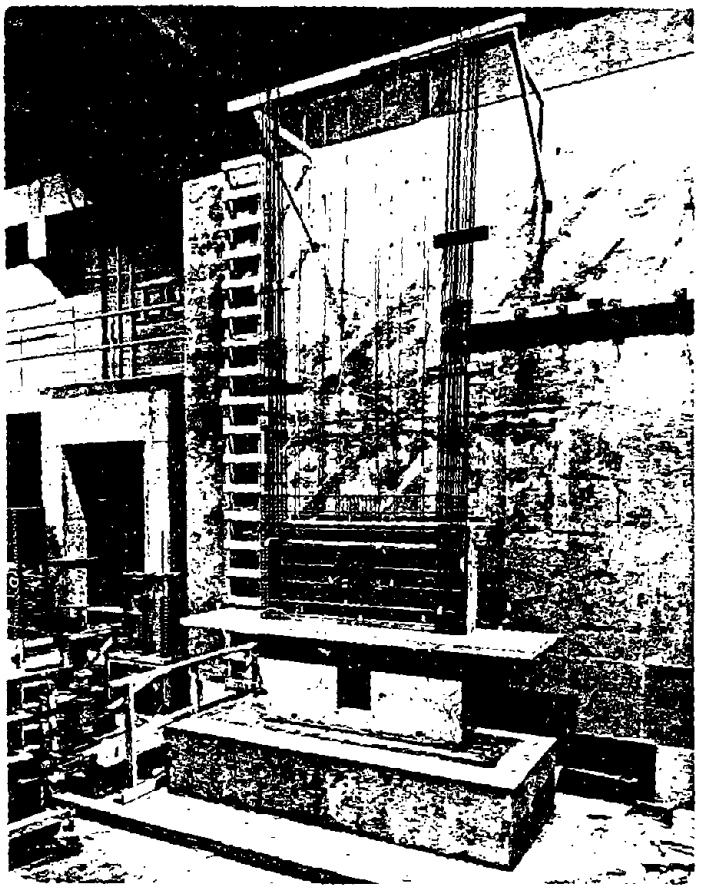

Fig. A-14 Specimen PW-1 During Construction

After casting, concrete was cured for four days prior to removing formwork. During this period, reinforcement for the next story was tied in position. Construction joints between lifts were prepared according to specifications in the 1971 ACI Building Code.[14] Concrete surfaces were roughened with a chisel. Laitance and loose particles were removed before placing fresh concrete.

Test Setup

Detailed descriptions of the test setup, loading apparatus, and instrumentation are presented in this section.

General Description

Photographs of the test setup for Specimens CI-1 and PW-1 are shown in Fig. A-15. Specimens were located between two pairs of reaction abutments and post-tensioned to the test floor. A schematic drawing of the test setup is shown in Fig. A-16.

Lateral loads were applied to the top of the specimens as fixed vertical cantilevers. External vertical frames were used to guide lateral movement of the specimens. The vertical guide frames were constructed of structural tubing located on each side of the specimen. Ball casters, mounted to the frames, were used to align floor slabs over the first three stories. Contact was maintained between ball casters and steel plates which were attached to the slabs. In this way, out-of-plane movement of walls during load reversals was minimized.

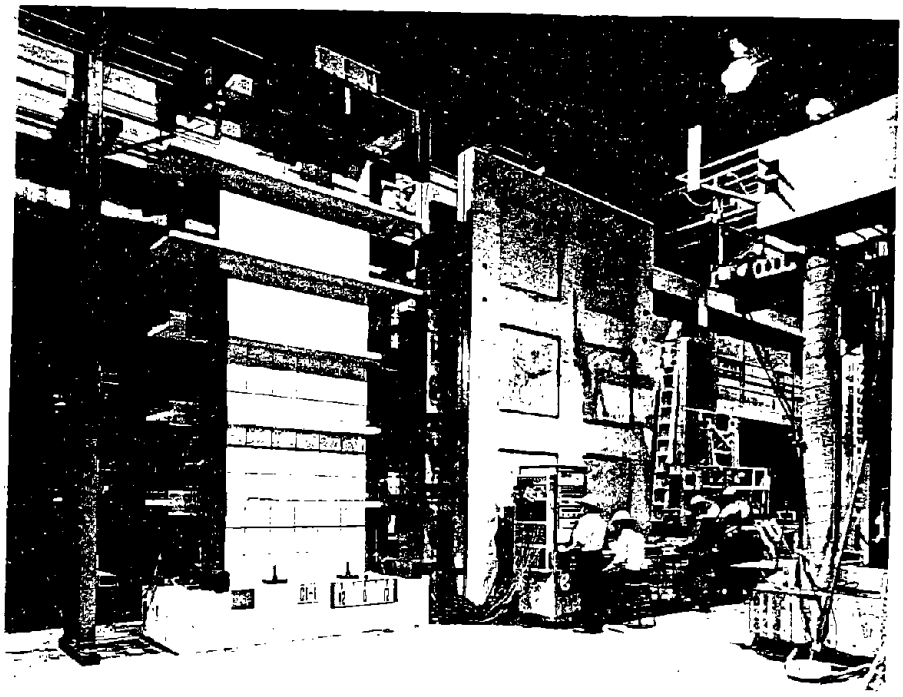

a) Specimen CI-1

b) Specimen PW-1

Fig. A-15 Photographs of Test Setup

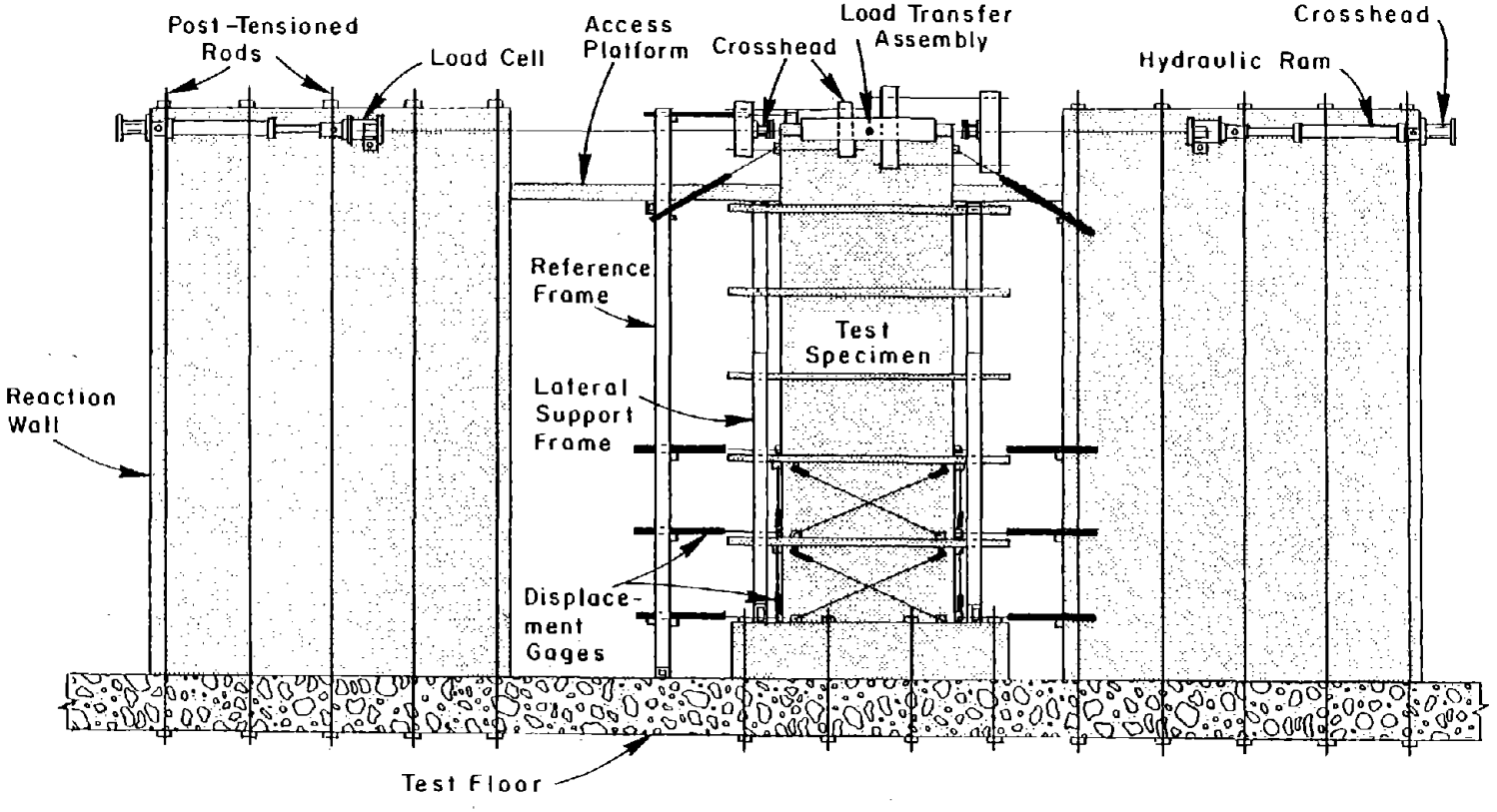

Fig. A-16 Test Setup and External Instrumentation

Loading System

Specimens were loaded laterally in the plane of wall specimen. Concentrated reversing loads were applied to the top of the specimens by four hydraulic rams. Rams were double acting, with 60-ton capacity and a maximum stroke of 36 in. (30 mm). Rams were located between reaction walls on both sides of the specimen as shown in Fig. A-16. Rams on opposite sides of the specimen were hydraulically coupled together so that applied loads were distributed evenly to eliminate twisting. Loading pistons of both rams were connected to a common crosshead and in turn to the specially designed loading assembly.

The loading assembly, shown in Fig. A-17, assured that forces would be applied horizontally. The load assembly consisted of inside and outside hardware. The outside loading hardware was fastened directly to the top slab. The inside loading hardware was connected to the outside hardware through a pin. Therefore, the inside hardware was free to rotate about its center.

Lateral loads were applied by pulling forces. Pulling action was used as a natural aid to avoid out-of-plane wall movements.

Instrumentation

Instrumentation was used to determine applied loads, deflections, rotations, shear distortions, and reinforcement strains. Specimens were instrumented both externally and internally.

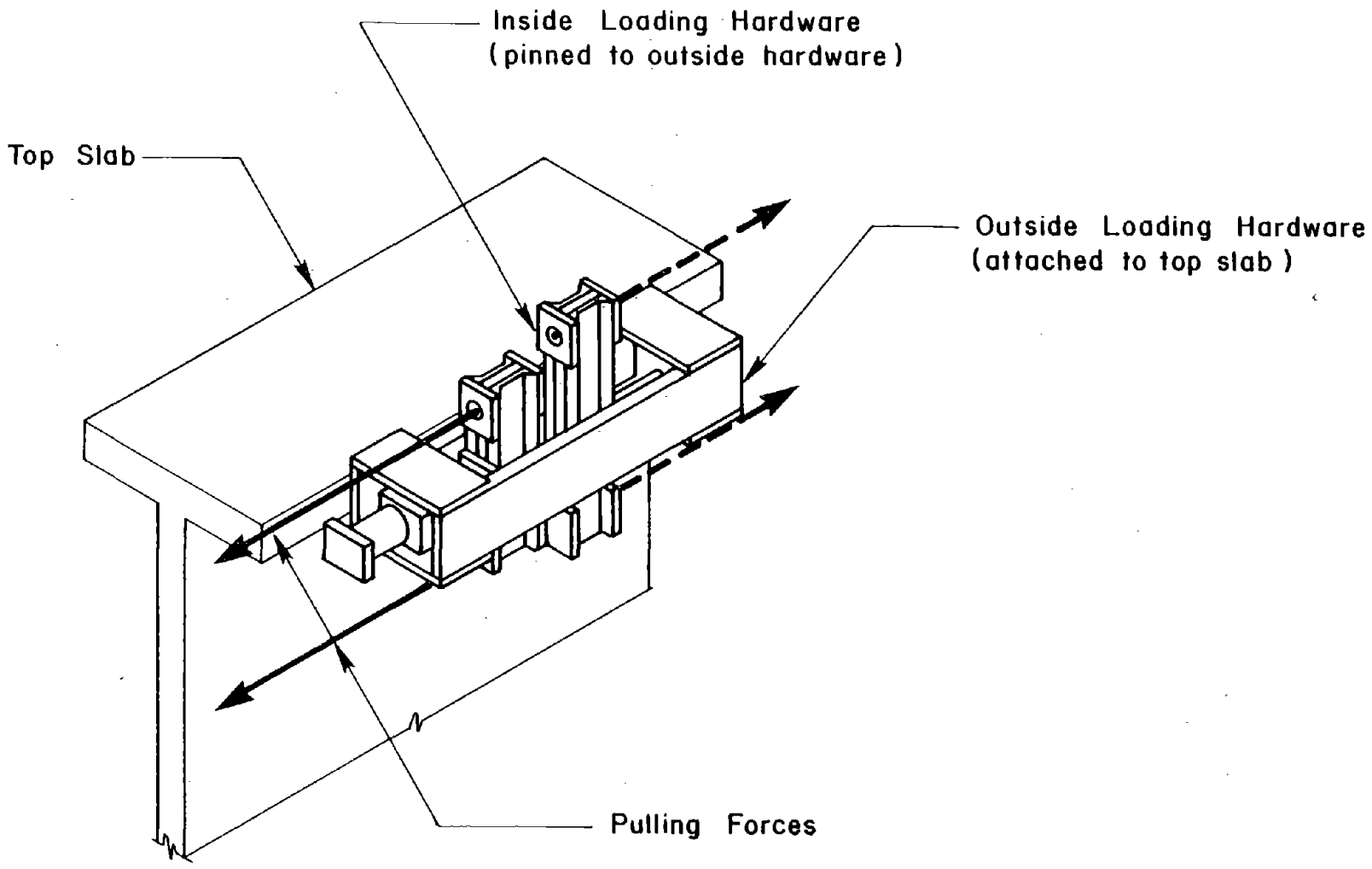

Fig. A-17 Loading Assembly

External Instrumentation - Locations of external measuring devices are shown in Fig. A-16. Four load cells were used to measure applied loads. They were positioned at the end of each ram piston. Lateral deflections were measured on both sides of the specimen using 36-in. (914 mm) stroke linear potentiometers. Potentiometers were located at the first, second, third, and sixth floor levels. In addition, displacements at 3 in. (76 mm) above the base of the wall and lateral movement of the base block were monitored.

Average rotation over selected wall segments were calculated using the output from two 4-in. (10 mm) stroke potentiometers mounted on both sides of the specimen. Using measured deformations, average rotation was determined as illustrated Fig. A-18. Rotations over the lower 3 in. (76 mm), first story, and second story wall segments were determined. Rotation at the top of the wall was directly measured using a rotation meter which was developed at the Construction Technology Laboratories.

Shear deformations of selected wall segments were determined from the output of two Direct Current Differential Transducers (DCDT) diagonally mounted across the segment. Using measured deformations, average shear strain of the instrumented segment was calculated as illustrated in Fig. A-19. Shear distortions over the first and second stories were measured.

During the test of Specimen CI-1, a major horizontal crack formed at the mid-height of the first story. To measure slip along this crack, a dial gage was used as shown in Fig. A-20.

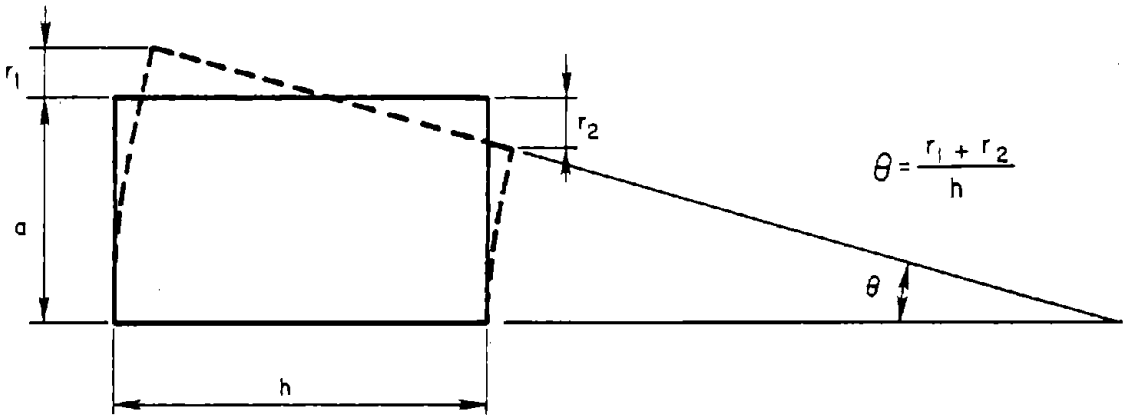

Fig. A-18 Procedure for Determining Rotation

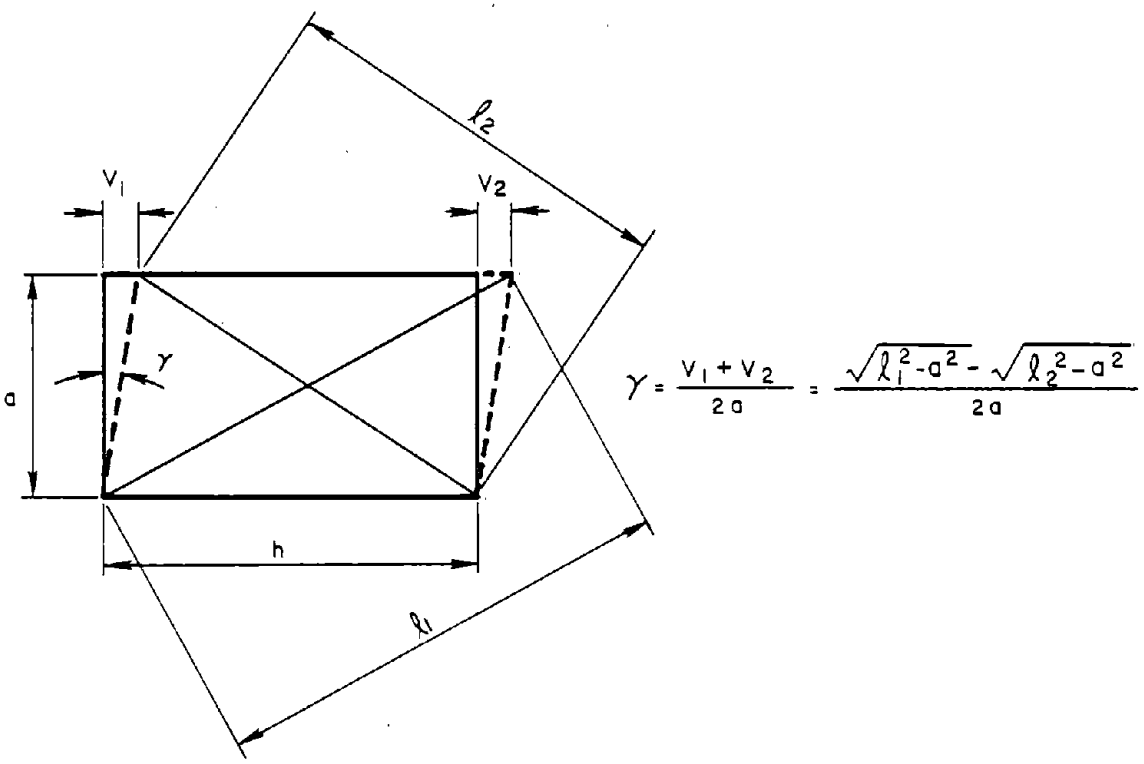

Fig. A-19 Procedure for Determining Shear Distortion

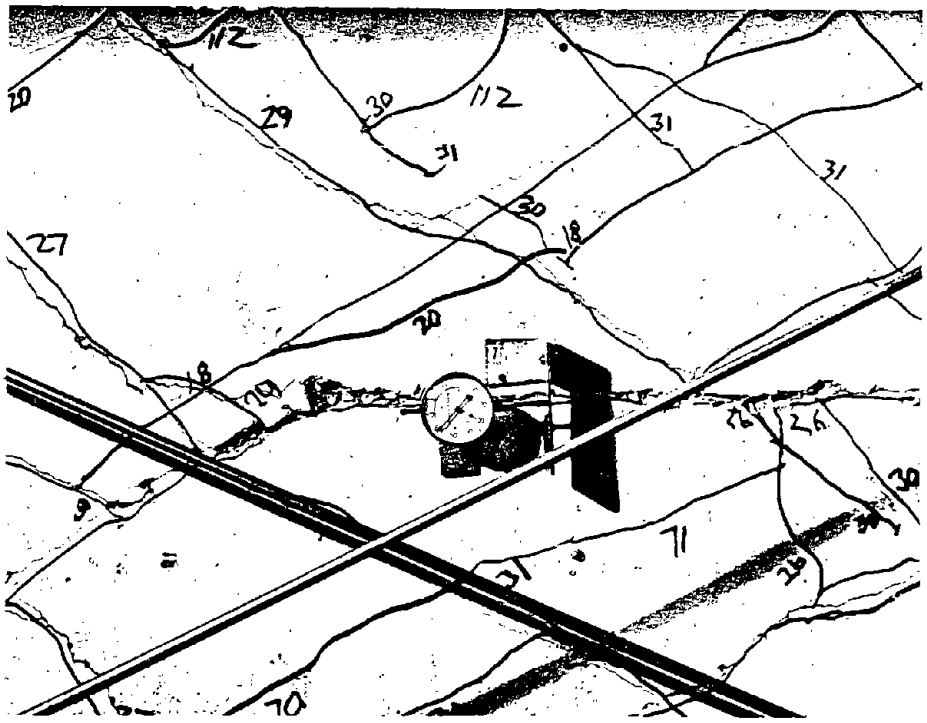

Fig. A-20 Dial Gage at Horizontal Crack

Other dial gages were also used to measure slip along construction joints at the first and second story levels of Specimen CI-1. Slip along cracks in Specimen PW-1 was not measured.

Internal Instrumentation - Steel strains at selected locations were measured by electrical resistance strain gages. Strain gages were attached to the surface of steel bars before casting. Over 150 strain gages were used in each specimen.

Locations of strain gages mounted on vertical and horizontal reinforcement in Specimens CI-1 and PW-1 are shown in Figs. A-21 and A-22, respectively. In addition, strain gages were attached to reinforcement in floor slabs at the first, second, and third story levels as shown in Fig. A-23. Strains in confinement hoops of boundary elements were also measured in the first two stories. Locations of strain gages on hoop reinforcement are shown in Fig. A-24.

Recording Equipment - Data from load cells, potentiometers, DCDTs, and electrical resistance strain gages were recorded using a digital data acquisition system and stored on cassette tapes. In addition, X-Y plotters were used to obtain continuous records of selected data. Slip data along construction joints and the movement of the major horizontal crack in Specimen CI-1 were recorded manually.

A complete photographic record was kept for both specimens. This included color slides and black and white prints taken at every load stage. In addition, movies were taken of both tests.

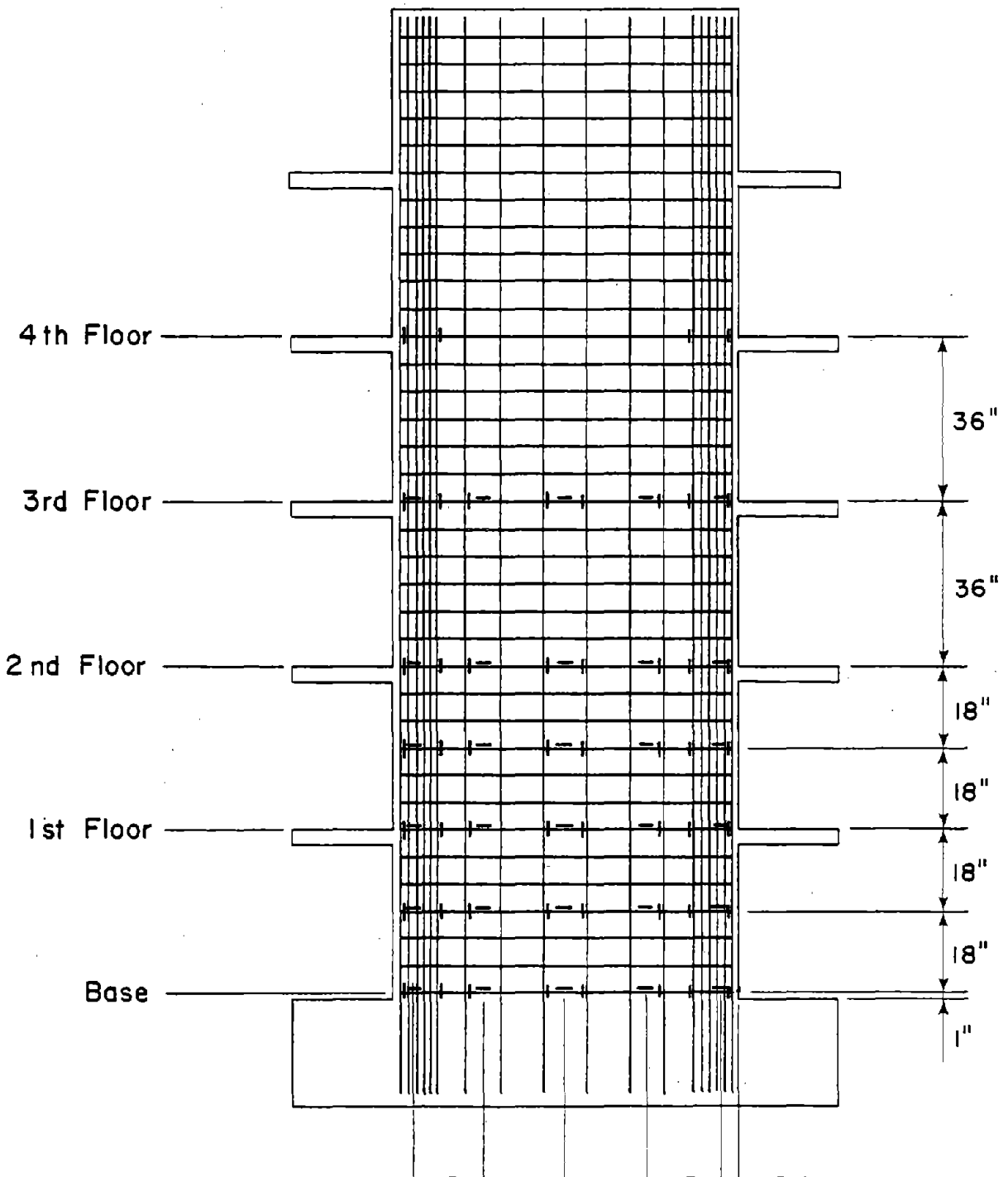

Fig. A-21 Strain Gage Locations on Vertical and Horizontal Reinforcement for Specimen CI-1

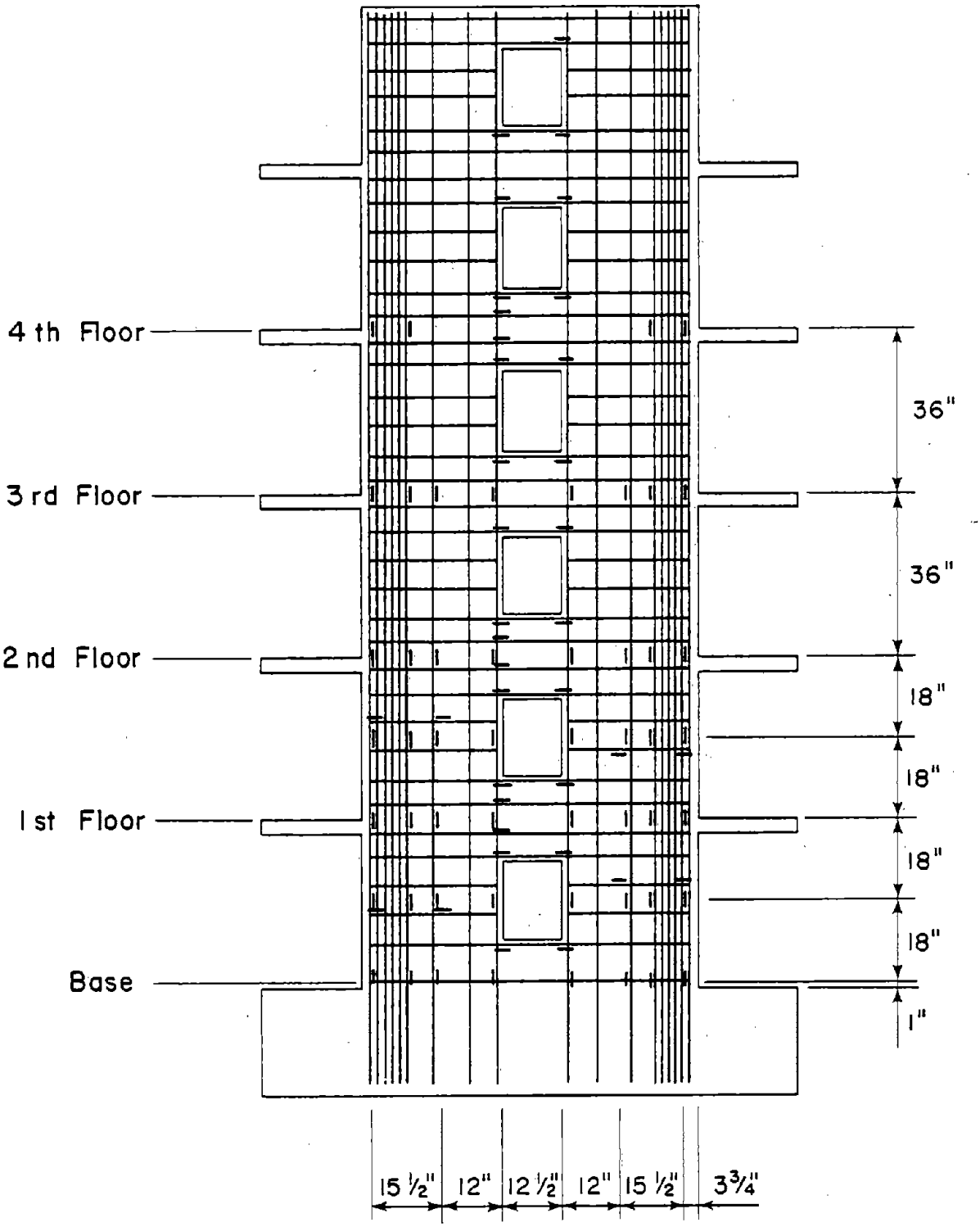

Fig. A-22 Strain Gage Locations on Vertical and Horizontal Reinforcement for Specimen PW-1

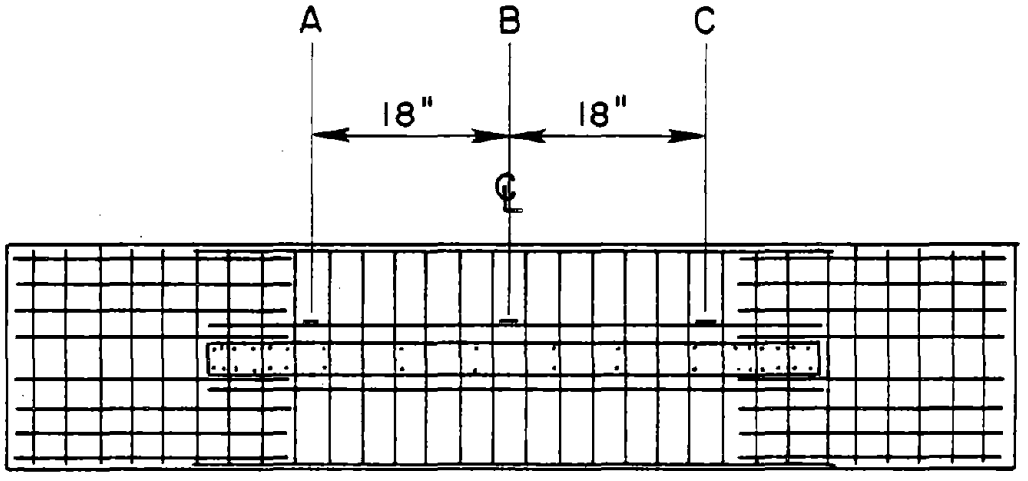

Fig. A-23 Strain Gage Locations on Slab Reinforcement

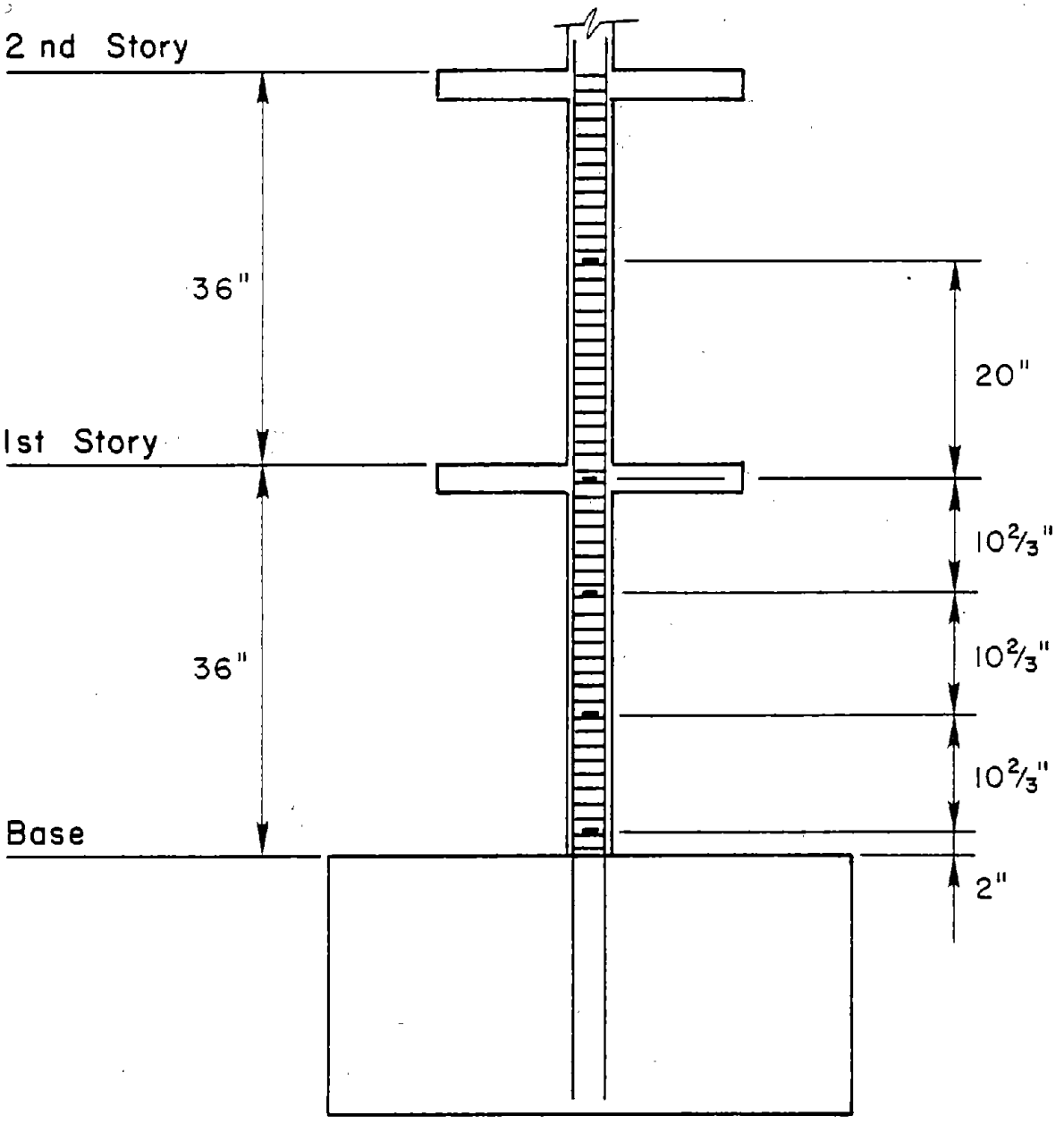

Fig. A-24 Strain Gage Locations on Hoop Reinforcement

Load History

The first two phases of the modified load history were developed to represent severe earthquakes of 20 second duration. Factors considered in the simulation included maximum inelastic response of the specimen and the number of inelastic cycles.

The load history was derived from the dynamic response of a 6-story prototype structure, shown in Fig. A-3, using a modified DRAIN 2-D computer program.[16] Two actual earthquake records were used for input ground motions. They were the East-West component of the 1940 El Centro Earthquake record, and the 16° South component of the 1971 Pacoima Dam Earthquake record. Damping of the prototype structure was assumed to be 5%. The two earthquake records were selected for their distinct dynamic characteristics.

The East-West El Centro record exhibits a "broad band" velocity spectrum whereas the Pacoima record exhibits a "peaking" response spectrum. Estimated lateral deflections of the prototype structure in response to the two earthquake excitations are shown in Figs. A-25 and A-26. It is noted that lateral deflections at each story were in phase. This indicates that first mode response predominated.

Based on dynamic response of the prototype, load histories for the test specimens were developed. Each load history was comprised of three load phases. Phase I and II consisted of ten reversing load cycles to simulate the two 20-second earthquakes. Among the ten load cycles, five were within the

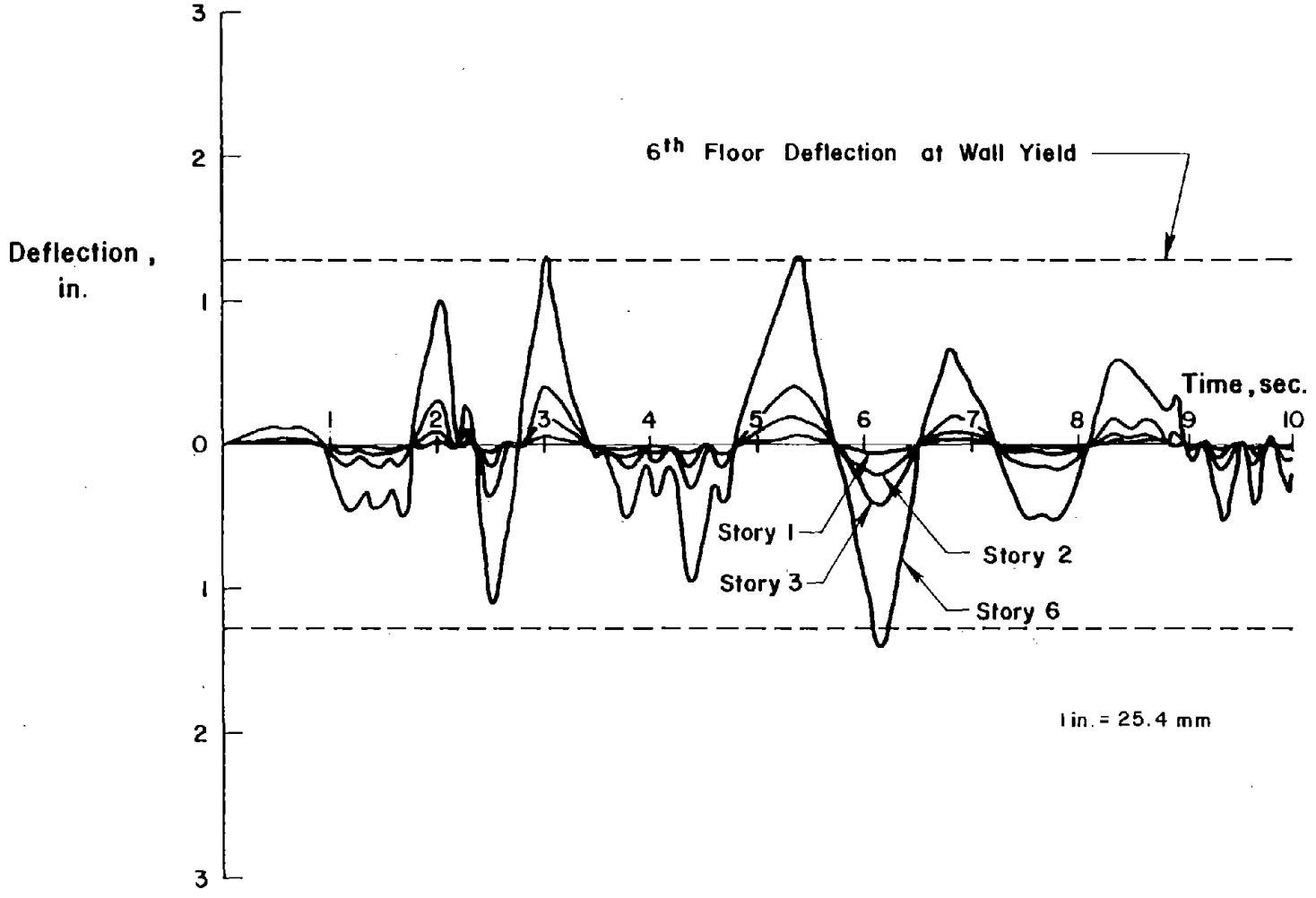

Fig. A-25 Time versus Deflection History for Prototype Structure (1940 E-W El Centro Earthquake)

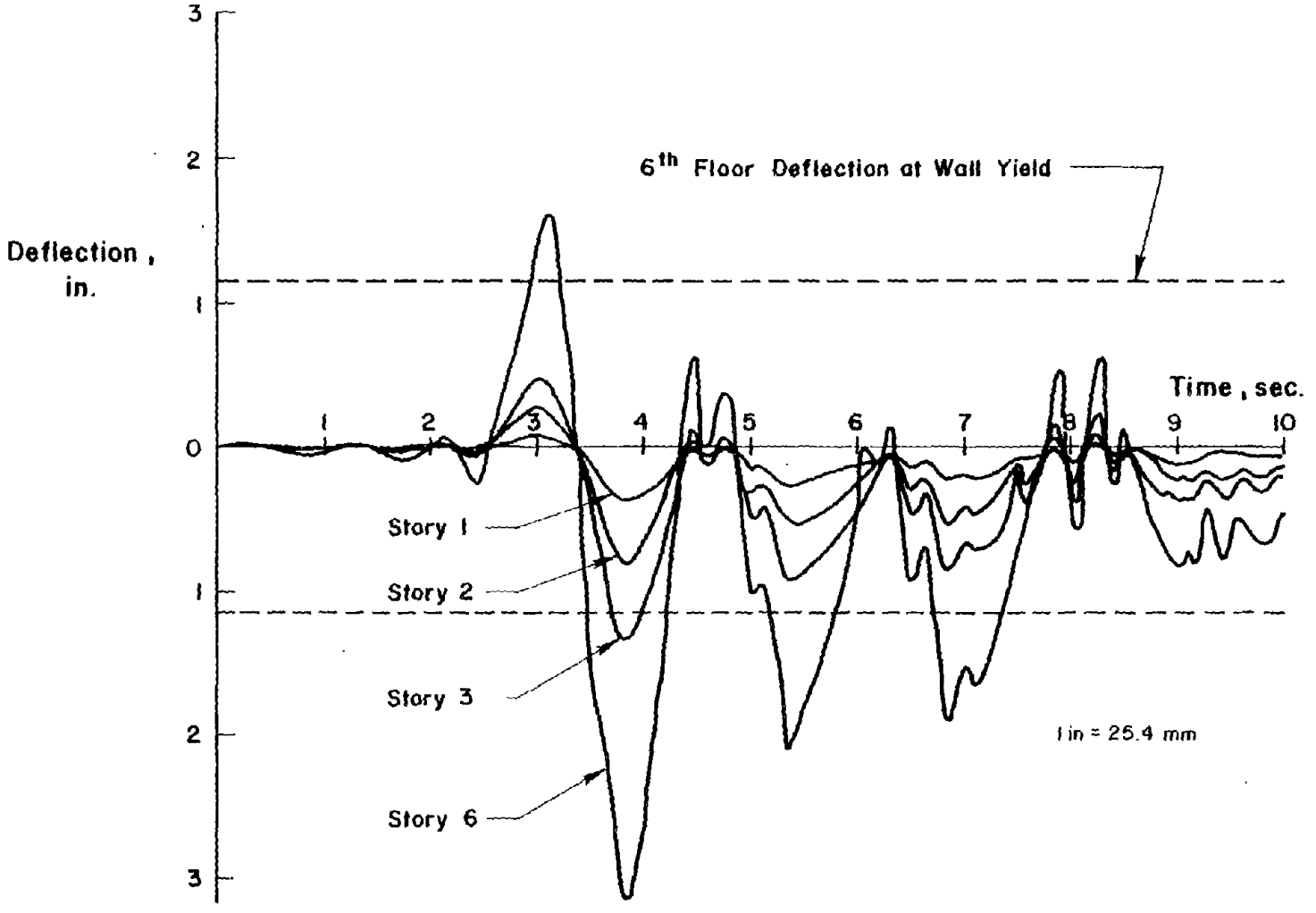
Deflection , in.
3
2
1
0
1
2
3
6th Floor Deflection at Wall Yield
Time , sec.
1
2
3
4
5
6
7
8
9
10
Story 1
Story 2
Story 3
Story 6
1 in = 25.4 mm

inelastic range. Phase III consisted of incrementally increasing load reversals. Each increment consisted of three load cycles of approximately equal deflections. Testing continued until loss of capacity was observed. Load histories for Specimens CI-1 and PW-1 are presented in Figs. A-27 and A-28, respectively.

Rotational ductility over the lower 6 ft (1.83 m) was selected as the controlling parameter for the initial cycle of each phase. However, once the given rotational ductility was achieved, deflections were used to control loading for subsequent inelastic cycles. Deflection histories for Specimens CI-1 and PW-1 are presented in Figs. A-29 and A-30, respectively. Numbers in brackets are rotational deformations that controlled loading for initial cycles in each phase.

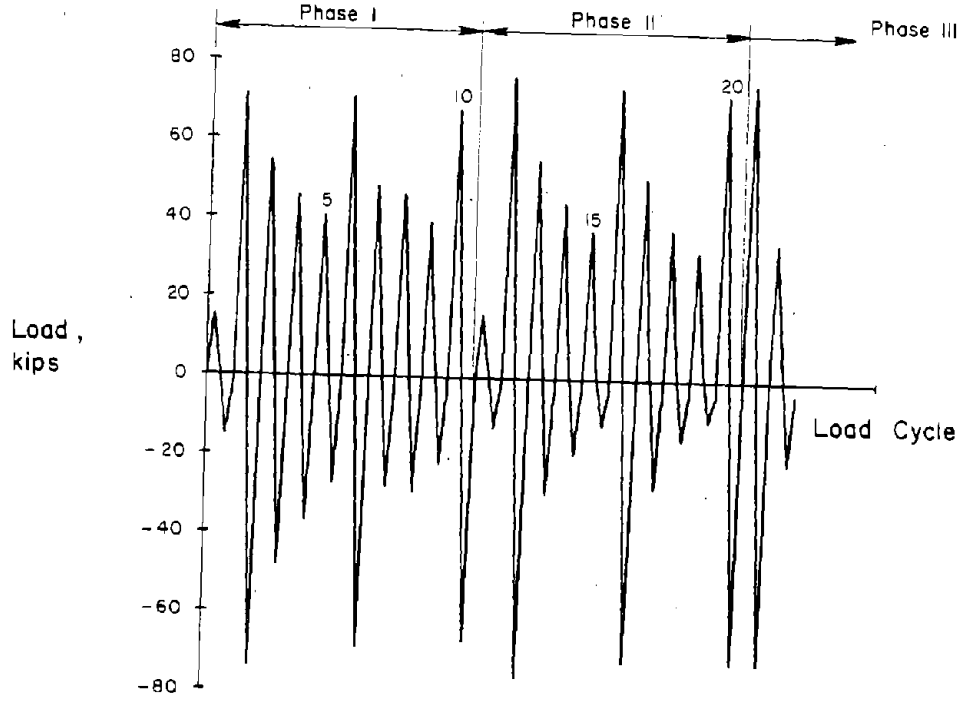

Fig. A-27 Load History for Specimen CI-1

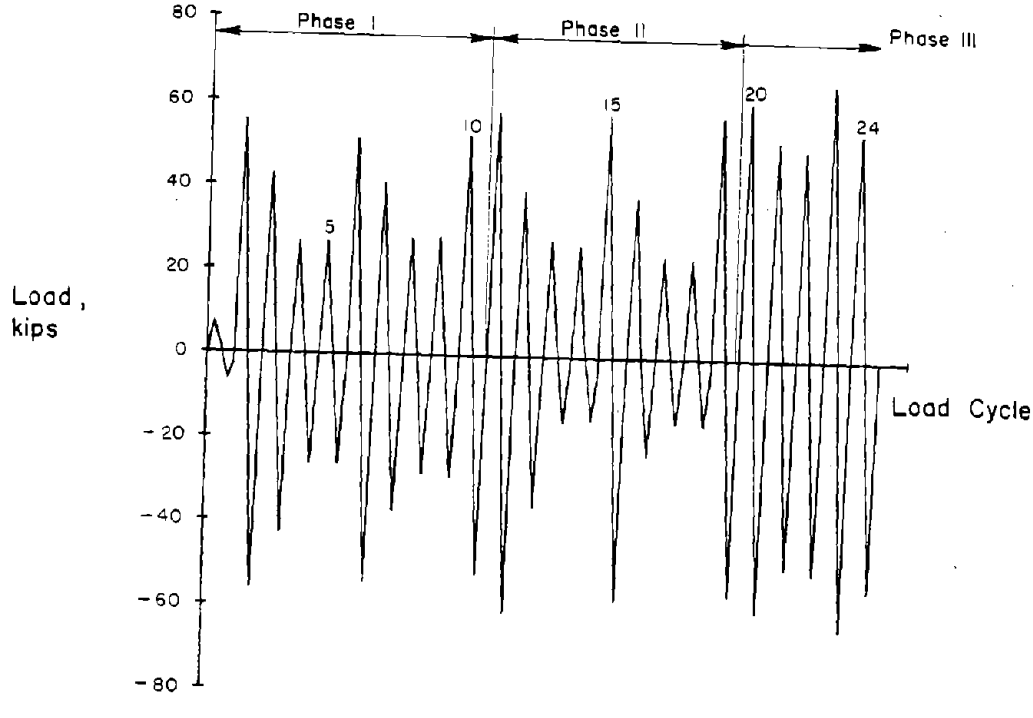

Fig. A-28 Load History for Specimen PW-1

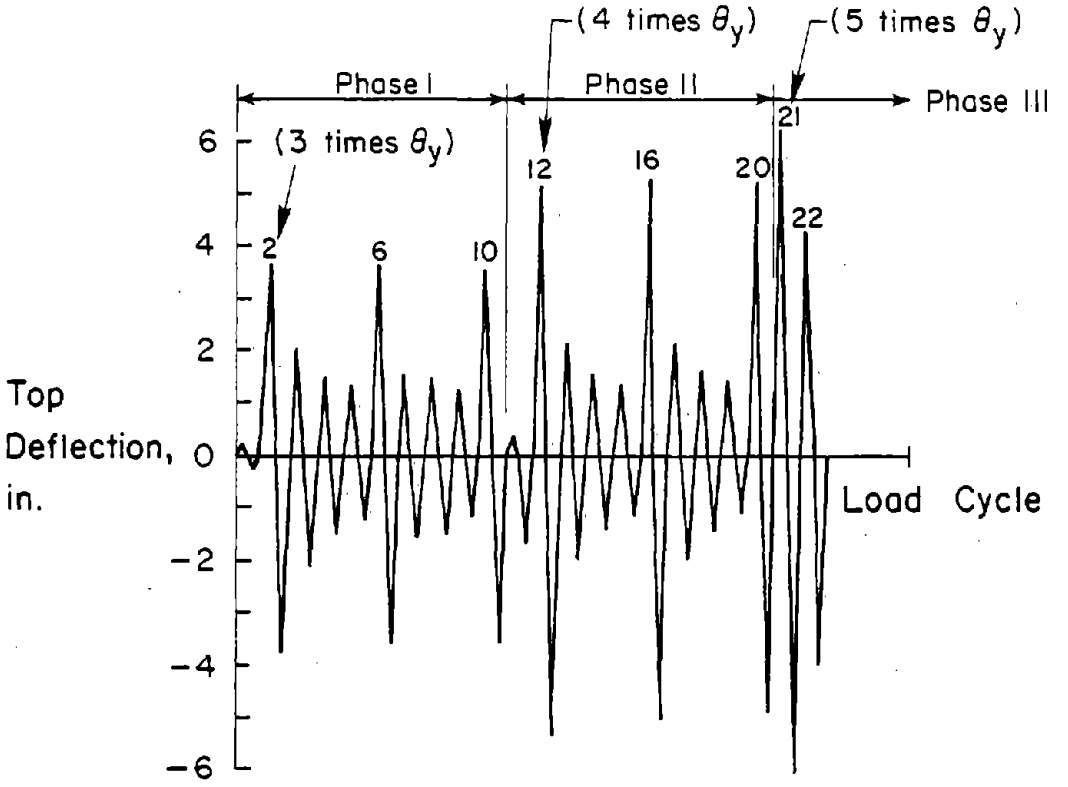

Fig. A-29 Deflection History for Specimen CI-1

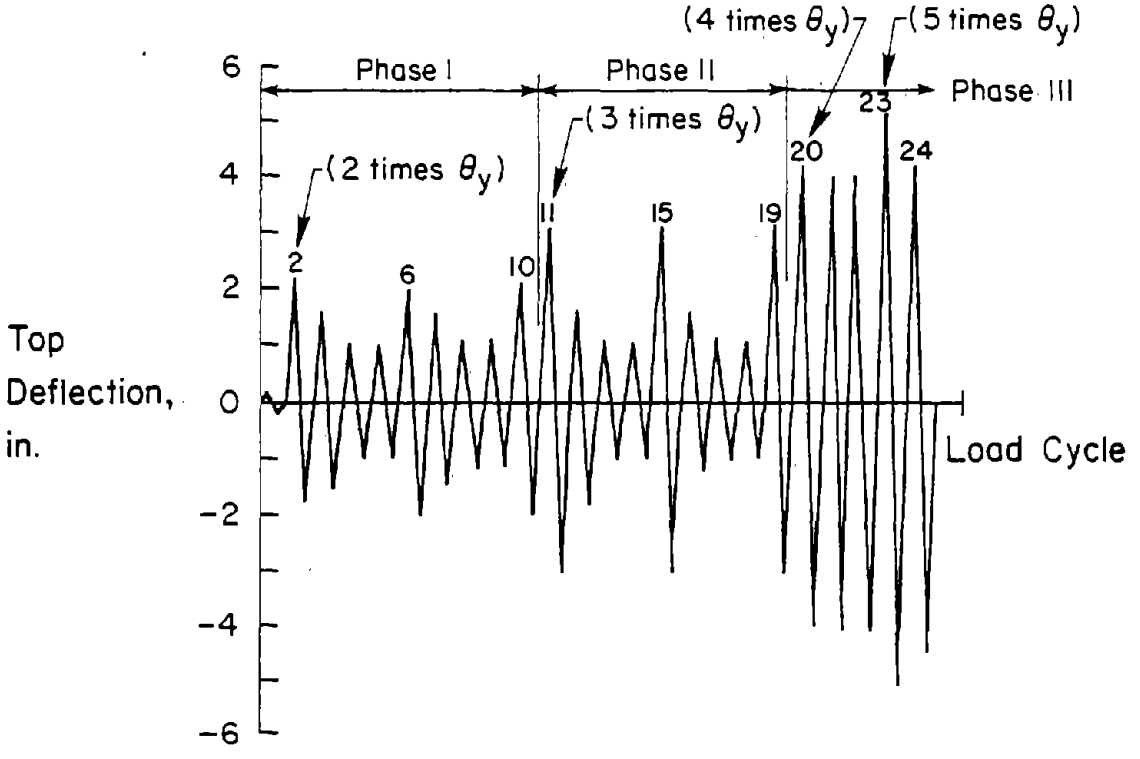

Fig. A-30 Deflection History for Specimen PW-1

APPENDIX B - TEST RESULTS

This appendix describes methods adopted for data analysis and presents a detailed account of all test data for Specimens CI-1 and PW-1. Specimen behavior during testing is also described.

Calculation of Deflection Components

Total lateral deflections at the 3-ft (0.92 m), 6-ft (1.83 m), and top levels were divided into deflections attributed to rotations and shear distortions.

Rotational deflection components were calculated assuming measured rotations over a segment to be concentrated at the center of that segment. To determine top deflection, the wall was considered essentially rigid above the last measured segment. Measured rotations over the first and second stories were obtained as described in Appendix A. It should be noted that base rotation is included in the first story rotation measurement. Therefore, using the notation defined in Fig. B-1, deflection attributed to rotation was calculated as follows:

$$\Delta_{ft} = \frac{11\ \theta_1 h}{2} + \frac{9\ \theta_2 h}{2}$$

$$\Delta_{f2} = \frac{3\theta_1 h}{2} + \frac{\theta_2 h}{2}$$

$$\Delta_{f1} = \frac{\theta_1 h}{2}$$

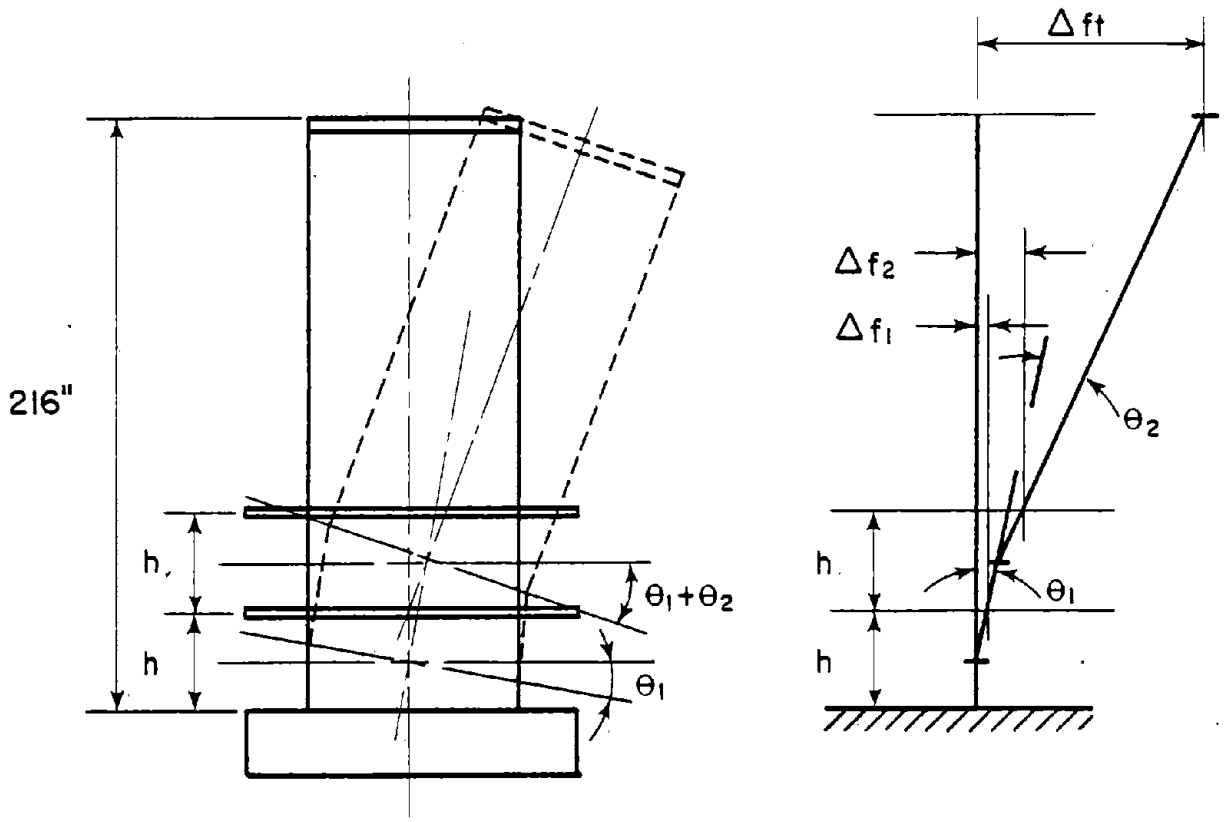

Fig. B-1 Calculation of Rotational Deflection Components

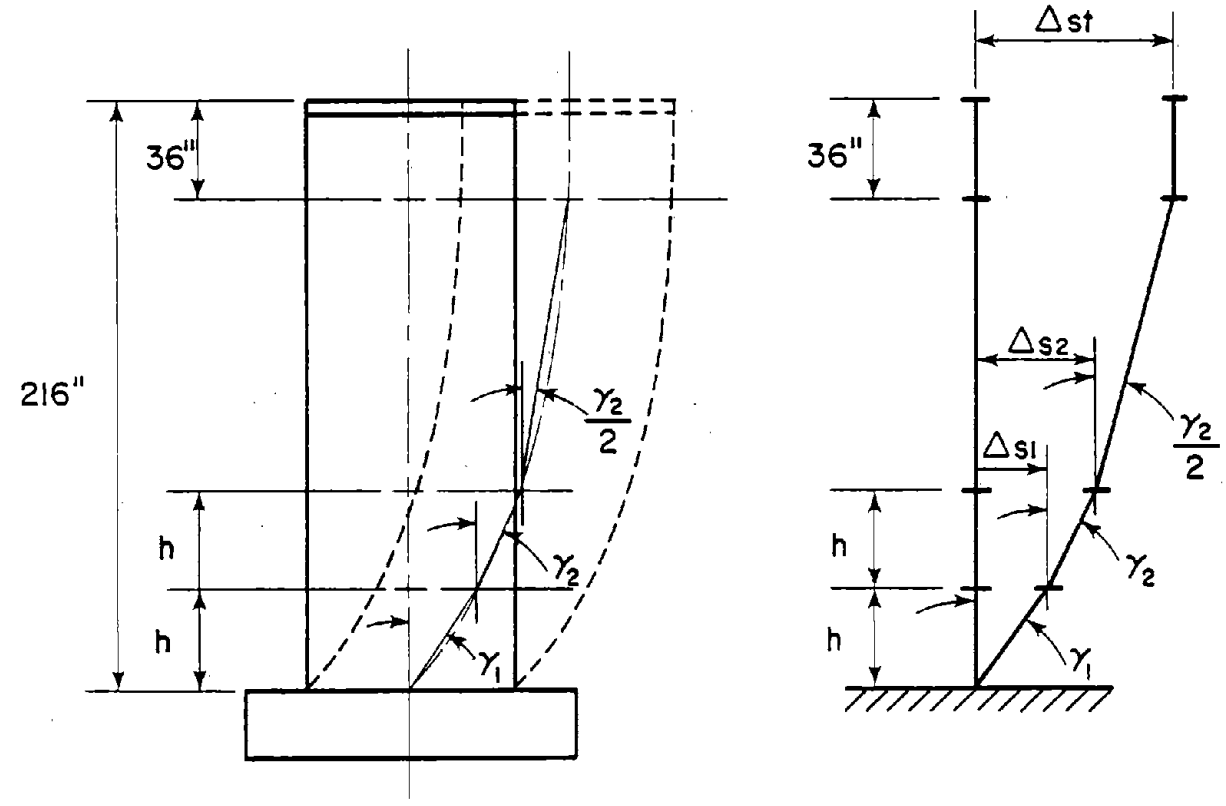

Fig. B-2 Calculation of Shear Distortion Deflection Components

Shear deflection components for each segment were calculated assuming measured shear distortions were constant over that segment. Measured shear distortions over the first and second stories were obtained as described in Appendix A. To estimate the shear deflection at the top of the walls, two assumptions were made. First, an average shear distortion of $\frac{\gamma_2}{2}$ was assumed constant over the distance between the 6-ft (1.83 m) level and the 15 ft (4.57 m) level. Second, shear distortion in the top 3 ft (0.93 m) of the wall was assumed to be zero. There would actually be some elastic shear strain in this top segment, however, it is negligible. Therefore, using the notation defined in Fig. B-2, deflection at respective levels attributed to shear was calculated as follows:

$$\Delta_{st} = (\gamma_1 + \gamma_2)h + \frac{\gamma_2}{2}(3h)$$

$$\Delta_{st} = (\gamma_1 + \gamma_2)h$$

$$\Delta_{s1} = \gamma_1 h$$

Specimen CI-I

Observed Behavior

Specimen CI-1 was subjected to 22 complete load reversals. The applied load history consisted of three phases. The first two phases represented two separate major earthquake excitations. The final phase consisting of incrementally increasing load reversals. Loads were applied until significant loss of load capacity was experienced by the specimen.

First cracking was observed in the first story at an applied load of 15.1 kips (67 kN). Cracks originated in the web of the wall and extended horizontally into the boundary elements. Because of heavy confinement in the boundary elements, small, closely spaced flexural cracks developed. With subsequent large inelastic load reversals, a major horizontal crack extended across the web at mid-height of the first story. As loads were reversed, slipping and grinding were noted along this crack. A dial gage was installed to measure horizontal movement along the crack. During Phase I loading, a maximum horizonal slip of 0.29 in. (7 mm) was measured along the crack. Maximum slip along construction joints at the base and 3-ft levels were 0.09 in. and 0.14 in. (2 mm and 1 mm), respectively.

A photograph of the first and second stories at the end of Phase I loading is shown in Fig. B-3. Cracks were concentrated in the first and second stories which can be regarded as the hinging region.

The test was continued with Phase II loading representing a more severe earthquake. A photograph of the hinging region at the end of Phase II loading is shown in Fig. B-4. Sliding and grinding of concrete along the horizontal crack was observed. Maximum horizontal movement along the crack was 0.65 in. (17 mm). Maximum slip along construction joints at the base and 3-ft level were 0.16 in. and 0.07 in. (4 mm and 1 mm), respectively. The horizontal crack at mid height of the first story extended completely across the wall by the end of Phase II loading.

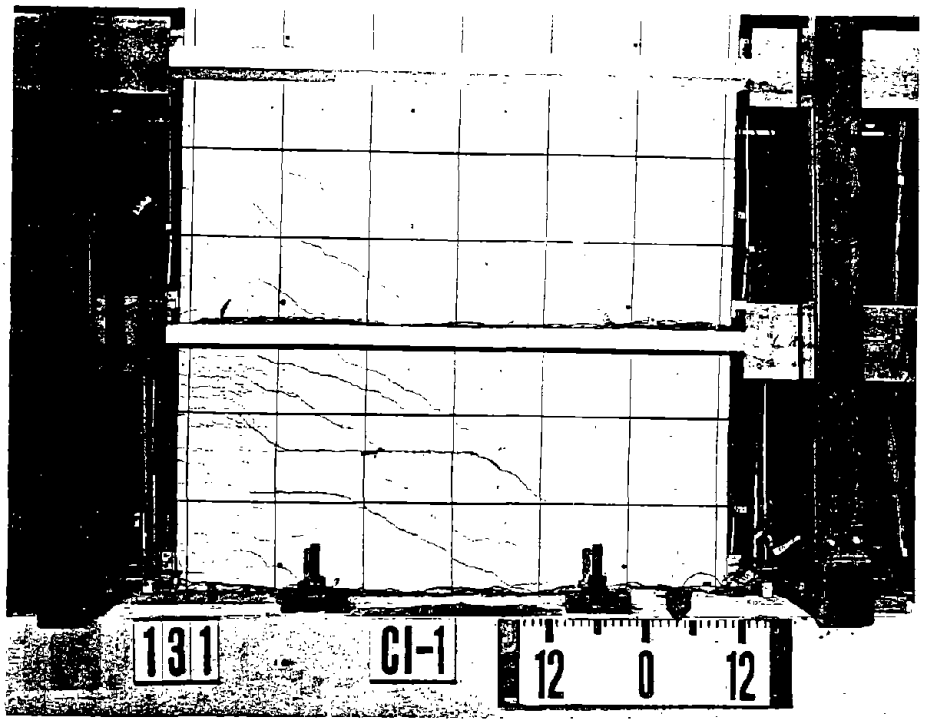

Fig. B-3 Crack Pattern of Specimen CI-1 at End of Phase I

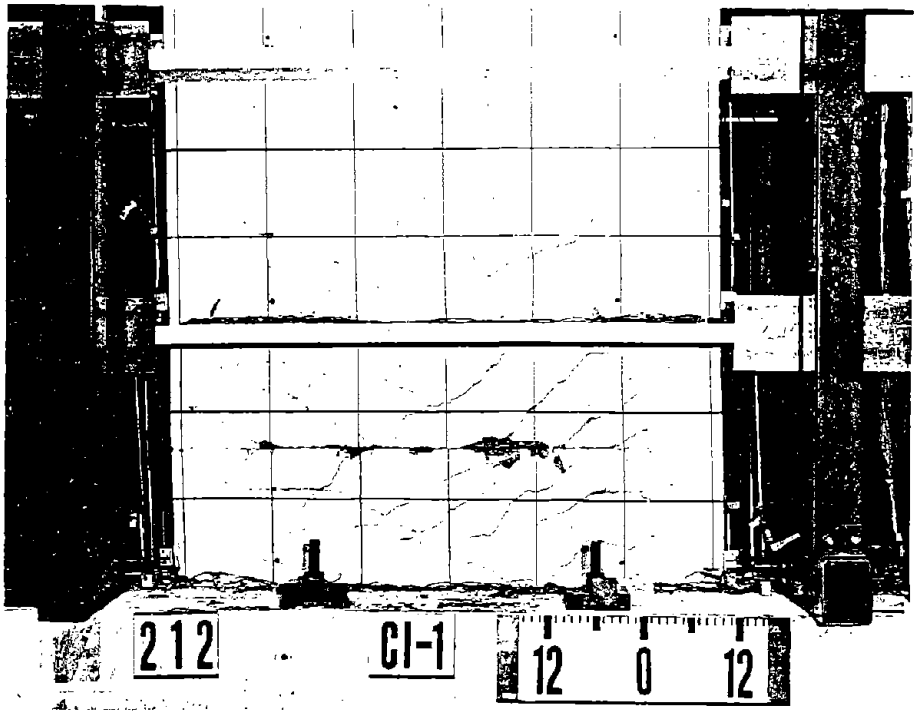

Fig. B-4 Crack Pattern of Specimen CI-1 at End of Phase II

Phase III consisted of Cycles 21 and 22. Shear resistance along the crack decreased as larger inelastic load cycles were applied. Shear resistance was primarily provided by the boundary elements through dowel action. Loss of shear capacity along the major horizontal crack and deterioration of the boundary elements ability to carry the applied shear through dowel action resulted in a "sliding shear" failure mode. A photograph of the hinging region of Specimen CI-1 at the end of the test is shown in Fig. B-5. Buckling of flexural reinforcement in spalled regions at the base of the wall is evident.

Load versus Deflection Relationships

The load versus top-deflection relationship for Specimen CI-1 is shown in Fig. B-6. Yielding of outer vertical bars in the boundary elements occurred during Cycle 2 at a load of 51.3 kips (22.8 kN) and a corresponding top-deflection of 1.24 in. (32 mm). Full yielding of the boundary elements occurred during Cycle 2 at a load of 62.4 kips (228.0 kN) and a corresponding top deflection of 1.45 in. (37 mm). Based on measured steel strains, tensile yielding in the primary flexural reinforcement on both sides of the wall spread to a level of 6 ft (1.8 m) above the base during Cycle 2.

The maximum load carried by Specimen CI-1 was 76.1 kips (338.5 kN) in the negative half of Cycle 12. The peak load carried to the positive half of Cycle 22 was 53.3 kips (237 kN) which corresponds to a 30% loss in load carrying capacity. A 69% loss of load carrying capacity was observed during the negative half of Cycle 22.

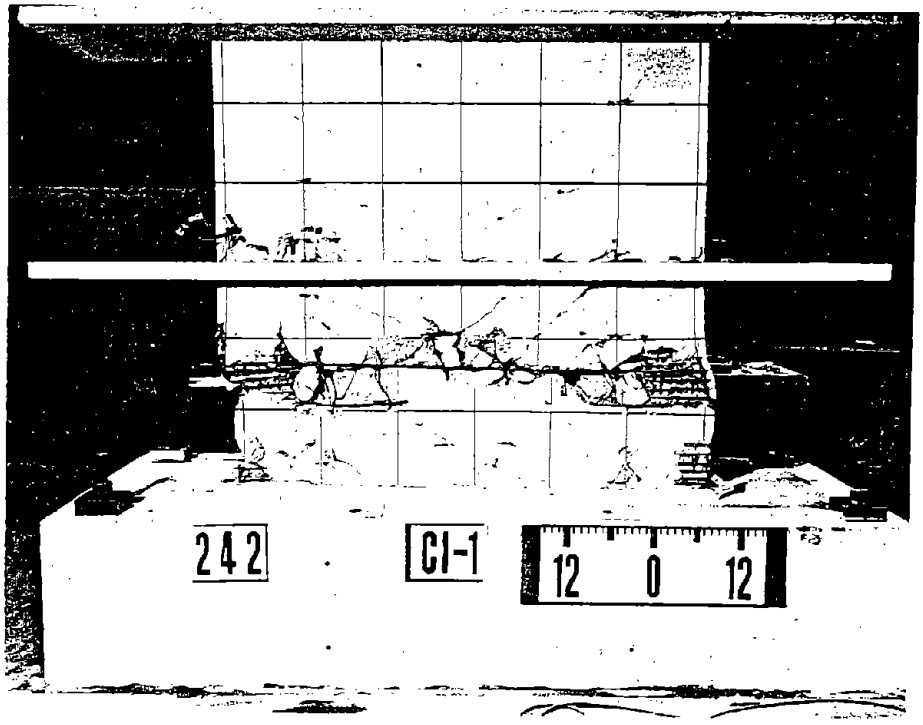

Fig. B-5 Specimen CI-1 at End of Test

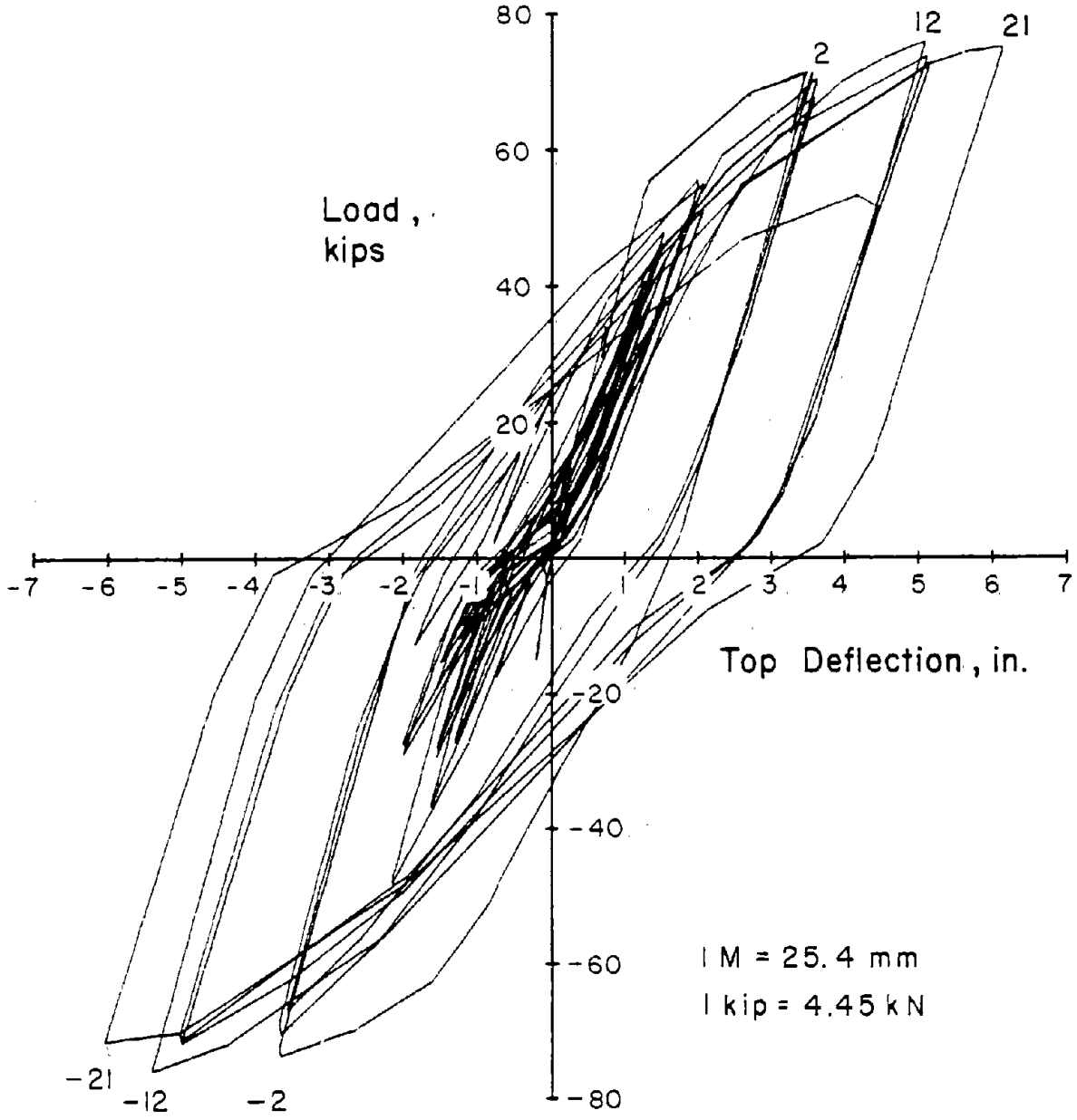

Fig. B-6 Load versus Top Deflection Relationship for Specimen CI-1

Complete load versus deflection relationships for the first and second story levels are shown in Fig. B-7.

Load versus Rotation Relationships

Complete load versus rotation relationships are shown in Fig. B-8. Base rotations were included in the first story data. Maximum rotation at the base, measured over the first 3 in. (76 mm) of wall, was 0.005 rad. in Cycle 21 at a corresponding load of 71.7 kips (318.9 kN). Base rotations were relatively small as shown in the figure.

Rotational deformations were concentrated in the first story region as shown in Fig. B-8b. The maximum rotation over the first story was 0.015 rad. in Cycle 21. Load versus the sum of first and second story rotations is shown in Fig. B-8a. The maximum rotation over the 6-ft (1.83 m) hinging region was 0.020 rad. in Cycle 21.

Load versus Shear Distortion Relationships

Complete load versus shear distortion relationships are shown in Fig. B-9. The largest shear distortions were measured in the first story as shown in Fig. B-9b. The maximum first story shear distortion was 0.042 rad. in Cycle 21. A large amount of sliding along the major horizontal crack in the first story was evident as shown by the extreme pinching in the last few load cycles of Fig. B-9b. By comparison, less pinching was observed in the shear distortion hysteresis loop of the second story as shown in Fig. B-9a. Maximum shear distortion in the second story was 0.010 rad. in Cycle 21.

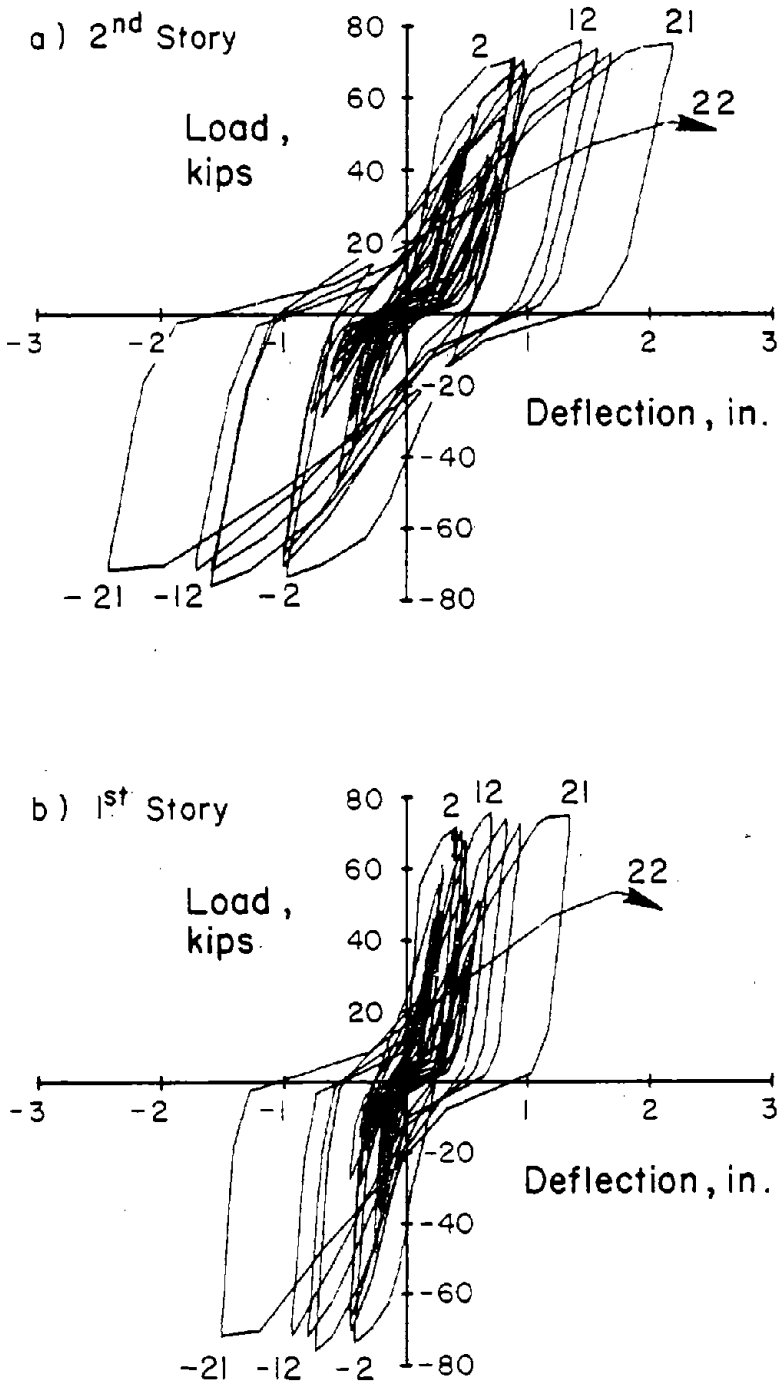

Fig. B-7 Load versus Deflection Relationships for Specimen CI-1

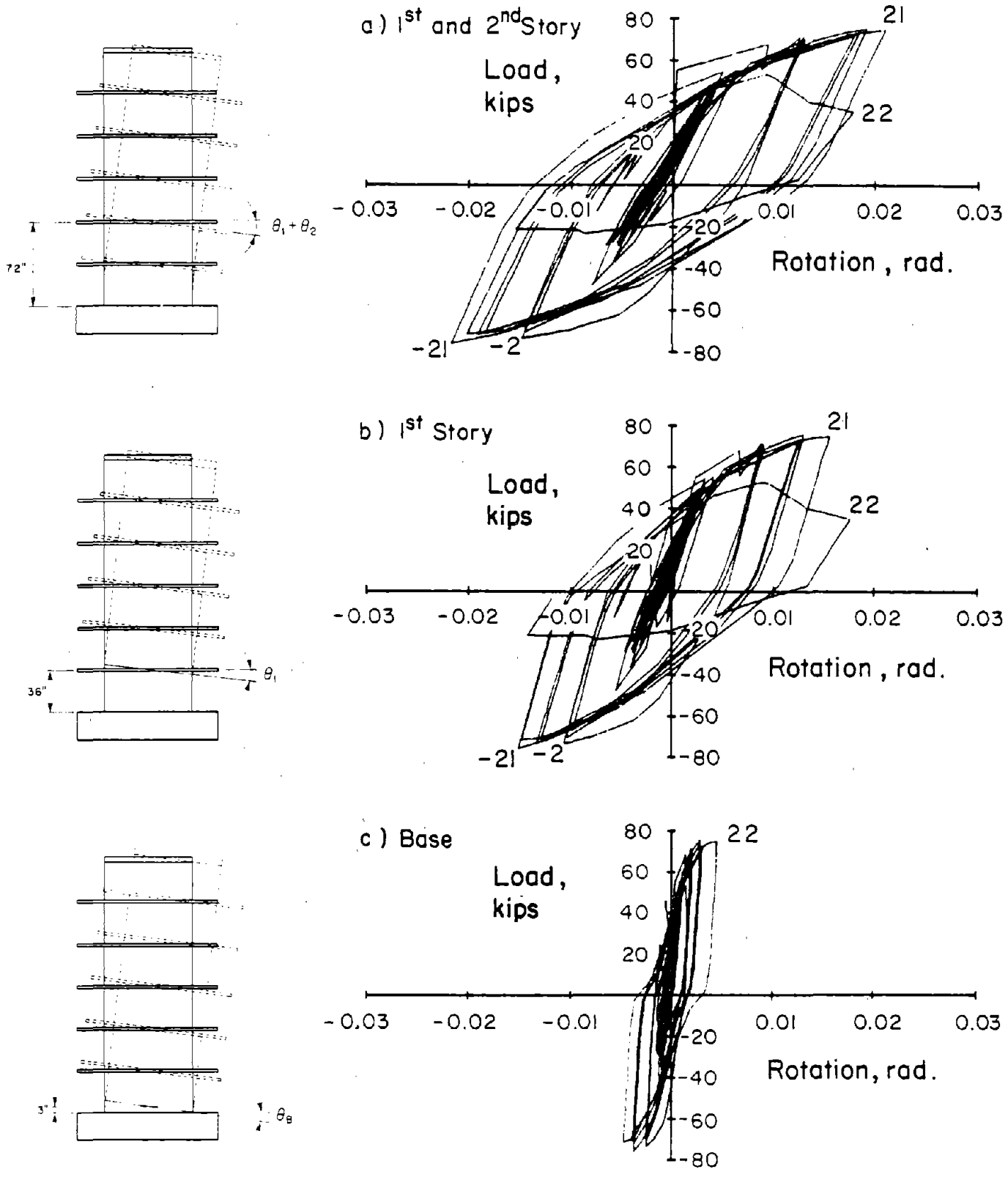

Fig. B-8 Load versus Rotation Relationships for Specimen CI-1

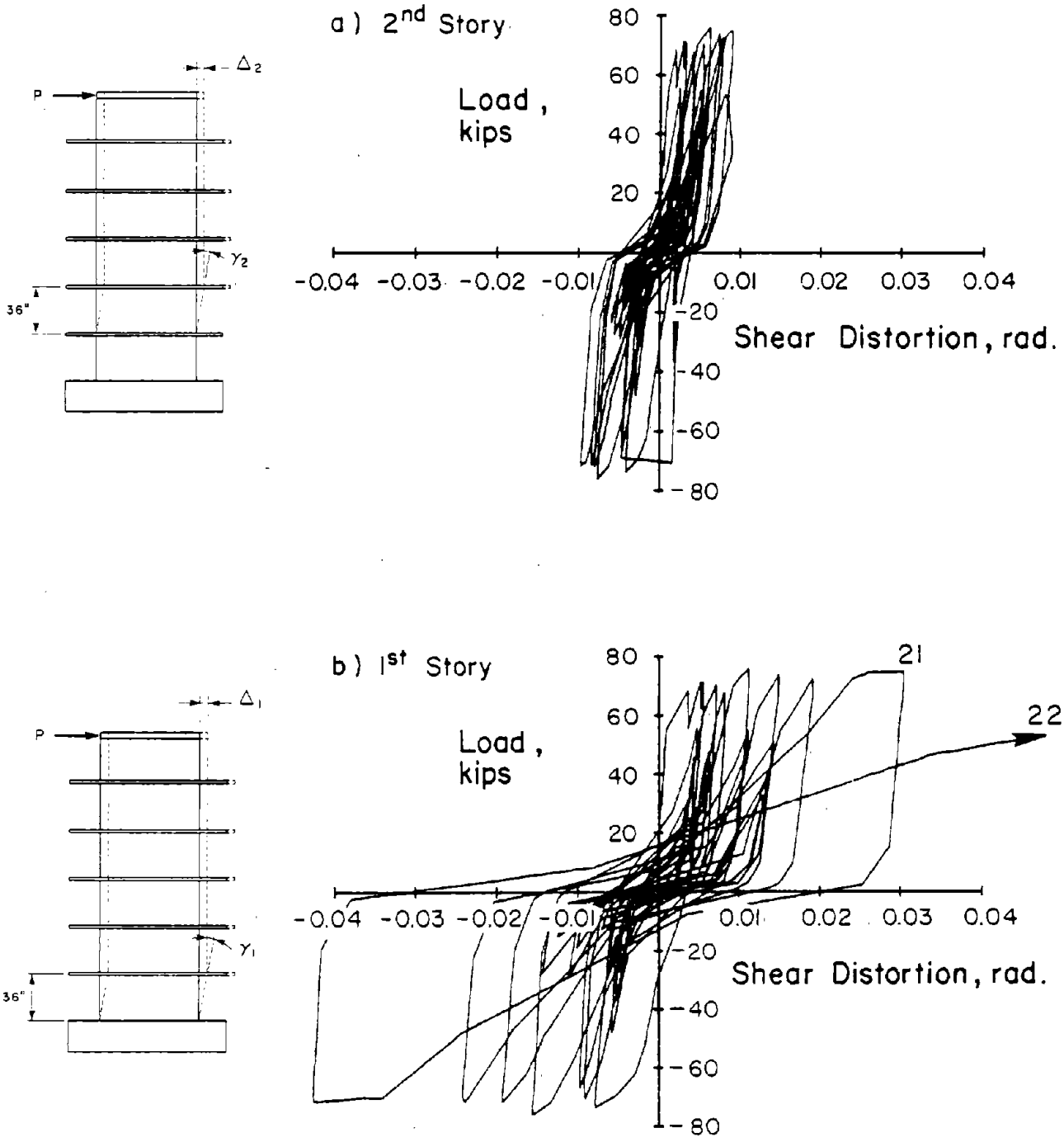

Fig. B-9 Load versus Shear Distortion Relationships for Specimen CI-1

Deflections

Deflection components for Specimen CI-1 are shown in Fig. B-10 for Cycles 10, 20, and 21. These cycles represent the end of Phase I, the end of Phase II, and the last stable load cycle. Dashed lines in the figures indicate extrapolated data.

The figures show that shear deformation was dominant within the first story region. Shear distortions were fairly constant between the 3-ft (0.91 m) and 6-ft (1.83 m) levels. On the other hand, rotational deflection within the first 3 ft (0.91 m) was relatively small. However, rotation is shown to increase from the 3-ft (0.91 m) to 6-ft (1.83 m) level, bringing the shear and rotational deflections to near equal proportions at the 6-ft level.

Reinforcement Strains

Figures B-11 through B-13 present load versus reinforcement strains at various locations in Specimen CI-1. Figures B-14 through B-18 present strain gradients across selected sections through the wall and slabs. Small numbers next to successive curves indicate load cycles.

Specimen PW-1

Observed Behavior

Specimen PW-1 was subjected to 24 complete reversing load cycles. The load history of Specimen PW-1 was similar to that of Specimen CI-1. First cracking was observed in the first story at an applied load of 7.2 kips (32 kN).

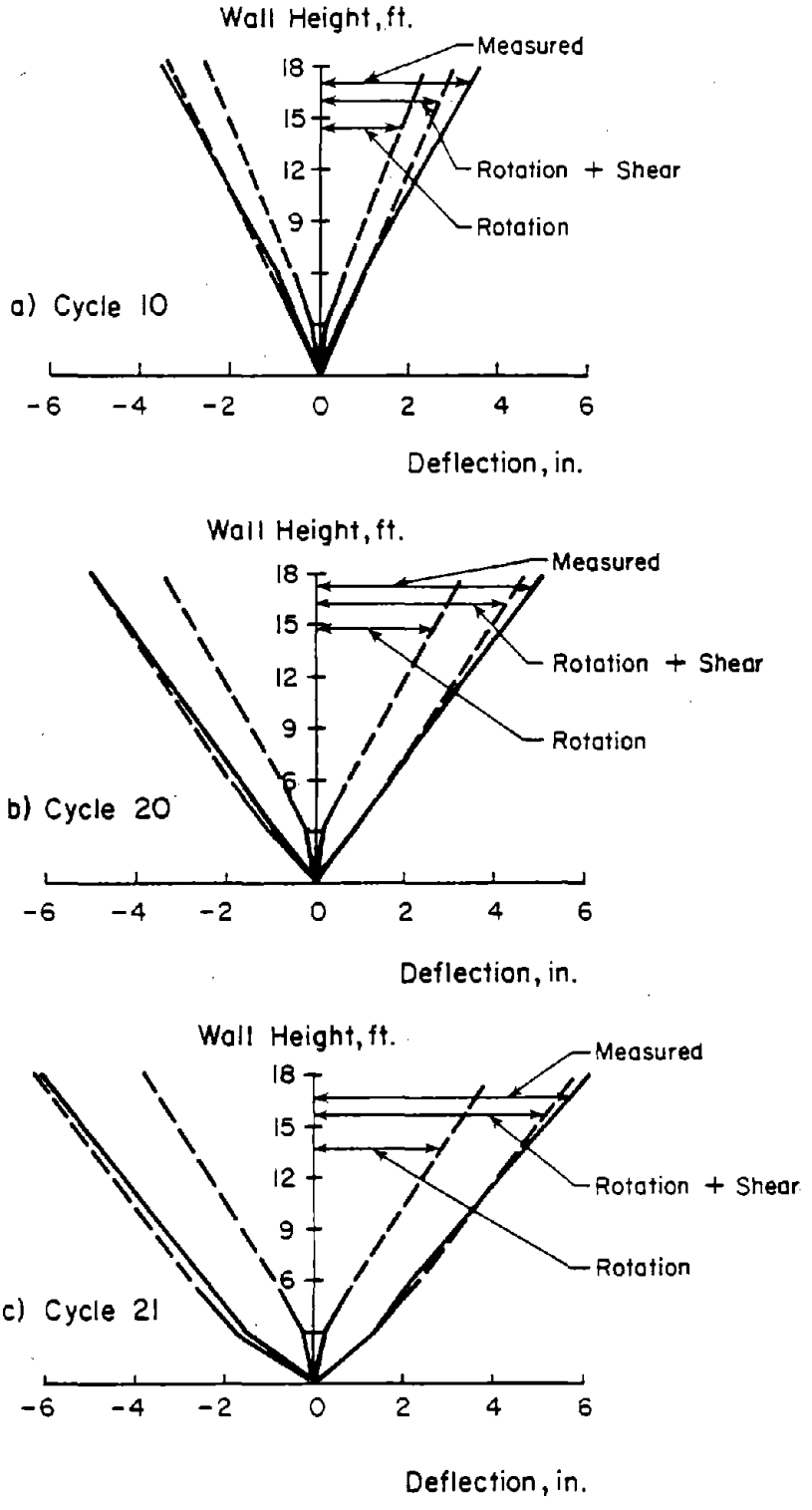

Fig. B-10 Deflection Components for Specimen CI-1

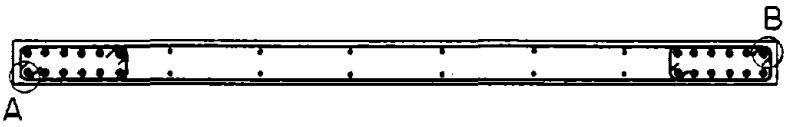

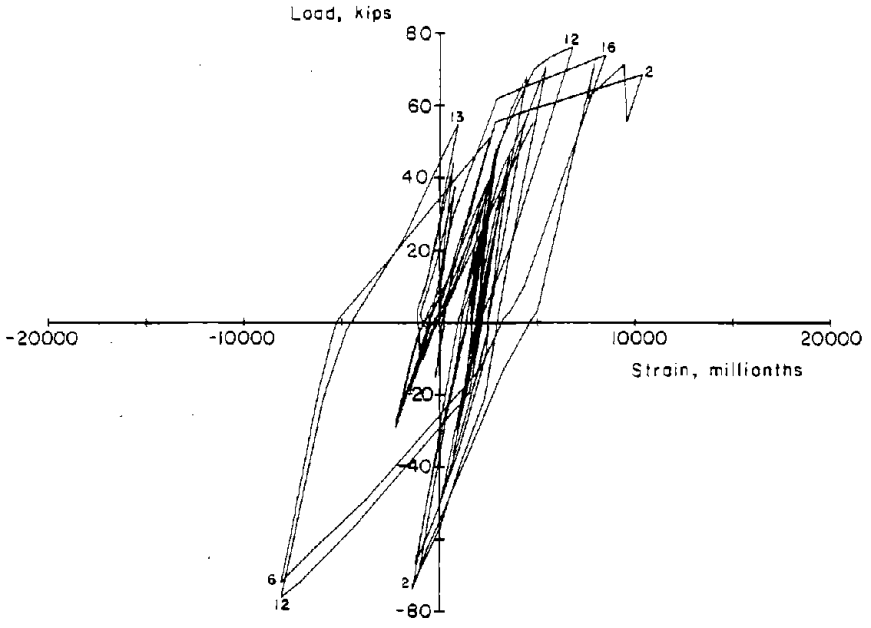

a) 1.5 ft above Base at Location A

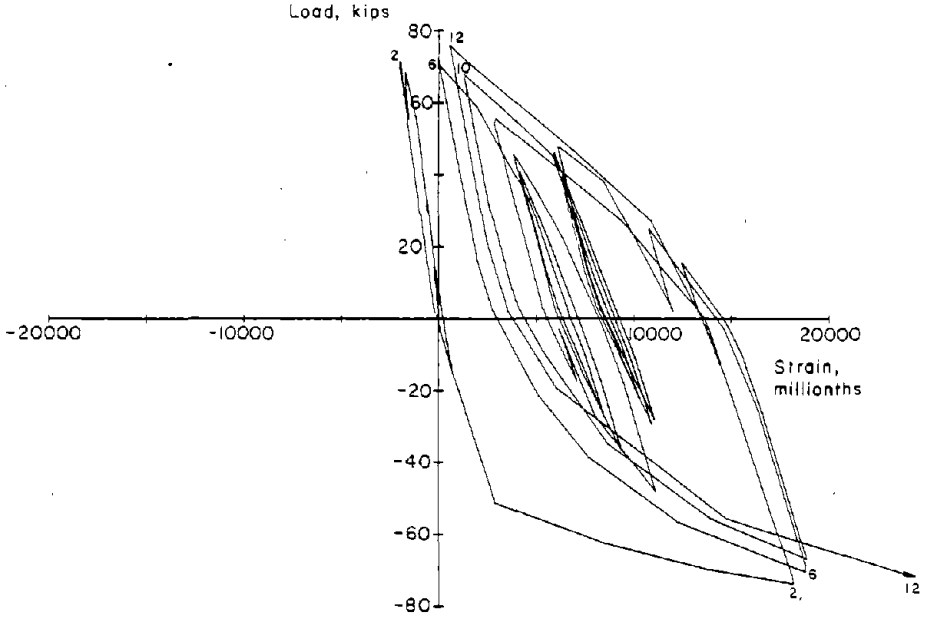

b) 1.5 ft above Base at Location B

Fig. B-11 Load versus Vertical Steel Strains for Specimen CI-1

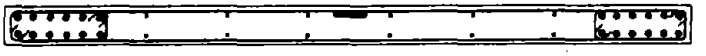

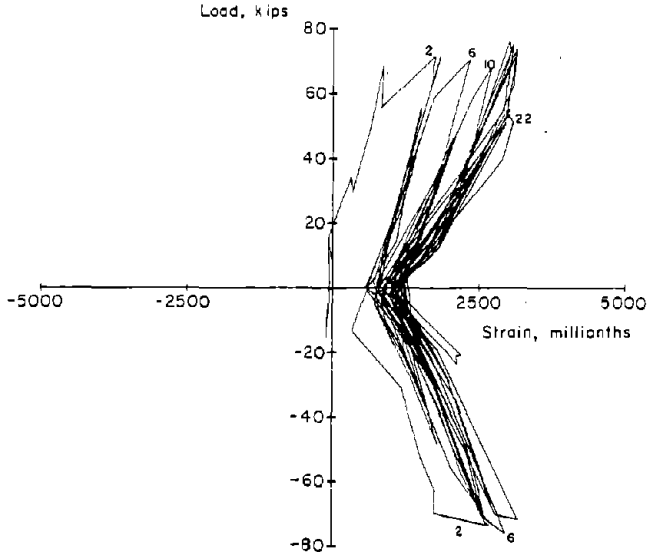

a) 3 ft above Base at Center

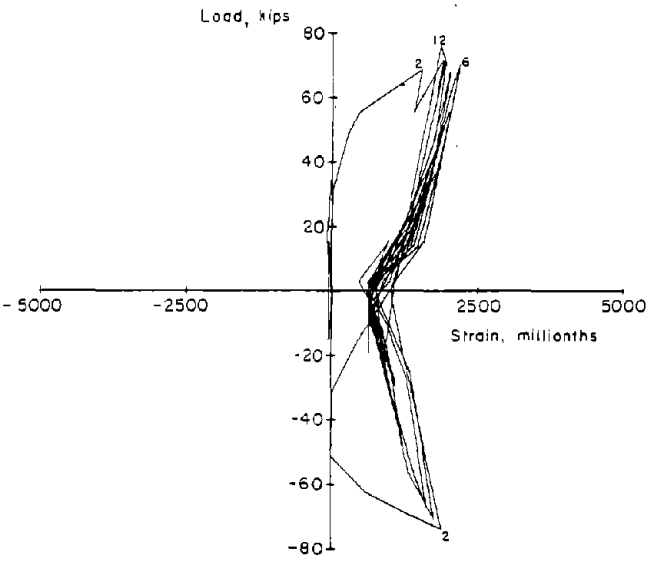

b) 1.5 above Base at Center

Fig. B-12 Load versus Horizontal Steel Strains for Specimen CI-1

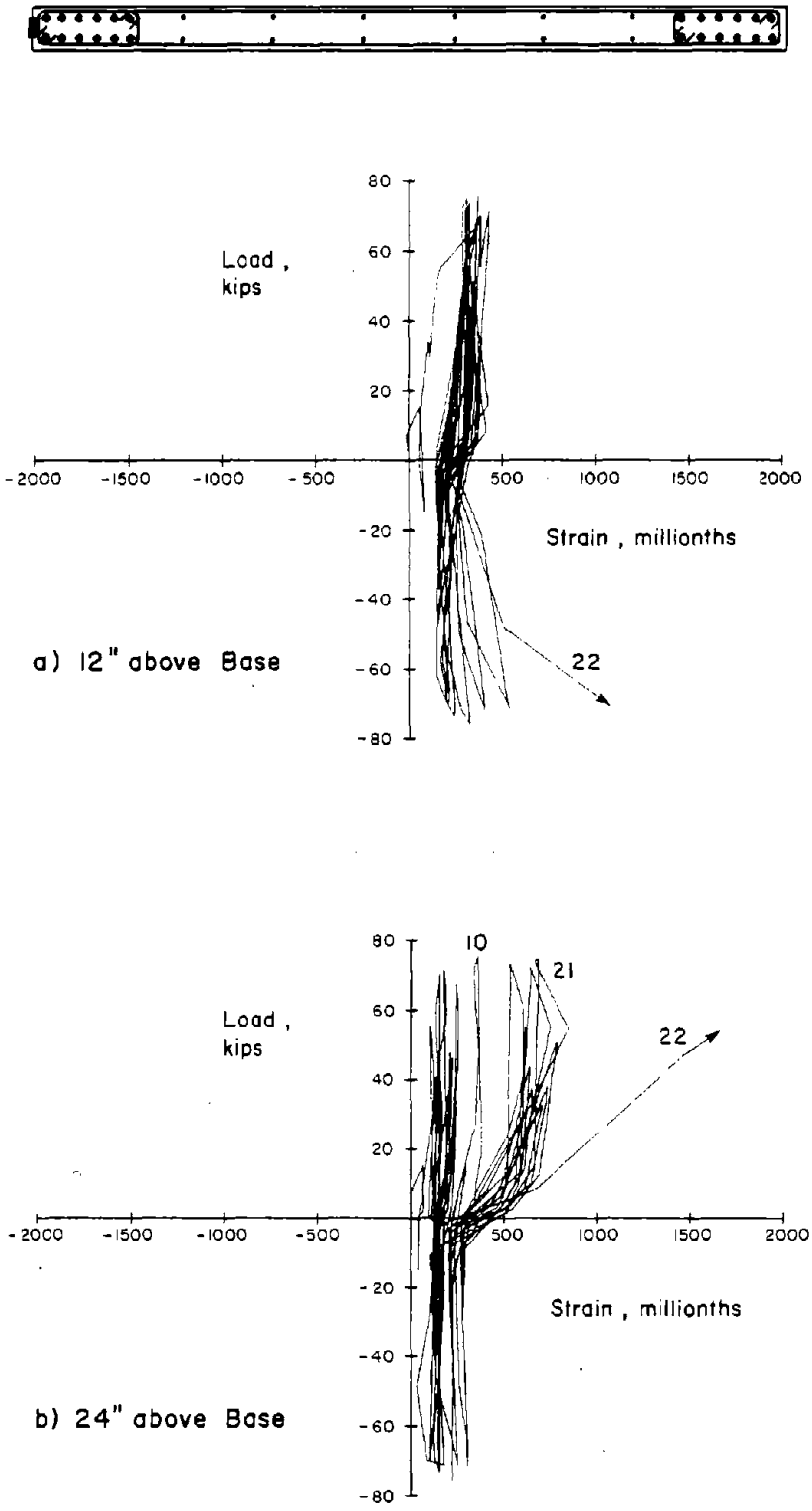

Fig. B-13 Load versus Confinement Hoop Strains for Specimen CI-1

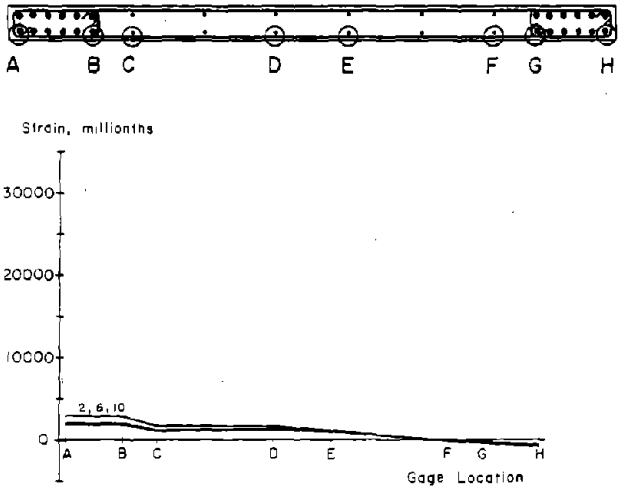

a) 6 ft above Base

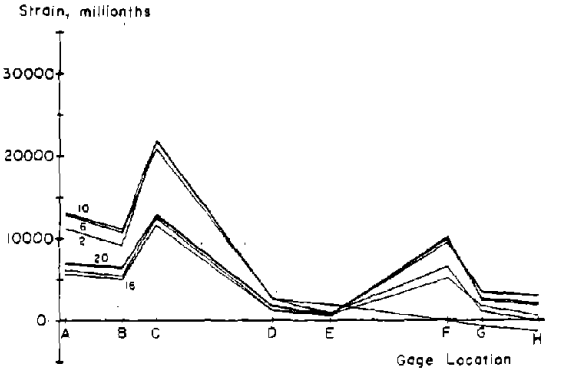

b) 3 ft above Base

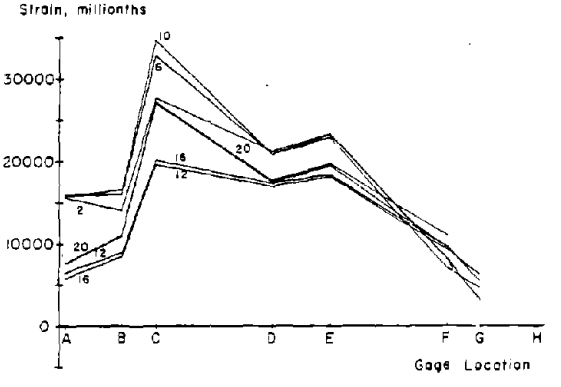

c) Base

Fig. B-14 Strain Distribution Across Wall for Vertical Reinforcement in Specimen CI-1

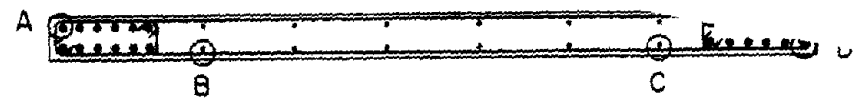

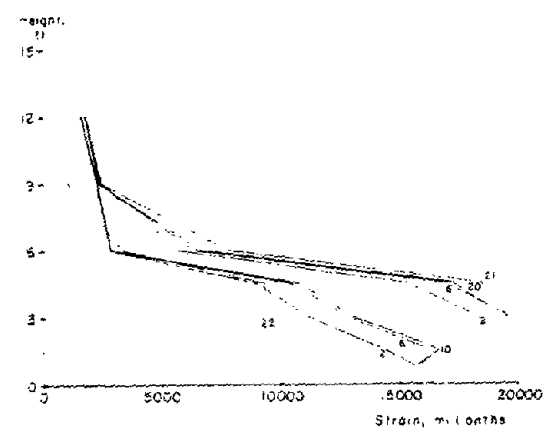

a) Location A

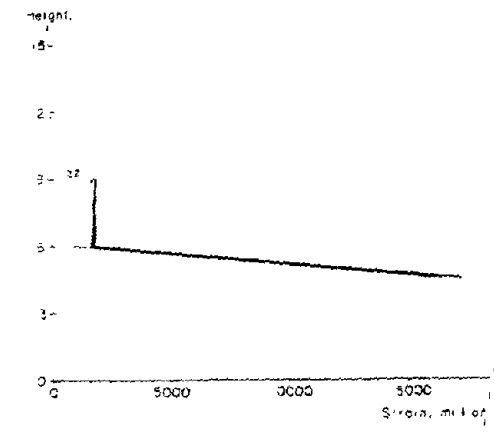

b) Location B

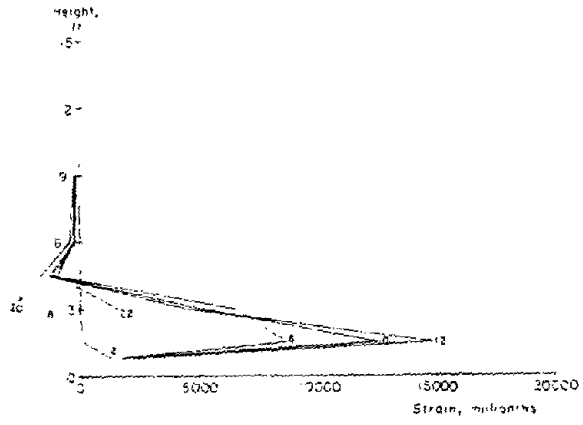

c) Location C

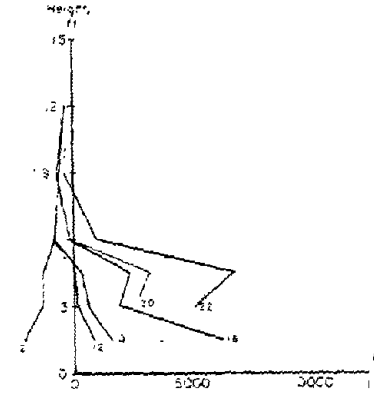

d) Location D

Fig. B-15 Strain Distribution Over Height Abov
for Vertical Reinforcement in Specir

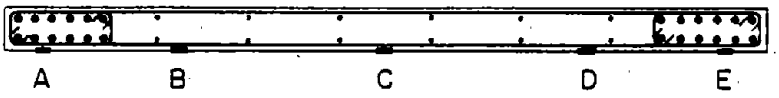

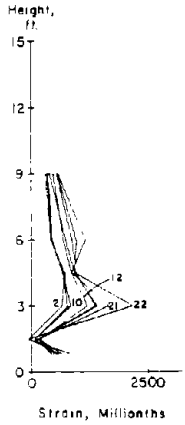

a) Location A

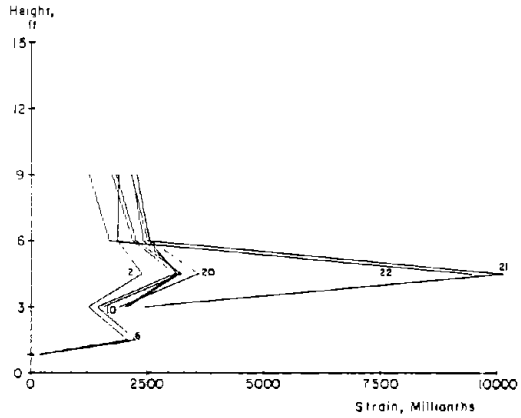

b) Location B

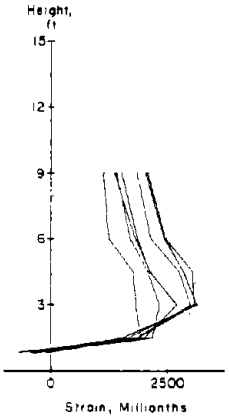

c) Location C

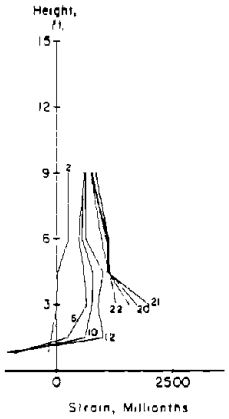

d) Location D

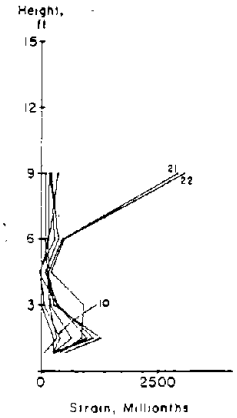

e) Location E

Fig. B-16 Strain Distribution Over Height Above Base for Horizontal Reinforcement in Specimen CI-1

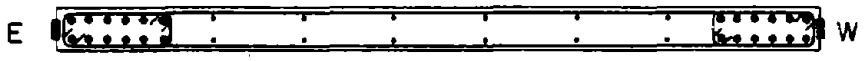

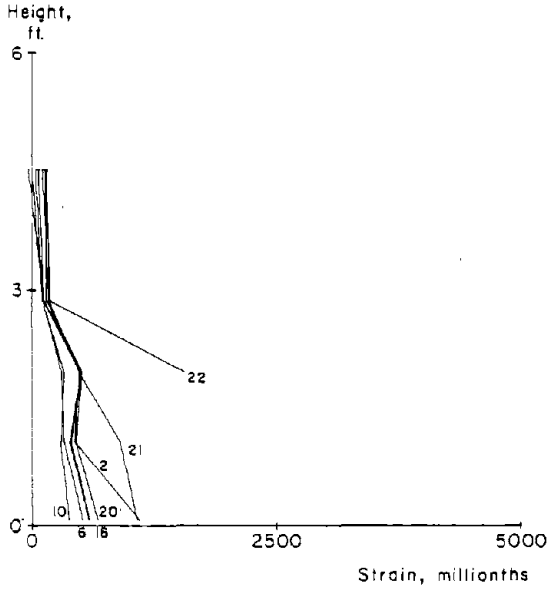

a) East Boundry Element

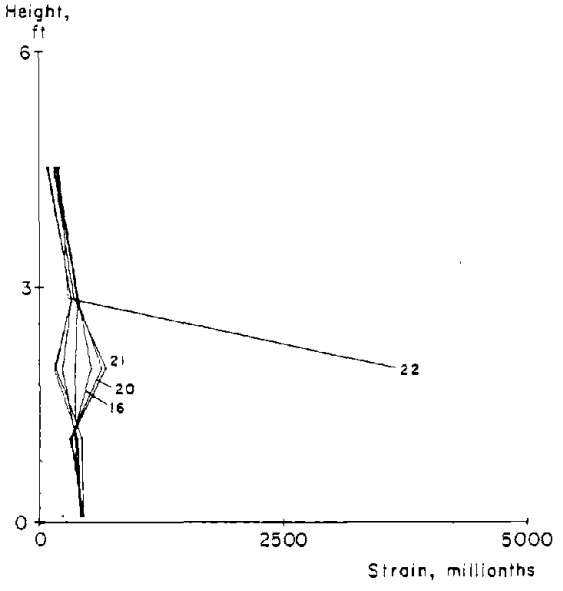

b) West Boundry Element

Fig. B-17 Hoop Strain Distribution Over Height Above Base for Specimen CI-1

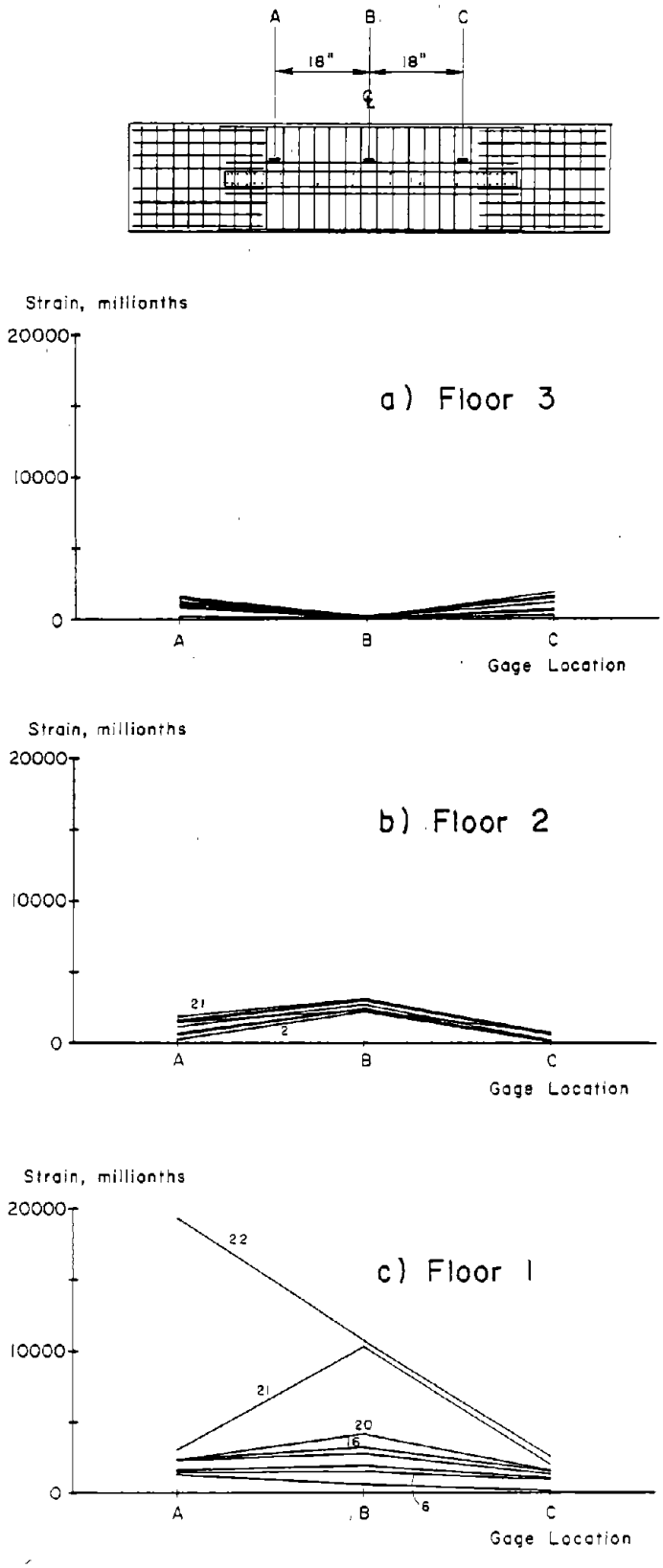

Fig. B-18 Strain Distribution in Slab Reinforcement for Specimen CI-1

Cracks ran horizontally from the top of the first story opening to the boundary elements. Diagonal cracks were also found in the first story wall piers. As inelastic load cycles were applied to the specimen, cracks in wall piers propagated into the boundary elements. A photograph of the hinging region at the end of Phase I is shown in Fig. B-19. Crack widths were about 0.1 in. (3 mm).

During Phase II loading crack widths in the first story widened. A photograph of the hinging region at the end of Phase II is shown in Fig. B-20. It is apparent from the photograph that the cracks in the first story differ from those in Specimen CI-1. Diagonal cracking was predominate in one pier whereas horizontal cracks dominated the other.

During Phase III loading Specimen PW-1 failed by shear-compression of a pier element. A photograph of the specimen at the end of testing is shown in Fig. B-21.

Load Versus Deflection Relationships

The load versus top-deflection relationship for Specimen PW-1 is shown in Fig. B-22. Yielding of outer vertical bars in the boundary elements was observed during Cycle 2 at a load of 28.0 kips (169.0 kN) and a corresponding top deflection of 0.98 in. (25 mm). Full yielding of all boundary element vertical steel occurred at a load of 54.5 kips (242 kN) and a corresponding top deflecton of 1.81 in. (46 mm). Based on measured steel strains, tensile yielding of the primary flexural reinforcement on both sides of the wall spread to a level of 6 ft (1.8 m) above the wall base during Cycle 2.

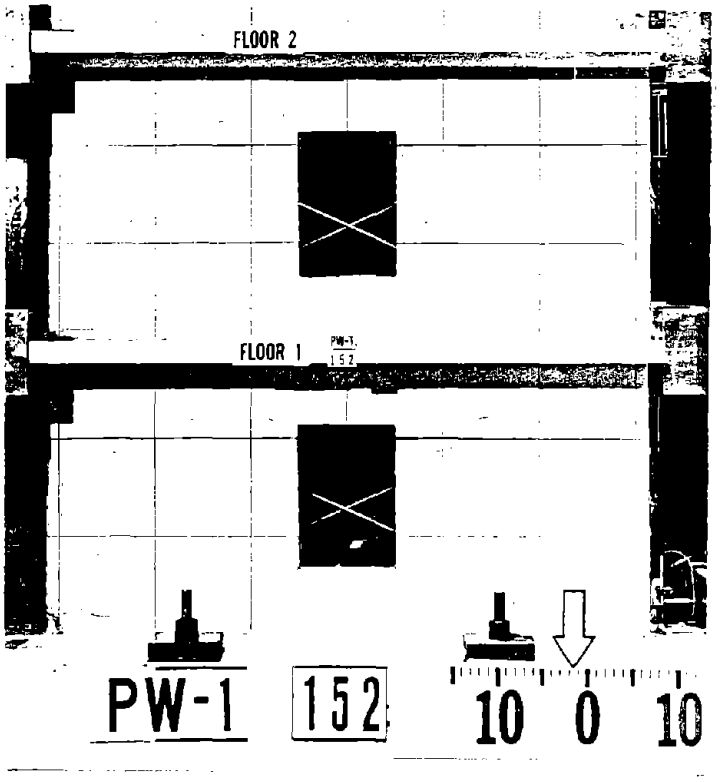

Fig. B-19 Crack Pattern of Specimen PW-1 at End of Phase I

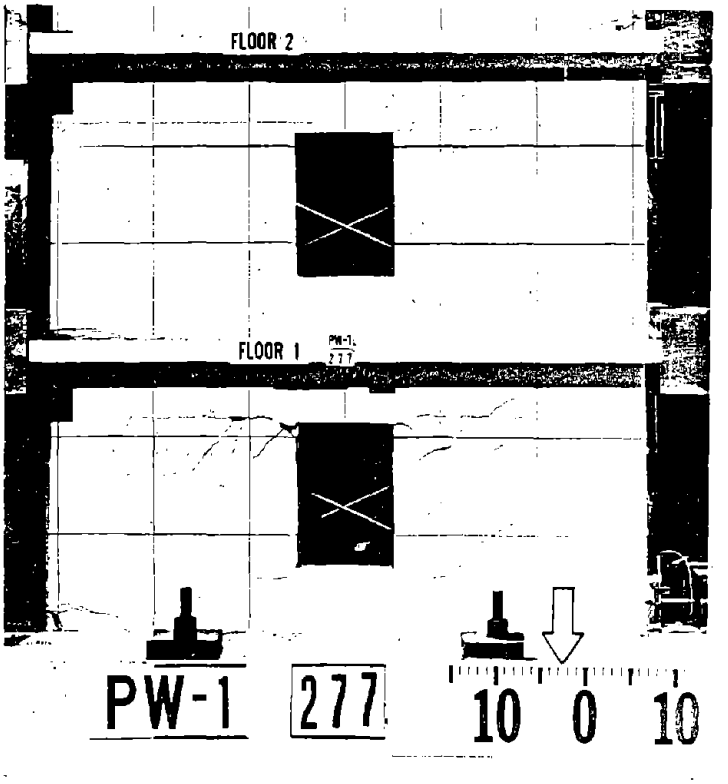

Fig. B-20 Crack Pattern of Specimen PW-1 at End of Phase II

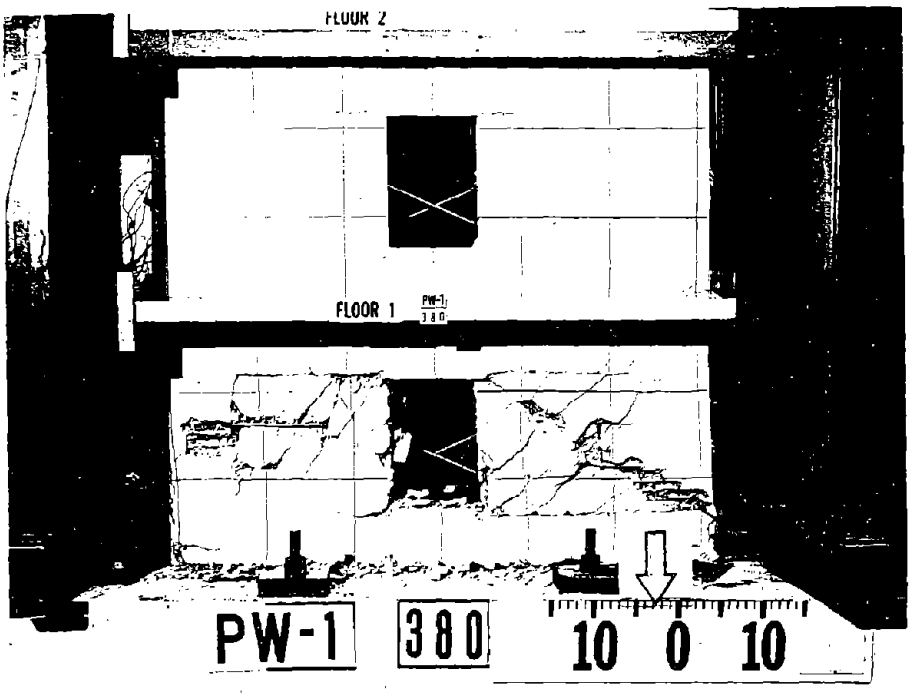

Fig. B-21 Specimen PW-1 at End of Test

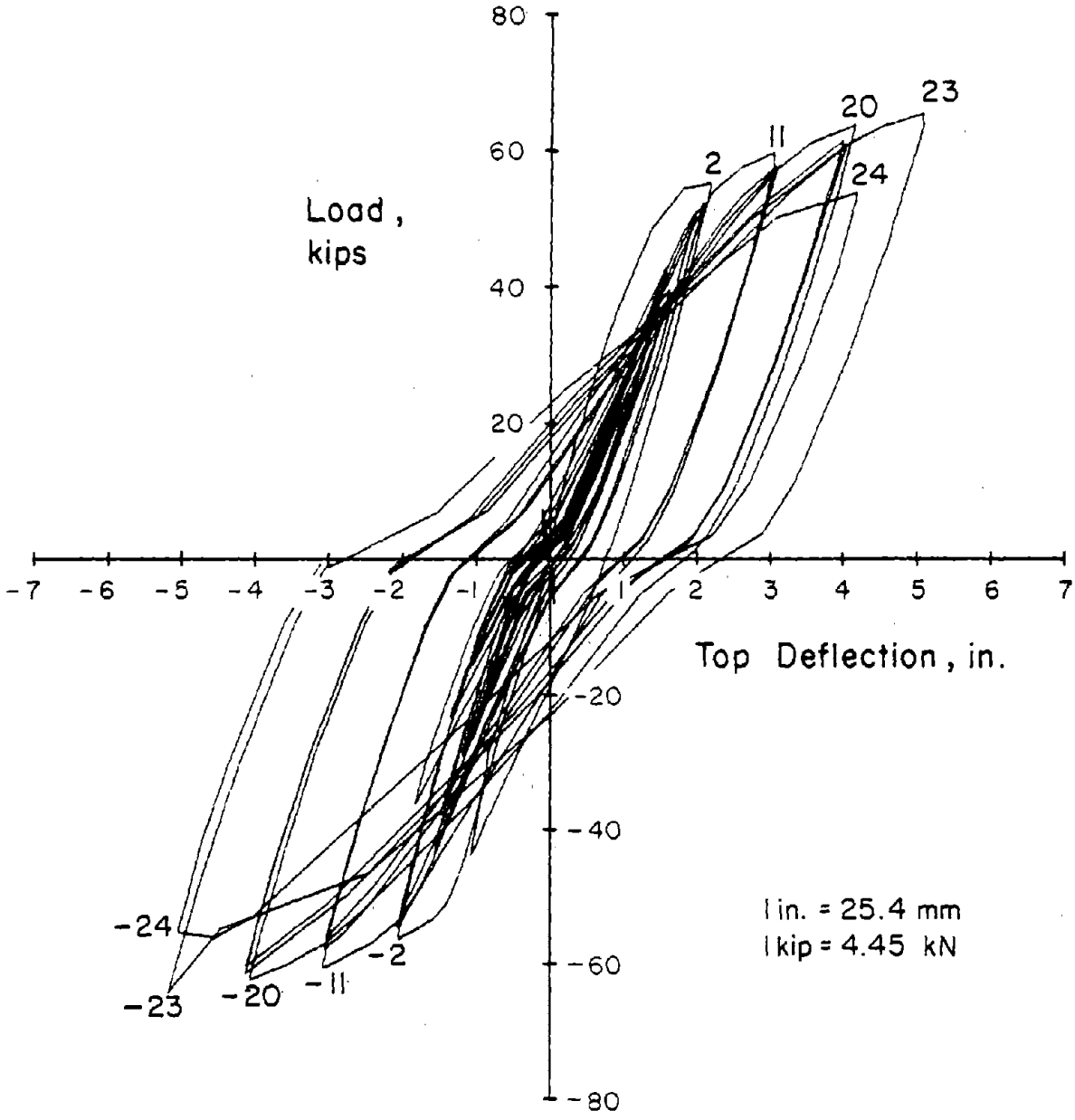

Fig. B-22 Load versus Top Deflection Relationship for Specimen PW-1

The maximum load carried by specimen PW-1 was 65.7 kips (292 kN) in Cycle 23. An 18% loss in load carrying capacity was observed in Cycle 24. As the load capacity began to drop in Cycle 24, significant loss of strength was observed and load was reversed.

Load versus deflection relationships for the first and second story levels are shown in Fig. B-23.

Load Versus Rotation Relationships

Load versus rotation relationships are shown in Fig. B-24. Rotation at the base, measured over the first 3 in. (76 mm), was 0.004 rad. in Cycle 23 at an applied load of 64.2 kips (285 kN). It is obvious that base rotations were small relative to first or second story rotations.

The first story load versus rotation relationship is shown in Fig. B-24b. Maximum rotation over the first story was 0.012 rad. in Cycle 3. Rotations tended to concentrate in the first story region.

Load versus rotation relationships for the first two stories are shown in Fig. B-24a. Maximum rotation over the 6-ft (1.83 m) region was 0.017 rad. in Cycle 23.

Load Versus Shear Distortion Relationships

Load versus shear distortion relationships for the first and second stories are shown in Fig. B-25. Shear distortions were concentrated in the first story. In Cycle 23, the maximum first story shear distortion was 0.034 rad. In the last few cycles, load versus first story shear distortion was characterized by

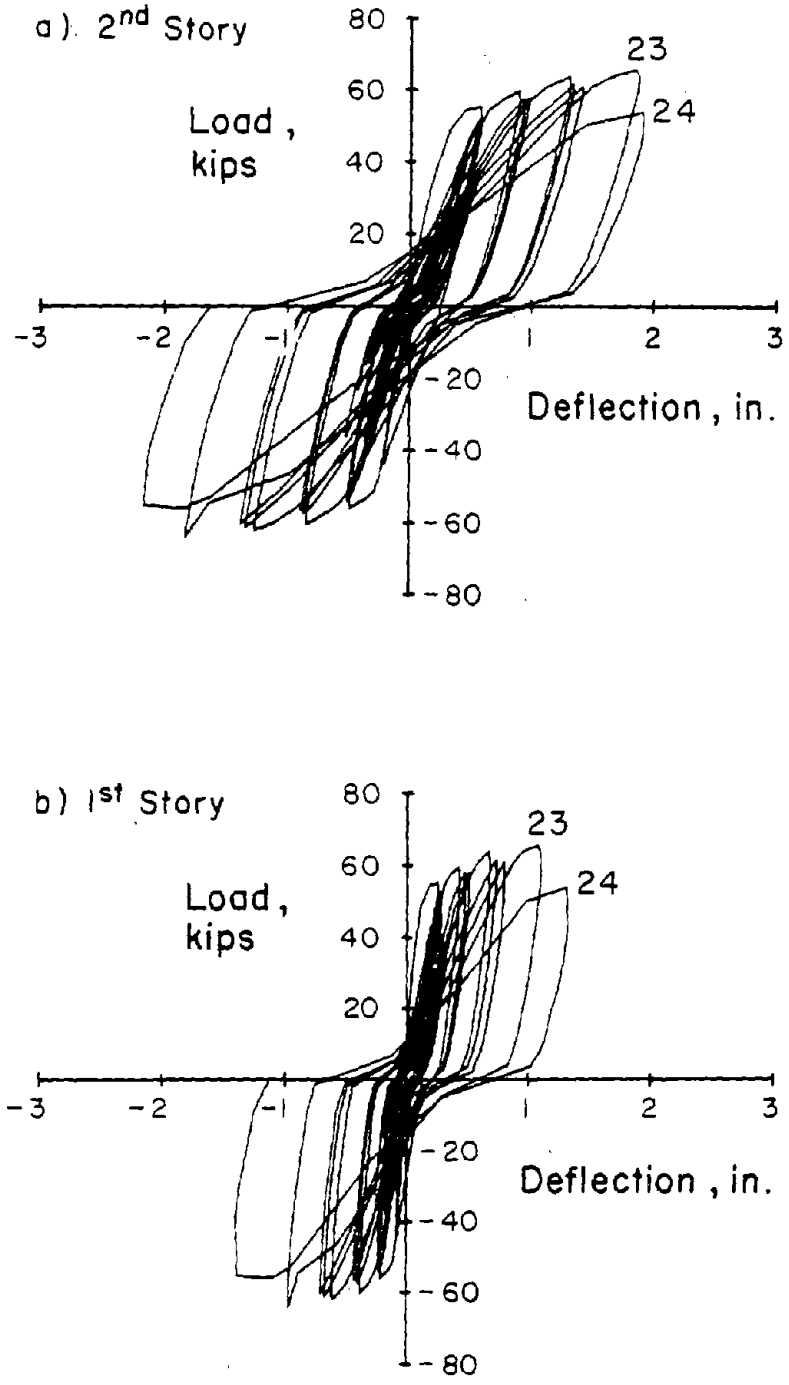

Fig. B-23 Load versus Deflection Relationships for Specimen PW-1

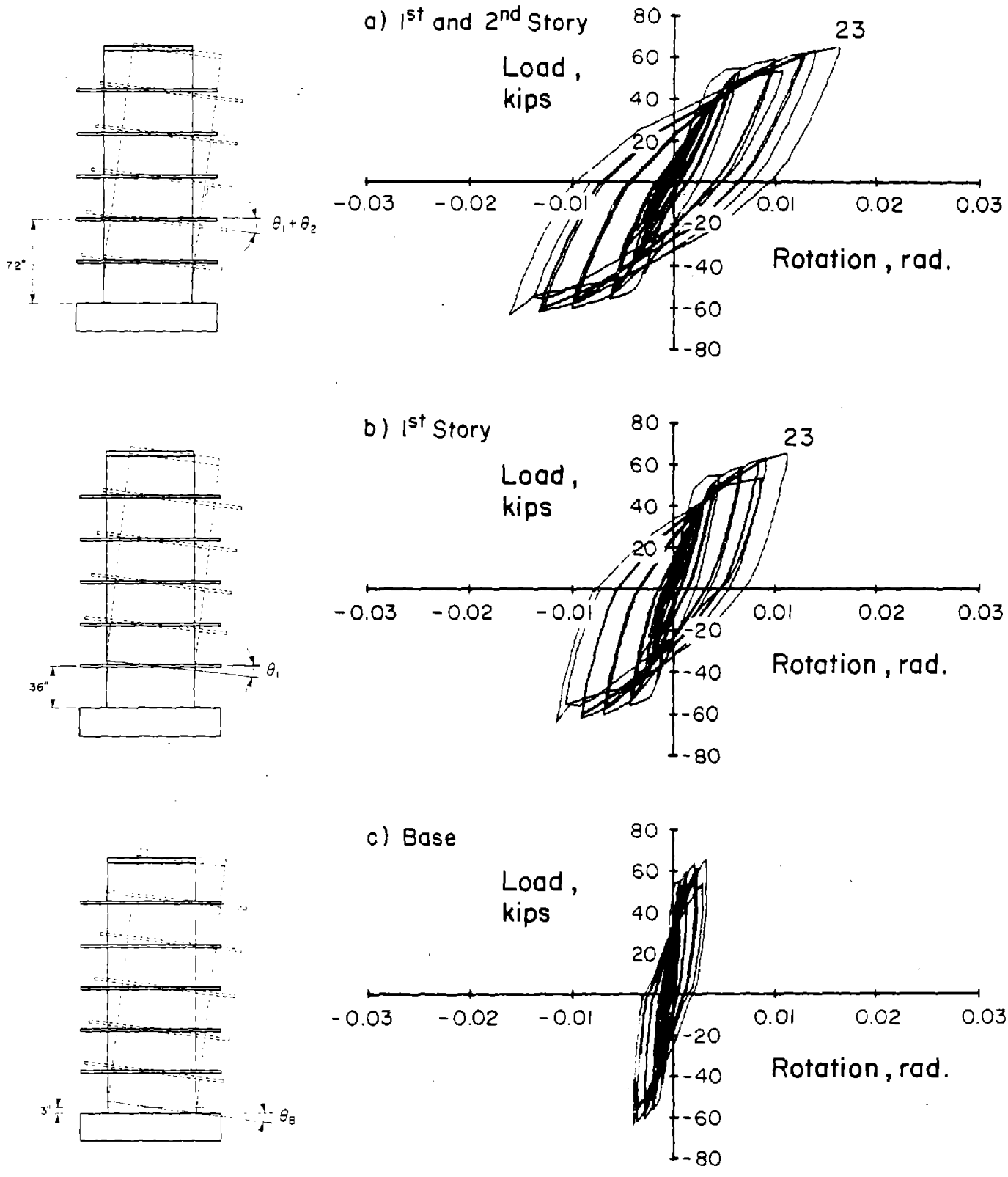

Fib. B-24 Load versus Rotation Relationships for Specimen PW-1

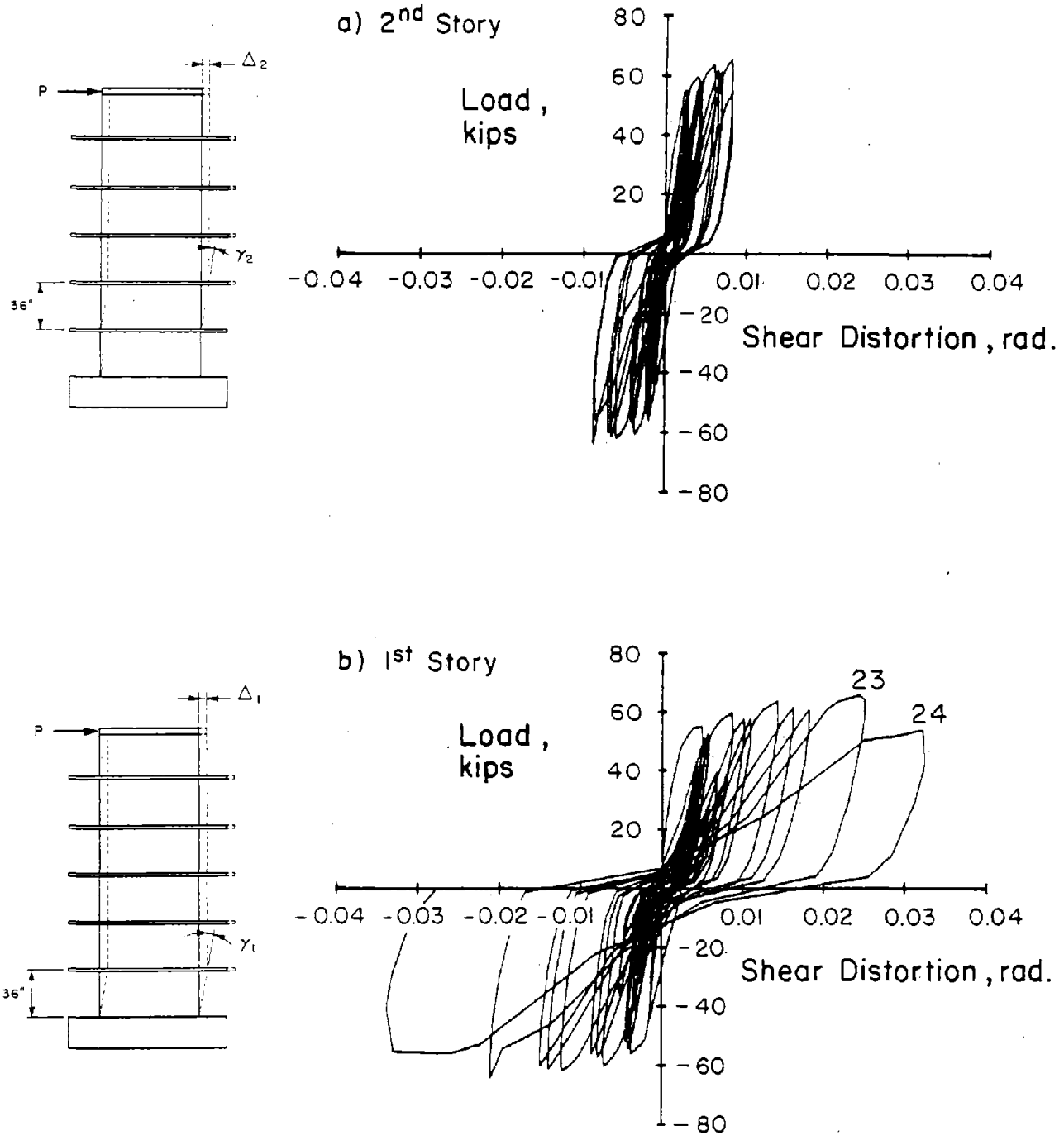

Fig. B-25 Load versus Shear Distortion Relationships for Specimen PW-1

severe pinching. This behavior indicates sliding along cracks during load reversals. Maximum shear distortion observed in the second story was 0.010 rad. in Cycle 23.

Deflections

Deflection components for Specimen PW-1 are shown in Fig. B-26 for Cycles 10, 19, and 23. These cycles occur at the end of Phase I, Phase II, and the last stable load cycle. Dashed lines in the figure indicate extrapolated data.

The figures indicate that shear deformations dominanted within the first story region. This behavior became more pronounced during Phase III loading. Significant slip along horizontal cracks in the first story was evident late in the test. From the 3-ft (0.91 m) level to the top of the wall, estimated shear deflections were relatively constant. The rotational component was relatively small in the first 3 ft (0.91 m). However, rotation increased steadily from the 3-ft (0.91 m) level to the top of the wall.

First story shear distortion measurements were lost because of malfunctioning instrumentation during testing. Therefore, shear deflection components were estimated by subtracting rotational deflection from measured lateral deflection. Assuming that calculated deflection components were in close agreement with the total measured, as was the case with specimen CI-1, this procedure provides a reasonable estimate of shear distortions.

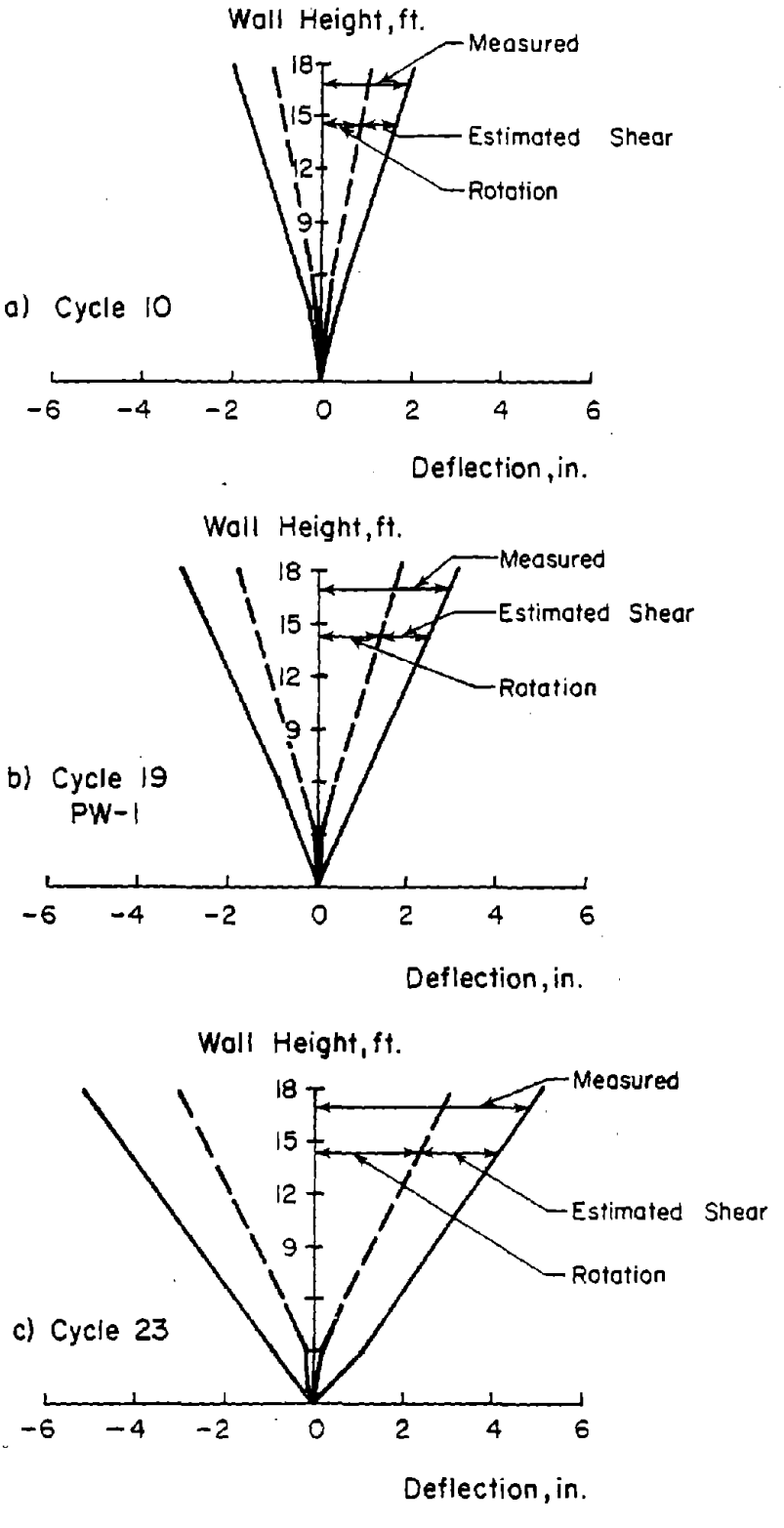

Fig. B-26 Deflection Components for Specimen PW-1

Reinforcement Strains

Figures B-27 through B-29 present load versus reinforcement strains at various locations in Specimen PW-1. Figures B-30 through B-34 present strain gradients across selected sections through the wall and slabs. Small numbers next to successive curves indicate load cycles.

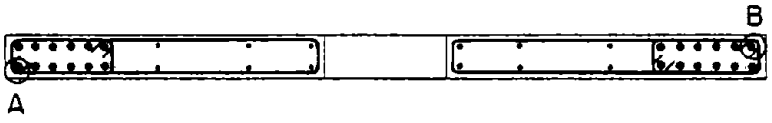

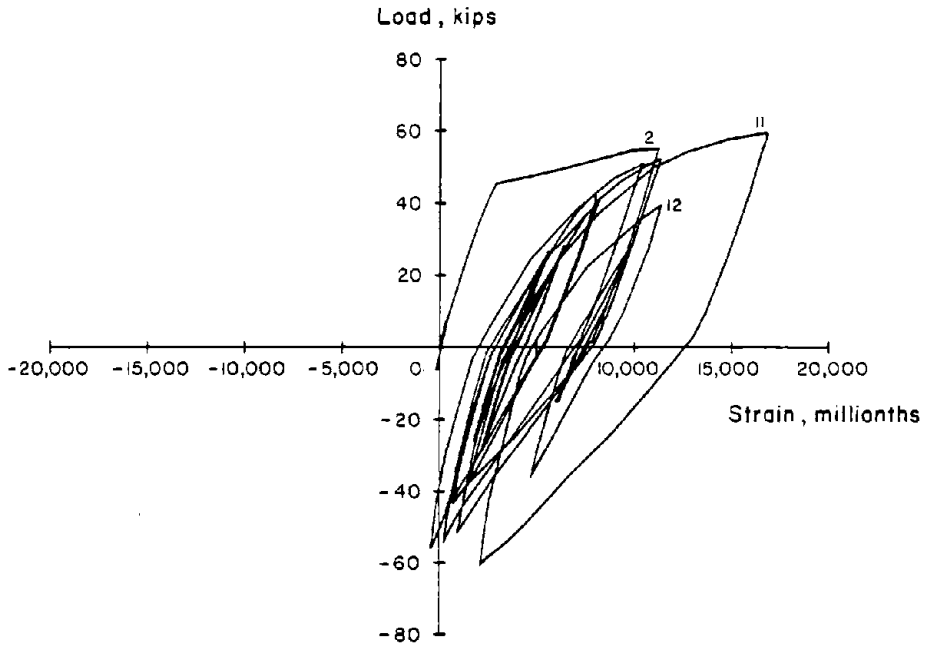

a) 1.5 ft above Base at Location A

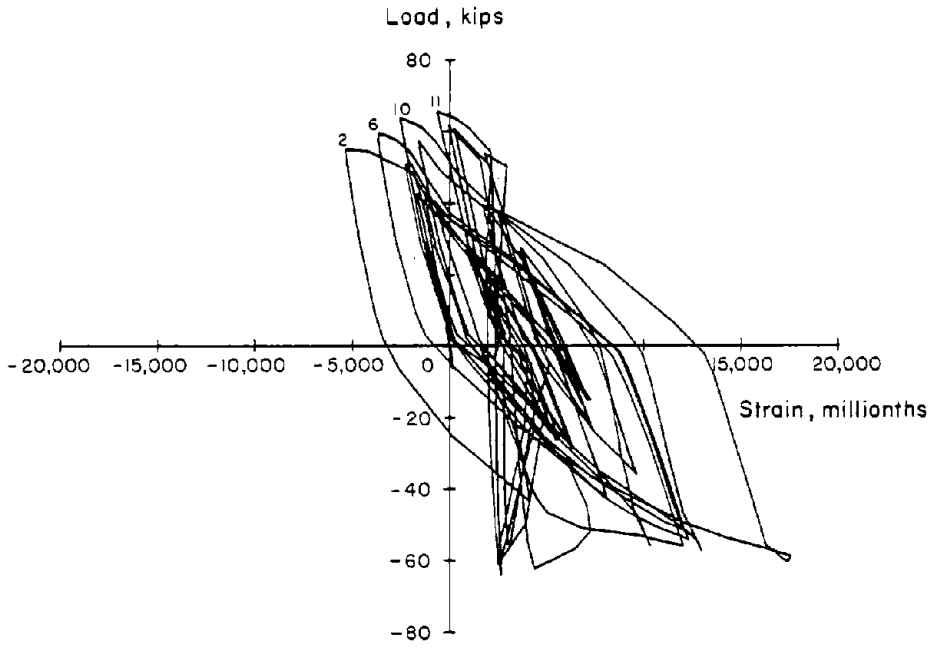

b) 1.5 ft above Base at Location B

Fig. B-27 Load versus Vertical Steel Strains for Specimen PW-1

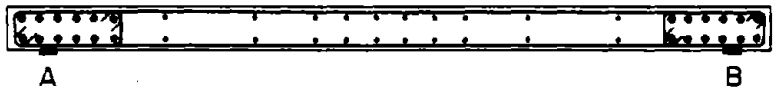

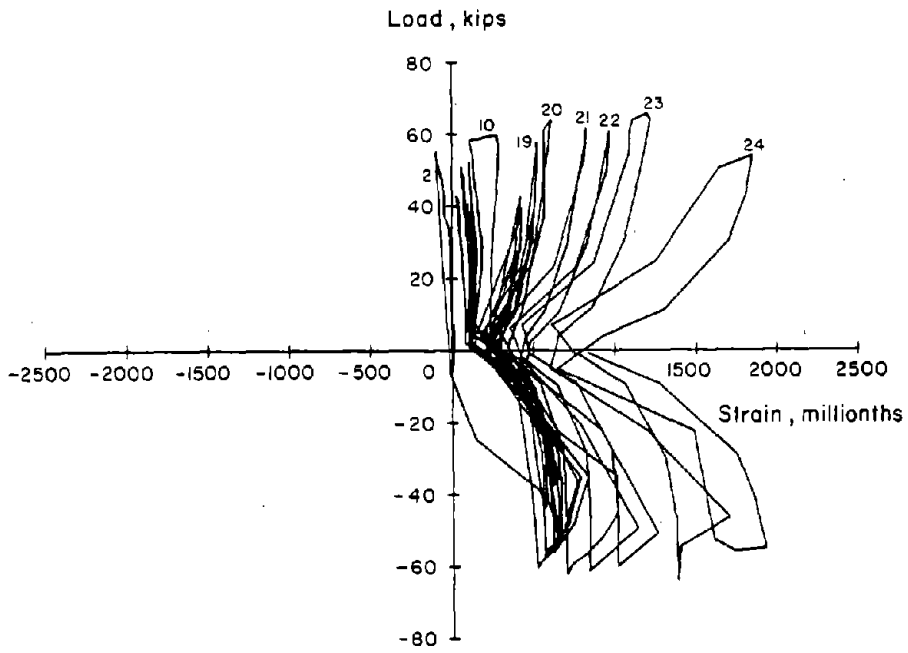

a) 3 ft above Base at Location B

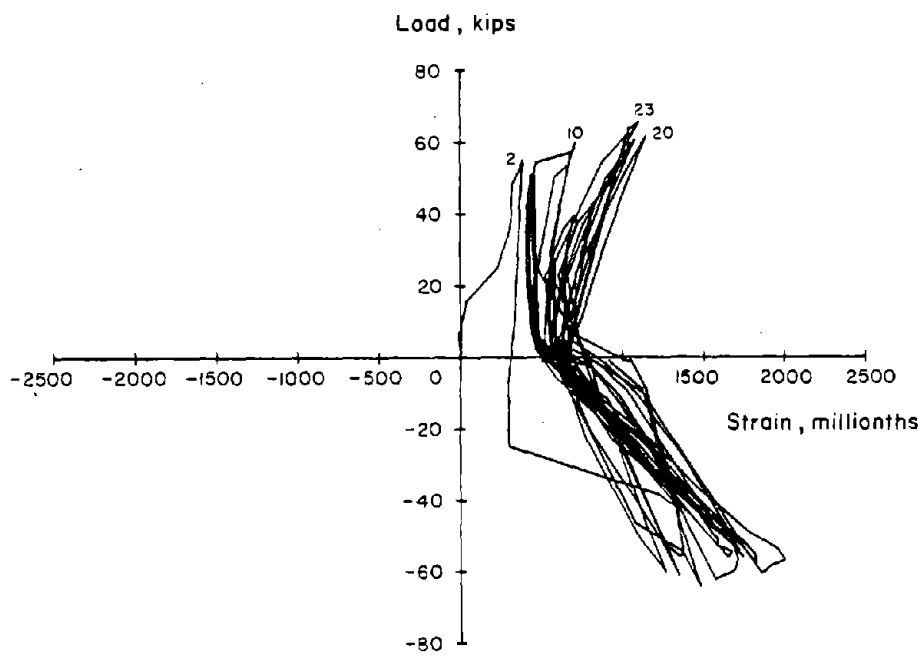

b) 1.5 ft above Base at Location A

Fig. B-28 Load versus Horizontal Steel Strains for Specimen PW-1

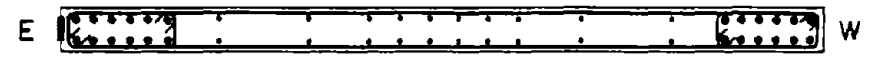

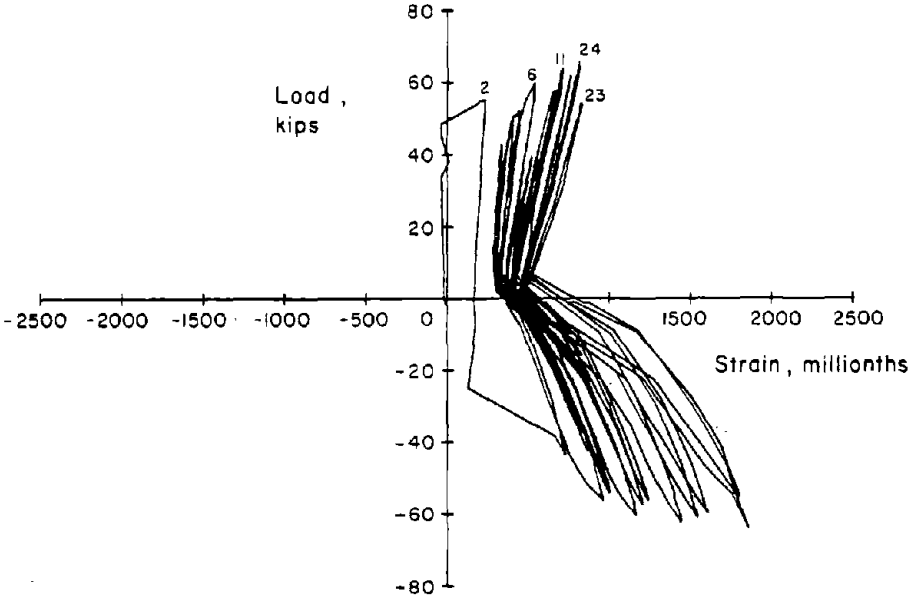

a) 12" above Base at East Boundry

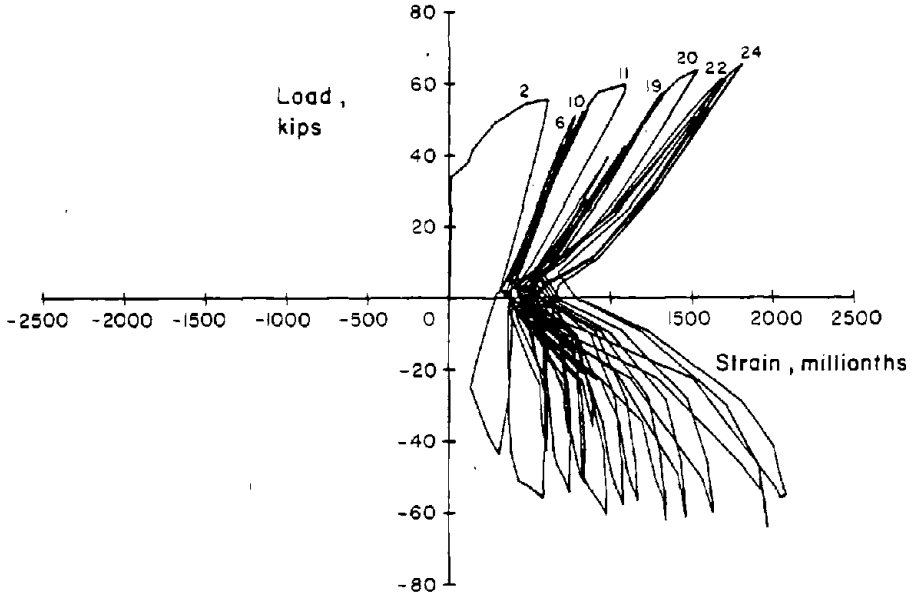

b) 6" above Base at East Boundry

Fig. B-29 Load versus Hoop Strains for Specimen PW-1

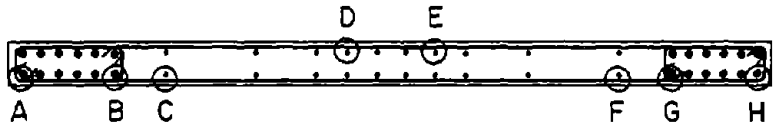

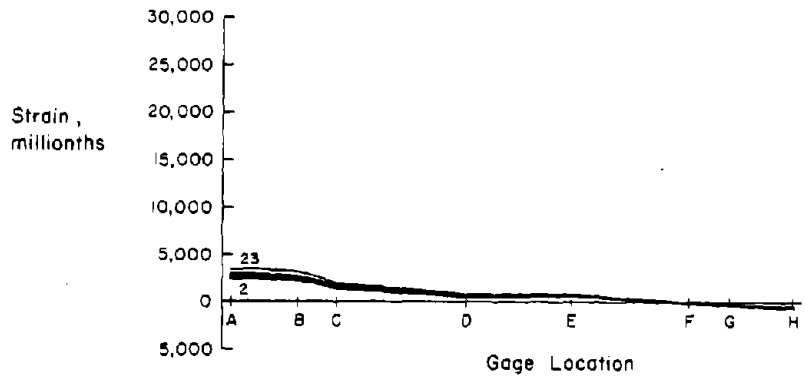

a) 6 ft above Base

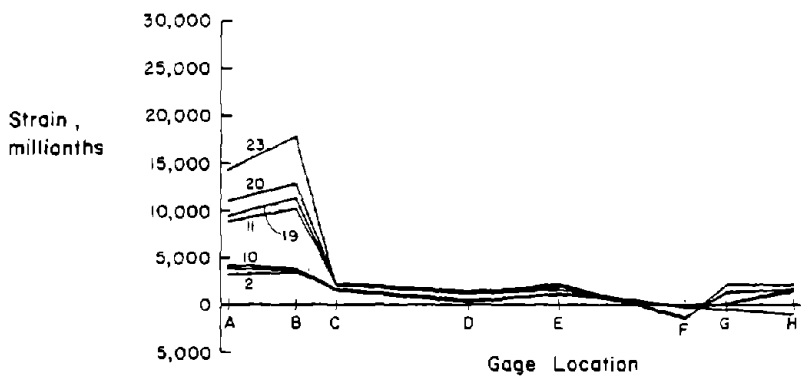

b) 3 ft above Base

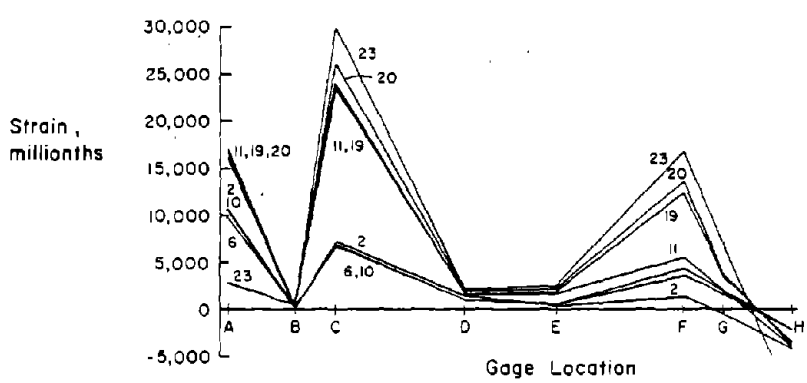

c) Base

Fig. B-30 Strain Distribution Across Wall for Vertical Reinforcement in Specimen PW-1

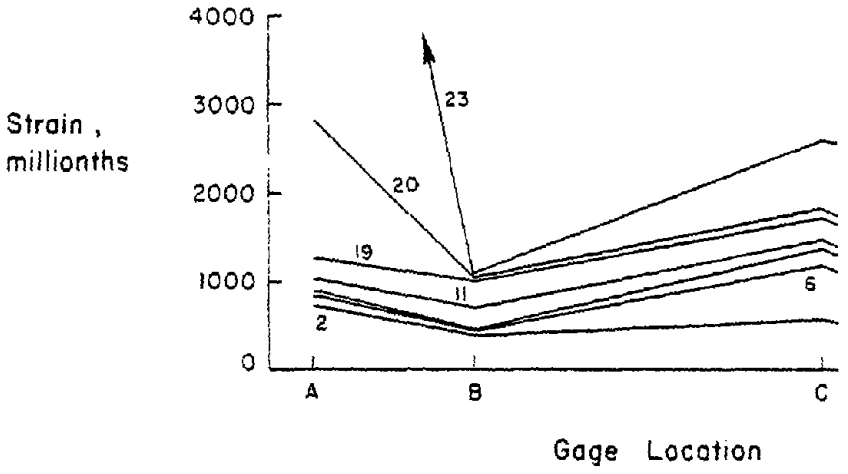

a) 4'-6" above Base

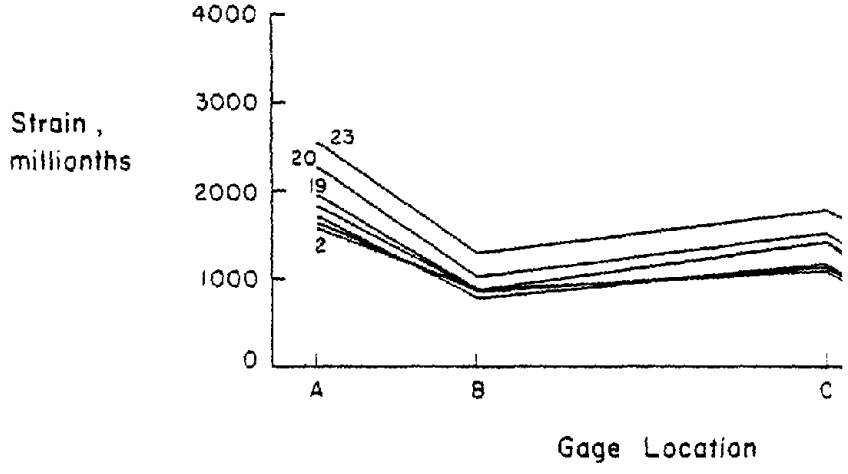

b) 1'-6" above Base

Fig. B-31 Strain Distribution Across Wall for Ho
Reinforcement in Specimen PW-1

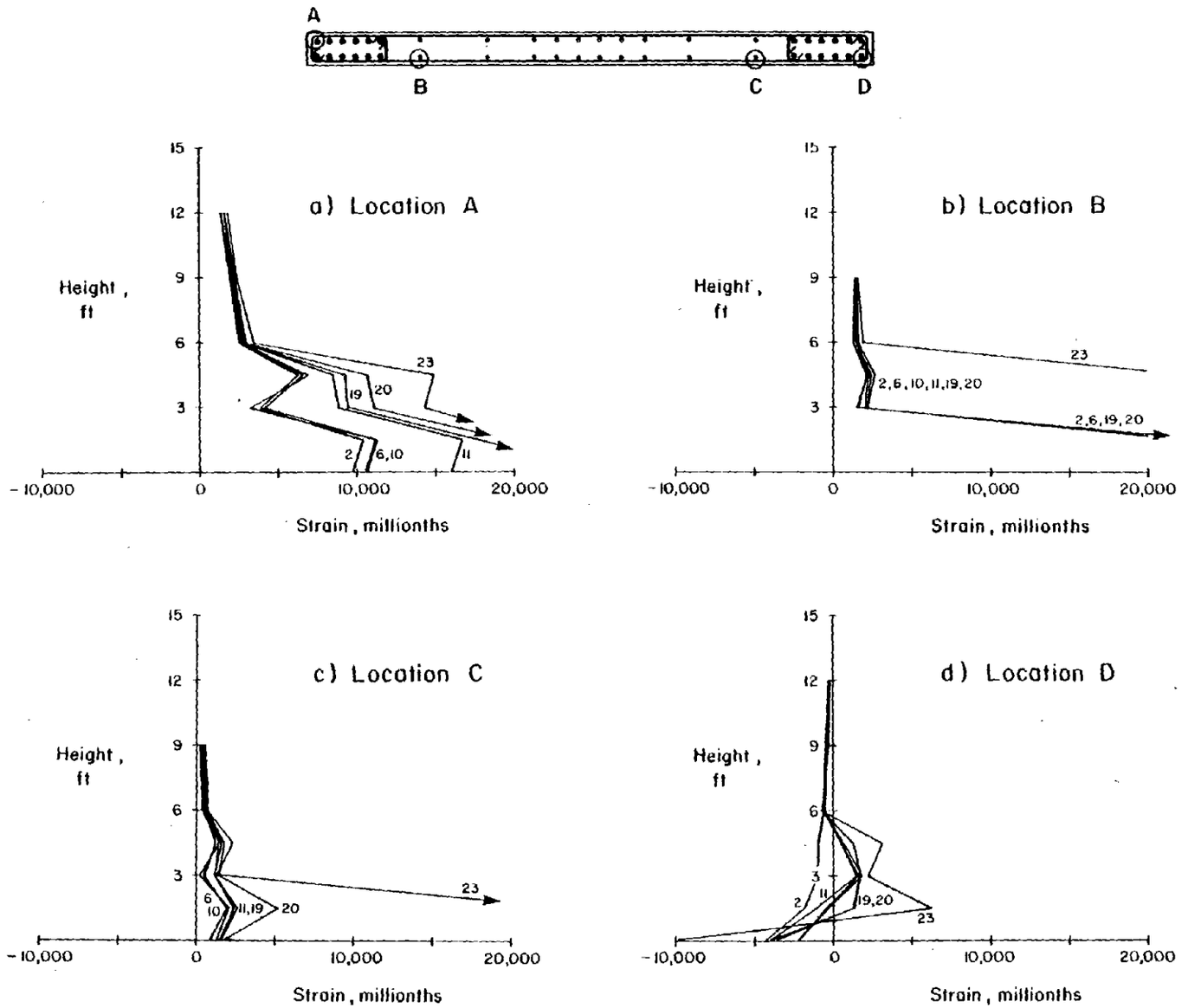

Fig. B-32 Strain Distribution Over Height Above Base for Vertical Reinforcement in Specimen PW-1

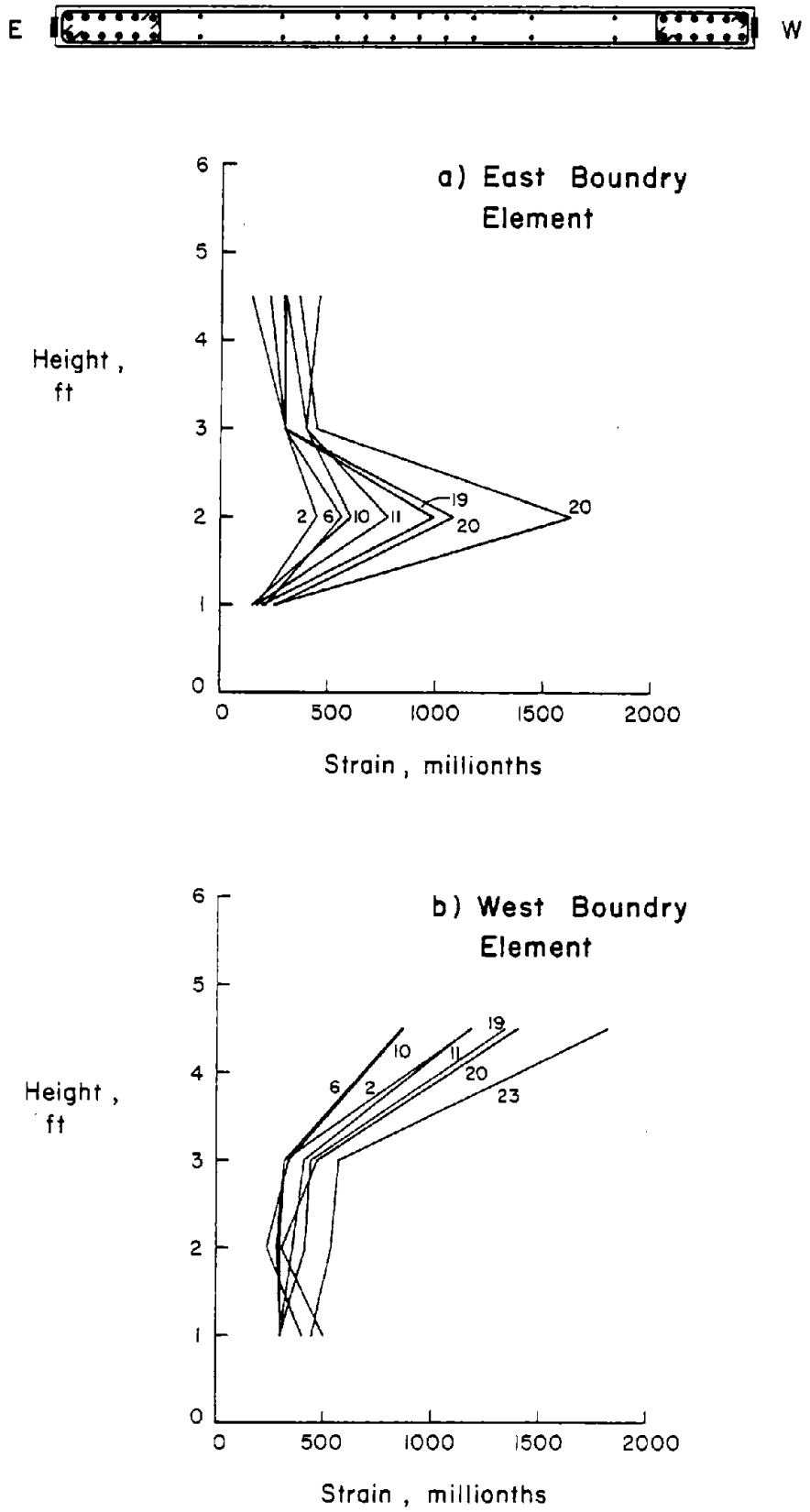

Fig. B-33 Hoop Strain Distribution Over Height Above Base for Specimen PW-1

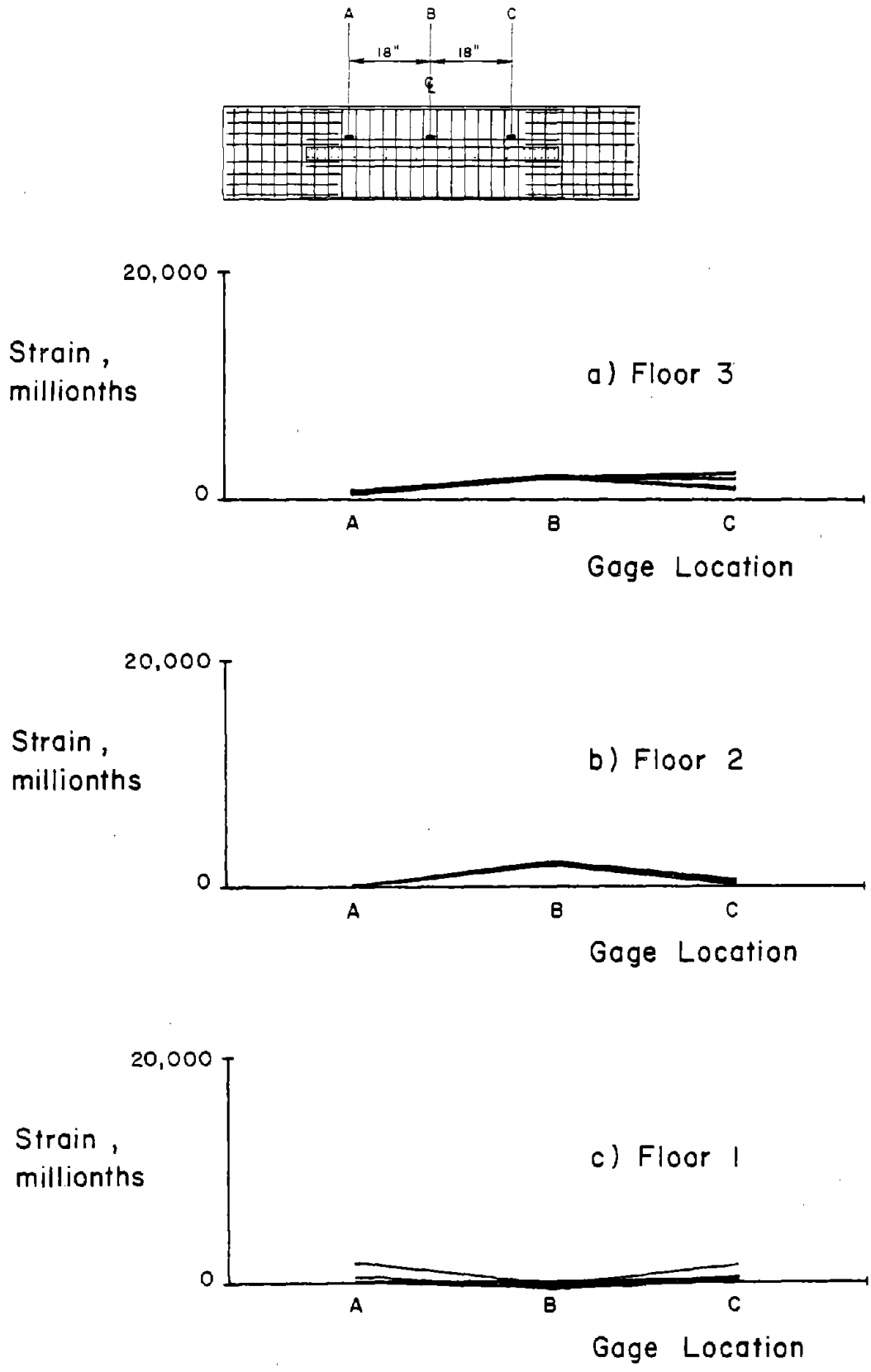

Fig. B-34 Strain Distribution in Slab Reinforcement for Specimen PW-1